

**FDS MODELLING OF HOT SMOKE TESTING,
CINEMA AND AIRPORT CONCOURSE**

Submitted as a Thesis

to the Faculty

of the

WORCESTER POLYTECHNIC INSTITUTE

In partial fulfilment of the requirement for the

Degree of Master of Science (M.S.)

in

Fire Protection Engineering

By

Alex Webb

Date: November 29, 2006

Approved:

Professor Jonathan Barnett, Advisor

Vince Dowling, Reader

Abstract

The construction of smoke hazard management systems in large buildings such as shopping malls, cinemas, airports and train stations are increasingly being based on performance based design. Hot smoke tests are a method of using simulated fire conditions to evaluate the functionality of the completed building and the installed systems without causing damage. The author amongst others performed hot smoke tests (HST) according to Australian Standard AS 4391 -1999 in several buildings. In some tests air temperatures, air speed and smoke optical density were recorded at several locations during the test of which two tests are reported.

These were later modelled by the author using Fire Dynamic Simulator (FDS) to show that typical fire protection engineering consultant applying the computer model may reasonably predict some results comparable to a full sized simulation scenario. However, some aspects were not well predicted. The modelling was improved by the outcomes of an investigation of the relationship between fuel properties, plume temperature and dynamics, and grid sensitivity. Areas of potential further improvement were identified. This work highlighted that the conditions witnessed in a hot smoke test can provide a guide, but do not represent all aspects of a real fire or design fire scenario. Although the FDS hot smoke model predicted comparable results to the hot smoke test, whilst suitable for system design, computer modelling should never be used as a system installation certification tool. Data from hot smoke tests, if gathered cost effectively, can be a valuable resource for computer model verification.

TABLE OF CONTENTS

1	INTRODUCTION	1
1.1	PERFORMANCE-BASED DESIGN	3
1.1.1	<i>Objectives</i>	3
1.1.2	<i>Acceptance Criteria</i>	3
2	HOT SMOKE TEST IN AUSTRALIA.....	5
2.1	DEFINITIONS FROM AS 4391-1999	5
2.2	TEST APPARATUS.....	6
2.3	ACCURACY OF HOT SMOKE TESTS	8
2.4	LIMITATIONS OF HOT SMOKE TESTS	8
2.5	HOT SMOKE TESTS INTERNATIONALLY	9
2.6	HOT SMOKE TESTS IN AUSTRALIA.....	11
3	FIRE DYNAMICS SIMULATOR (FDS)	13
3.1	COMPARISON OF METHODS OF TREATMENT OF TURBULENCE	13
3.2	HYDRODYNAMIC MODEL.....	16
3.2.1	<i>Conservation of mass</i>	17
3.2.2	<i>Conservation of species</i>	17
3.2.3	<i>Conservation of momentum</i>	17
3.2.4	<i>Conservation of energy</i>	18
3.2.5	<i>Equation of state</i>	18
3.3	TREATMENT OF TURBULENCE	19
3.4	LOW MACH NUMBER ASSUMPTION.....	19
3.5	COMBUSTION MODEL	20
3.6	RADIATION TRANSPORT.....	21
3.7	GEOMETRY	21
3.8	BOUNDARY CONDITIONS	22
3.9	OTHER FEATURES.....	22
3.10	LIMITATIONS.....	22
3.11	MODEL SENSITIVITY	23
3.12	VALIDATION AND VERIFICATION	24
3.12.1.1	Verification of model aspects relevant to HST	25
4	METHODOLOGY	27
5	FDS CALCULATIONS OF THE PLUME	28
5.1	SINGLE TRAY FIRE CORRELATION.....	28
5.1.1	<i>Sensitivity to radiant fraction and Heat Release Rate per unit area</i>	28
5.1.2	<i>Sensitivity to grid resolution</i>	29
5.1.3	<i>Ethanol and Methanol</i>	33
6	HST IN A CINEMA AUDITORIUM.....	35

6.1	TESTING AND COMMISSIONING	35
6.2	OBSERVATIONS	38
6.3	COMPARISON BETWEEN FDS AND TEST OBSERVATIONS.....	40
7	SCALING.....	40
8	AIRPORT CONCOURSE INTRODUCTION	42
8.1	TEST METHOD	42
8.1.1	<i>Instrumentation</i>	43
8.2	DESCRIPTION OF THE TEST SITE	44
8.2.1	<i>Smoke exhaust locations</i>	46
8.3	OBSERVATIONS AND DISCUSSION	49
8.3.1	<i>Test 1 –Departures Concourse</i>	50
8.3.1.1	Observations Test 1	50
8.3.1.2	Discussion of visual observations Test 1	50
8.3.1.3	Results Test 1	51
8.3.1.3.1	Results for location 1 - Test 1.....	52
8.3.1.3.2	Results for location 2 - Test 1.....	55
8.3.1.3.3	Results for location 3 - Test 1.....	59
8.3.1.3.4	Comparison of results for all locations - Test 1.....	61
8.3.2	<i>Test 2 – Departures Concourse repeat test</i>	63
8.3.2.1	Observations Test 2	63
8.3.2.2	Discussion of visual observations – Test 2	63
8.3.2.3	Results – Test 2.....	64
8.3.2.3.1	Results for Station 1 – Test 2.....	64
8.3.2.3.2	Results for Station 2 – Test 2.....	66
8.3.2.3.3	Results for Station 3 – Test 2.....	69
8.3.2.3.4	Comparison of results for all locations – Test 2.....	71
8.4	EXPERIMENT CONCLUSIONS	72
9	FDS MODELLING OF AIRPORT CONCOURSE HOT SMOKE TEST ..	73
9.1	INPUT FILE	73
9.2	GEOMETRY	74
9.2.1	<i>Grids</i>	76
9.2.2	<i>Sensitivity analysis of node number</i>	78
9.2.3	<i>Ventilation Openings</i>	78
9.2.4	<i>Mechanical Smoke Exhaust</i>	78
9.2.5	<i>Smoke detection</i>	80
9.3	SIMULATION OF TEST 1 EVENTS.....	80
9.4	SIMULATION OF TEST 2 EVENTS.....	81
9.5	RESULTS OF TEST 1 MODEL AND COMPARISON WITH TEST DATA.....	81
9.5.1	<i>Air velocity – test 1</i>	82
9.5.2	<i>Temperature – test 1</i>	82
9.5.3	<i>Smoke – test 1</i>	84
9.6	RESULTS OF TEST 2 MODEL AND COMPARISON WITH TEST DATA.....	85

9.6.1	<i>Air velocity – test 2</i>	86
9.6.2	<i>Temperature – test 2</i>	87
9.6.3	<i>Smoke – test 2</i>	88
9.7	DISCUSSION OF COMPARISON.....	89
9.8	RESULTS OF TEST 2 MODEL WITH CONCOURSE EXHAUST AT 50% AND COMPARISON WITH TEST DATA.....	90
9.8.1	<i>Air velocity – Test 2: 50% concourse extract</i>	91
9.8.2	<i>Temperature – Test 2: 50% concourse extract</i>	91
9.8.3	<i>Smoke – test 2: 50% concourse extract</i>	92
9.8.4	<i>Test 2: 50% concourse extract impact of gate lounge exhaust</i>	93
9.9	GRID SENSITIVITY ANALYSIS.....	95
9.10	COMPUTATION SENSITIVITY ANALYSIS.....	99
10	DISCUSSION	100
10.1	IMPROVEMENTS TO THE TESTING.....	102
10.2	IMPROVEMENTS TO THE MODELLING.....	102
11	CONCLUSIONS	103
12	ACKNOWLEDGEMENTS	105
13	REFERENCES	105

List of Figures

Figure 1. Typical Hot Smoke Test Layout using smoke canister.	7
Figure 2. Schematic representation of different treatments for turbulence.	14
Figure 3 Heat output for methylated spirit from AS 4391.	29
Figure 4. Variation in plume temperature calculations due to radiative fraction.	31
Figure 5 Variation in plume temperature calculations as a function of HRRPUA.	31
Figure 6. Variation in plume temperature calculations due to solver and number of cells (number in the legend denotes millions of cells).	32
Figure 7. Variation in plume temperature calculations due to fuel input data.	34
Figure 8. Small auditorium FDS model	36
Figure 9. Small auditorium FDS model results - visibility slice at 100 seconds.	37
Figure 10. Small auditorium FDS model results - visibility slice at 300 seconds.	38
Figure 11. Calculation of hot smoke test parameters	41
Figure 12. Smoke meter and thermocouple located 300mm from the ceiling.	44
Figure 13 Test 1 and 2. Departures concourse.	45
Figure 14 Location of test 1 and repeat showing instrumentation.	48
Figure 15. Smoke extinction coefficient station 1	53
Figure 16. Temperature station 1	53
Figure 17. Location of instrumentation station 1 in regard to the test fire looking east to west.	54
Figure 18. Location of instrumentation station 1 in regard to the smoke layer during test 1.	54
Figure 19. Smoke extinction coefficient station 2	56
Figure 20. Temperature station 2.	57
Figure 21. Air velocity station 2.	57
Figure 22. Comparison of air speed, temperature and smoke extinction coefficient station 2	58
Figure 23. Test fires and instrumentation station 2 during the test.	58
Figure 24. Smoke extinction coefficient station 3	60
Figure 25. Temperature station 3.	60
Figure 26. Location of instrumentation station 3 in regard to the test fire looking west to east.	61
Figure 27. Temperature comparison for all stations.	62
Figure 28. Smoke extinction coefficient comparison for all stations	62
Figure 29. Smoke extinction coefficient station 1	65
Figure 30. Temperature station 1	66
Figure 31. Smoke extinction coefficient station 2	67
Figure 32. Temperature station 2.	68
Figure 33. Air speed station 2.	68
Figure 34. Smoke extinction coefficient station 3	70
Figure 35. Temperature station 3.	70
Figure 36. Smoke extinction coefficient comparison for all stations	71
Figure 37. Temperature comparison for all stations.	72

Figure 38. Perspective view of the building from above	75
Figure 39. Perspective view of the building from below (Reflected ceiling plan view).....	75
Figure 40. Perspective view of the test fire location from east, looking toward the satellite (compare to showing the test site)	76
Figure 41. Perspective view of the domain grids from below (Reflected ceiling plan view).....	77
Figure 42. Perspective view of the building from below (Reflected ceiling plan view).....	79
Figure 43. Perspective view of the exhaust fans in gate lounges from below (Reflected ceiling plan view).....	79
Figure 44. Air velocity station 2 – Comparison of Test 1 simulation and measured data.....	82
Figure 45. Temperature all stations.....	83
Figure 46. Smoke extinction coefficient all stations	84
Figure 47. Smoke extinction coefficient all stations – station 2 smoothed.....	85
Figure 48. Air velocity station 2 – Comparison of Test 2 simulation and measured data.....	86
Figure 49. Air speed - Test 2 in the concourse and entrance to gate 1.....	87
Figure 50. Temperature all stations – test 2	88
Figure 51. Smoke extinction coefficient all stations – test 2	89
Figure 52. Air velocity station 2 – Comparison of Test 2: 50% simulation and measured data	91
Figure 53. Temperature all stations – test 2: 50%	92
Figure 54. Smoke extinction coefficient all stations – test 2: 50%.....	92
Figure 55 Pictures of the FDS rendering of smoke entering the Gate lounge 1.....	94
Figure 56. Grid sensitivity comparison of thermocouple readings 750,000 cells (Melbairtest2c) vs 114,000 cells (Melbairtest2e)	96
Figure 57. Grid sensitivity comparison of thermocouple readings 750,000 cells (Melbairtest2c) vs 1,440,900 cells (Melbairtest2g) for the first 200 seconds.....	97
Figure 58. Grid sensitivity comparison desktop and the HSPC temperatures	99
Figure 59. Grid sensitivity comparison desktop and the HSPC temperatures smoke and air speed.....	100

List of Tables

Table 1. Equations solved by FDS.....	16
Table 2. Sensitivity analysis of methylated spirit pool fire.	30
Table 3. Comparison of Methanol and Ethanol FDS input values.	33
Table 4. Hot smoke test event times and comments.....	38
Table 5 Test location and details	44
Table 6. Test 1: Hot smoke test event- times and comments.....	50
Table 7. Test 2 - Hot smoke test event times and comments.....	63
Table 9. Simulation of Test 1 – FDS Hot smoke test event times and comments.	80
Table 10. Simulation of Test 2 – FDS Hot smoke test event times and comments.	81
Table 11. FDS grid sensitivity runs.....	98

Nomenclature

List of Acronyms

AHJ	Authority Having Jurisdiction
AHU	Air Handling Unit – part of a mechanical air conditions system
CFD	Computational Fluid Dynamics
CSIRO	Commonwealth Scientific Industrial Research Organization
DNS	Direct Numerical Simulation
FDS	Fire Dynamic Simulator
HRR	Heat Release Rate
HRPPUA	Heat Release Rate Per Unit Area
HST	Hot Smoke Test
ISO	International Standards Organisation
LES	Large Eddy Simulation
NIST	National Institute of Standards and Technology
RANS	Reynolds-averaged form of the Navier-Stokes equations
SCS	Smoke control systems
SI	International System of Units

List of Terms

A1	International paper size complying with ISO 216
Cell Size	Dimensions of cell
Grid Size	Total number of cells within grid
KS	Thermal conductivity
Navier-Stokes Equations	Governing equations for particle flow in FDS
RAMP ID	Identifies description for ramp up function
Smokeview	Visualization of FDS prediction
OBST	Obstacle nameless group in FDS
p	Pressure
ρ	Density
t	Time
u or u	Velocity vector $= (u, v, w)$
τ	Stress tensor
f	Force term which excluding gravity
g	gravity
h	sensible enthalpy
q	heat flux (radiative and convective)

\dot{q}'''	heat release rate per unit volume
\dot{q}_r''	radiative flux to a solid surface
\dot{q}_c''	convective flux to a solid surface
Q	total heat release rate
Q_c	characteristic fire size
\mathcal{R}	Universal gas constant
M	Molecular weight of gas mixture
Φ	dissipation function
Y_i	mass fraction of i^{th} species
D_i	diffusion coefficient of i^{th} species

1 INTRODUCTION

The construction of smoke hazard management systems in large buildings such as shopping malls, cinemas, airports and train stations are increasingly performance based design. These systems are designed by fire protection engineers using design guides and computer modelling techniques such as Computational Fluid Dynamics (CFD) that have become more accepted among Fire Protection Engineers. One such program is Fire Dynamics Simulator (FDS) , developed by National Institute of Standards and Technology, (NIST), which allows a user to construct a three-dimensional model to investigate a given fire scenario.

Evaluation is critical in establishing both the acceptable uses and limitations of a model such as FDS. FDS has undergone various forms of evaluation. Roughly half of the studies referenced in the FDS technical guide (35) were aimed primarily at model evaluation, the other half describe limited work to validate FDS for a specific use. This paper attempts to model a hot smoke test with the resources available to the typical fire protection engineer and to add to the body of work that forms the basis of a model evaluation.

Hot smoke tests (HST) are a method of using simulated fire conditions to evaluate the functionality of a completed building and installed systems without causing damage. The HST comprises a small clean burning liquid fuel fire in which artificial smoke is injected and the flow of the simulated hot smoke layer is tracked and the response of the fire safety systems noted.

This paper discusses the smoke control designs for a cinema auditorium and an airport terminal concourse. HSTs have been carried out in both buildings. In the airport building an array of temperature, obscuration and air velocity instrumentation was installed. Both spaces have also been analysed using FDS(38). A comparison of the HTS results and the FDS results is made. Common smoke control system defects identified during these and the other tests are summarized.

As a precursor to the modelling of the buildings the ability of FDS to model a simple axis symmetric plume of a burning tray of methylated spirit (ethanol) was analysed.

Guidance to the design of smoke control systems (SCS) is readily available from the NFPA (45-49) and the BRE (24-27;44) and other sources (42), and provide the methodologies and bases for which designers can develop a performance based on an appropriate smoke control strategy. In undertaking a smoke control design, the process requires consideration of several factors including the potential fire hazard, the building configuration, and the methodology for fire, smoke and evacuation analysis. Key SCS objectives are identified along with the performance requirements as part of the design process. Installation of appropriate, testing and commissioning of the system in accordance with the final design must be correct if the system is to satisfy the objectives and performance criteria. But how does an Authority having Jurisdiction (AHJ) know when this is so? One way is by requiring a Hot smoke testing (HST) to be required as part of the testing and commissioning of implemented systems. The outcomes and relevance of a HST is dependant on the test parameters. NFPA 92 Clause 5.3.3.6 (45)states:

Much can be accomplished to demonstrate smoke control operations with resorting to demonstrations that use smoke or products that simulate smoke... Test criteria based on a systems ability to remove smoke from an area are not appropriate for zoned smoke-control systems, since these systems are designed for containment, not removal, of smoke.

This however is not the case with some performance based design which justifies non conformance by determining appropriate time to untenable conditions.

CSIRO has carried out over one hundred HSTs in accordance with the Australian Standard AS 4391 (54). Tests have been done in many building types and tunnel configurations.

The smoke control designs and tests for two different types of buildings have been selected. The first case is a cinema auditorium which in Australia is classified as an Assembly occupancy (Class 9B) by the Building Code of Australia (5). The hot smoke test has also been analysed using the Computation Fluid Dynamics (CFD) package Fire Dynamics Simulator (FDS) Version 4 (36;38;41). The second test was conducted in a airport terminal concourse (classified as assembly occupancy, Class 9b).

1.1 Performance-based Design

1.1.1 Objectives

In a performance based approach the main objective of the smoke control system is to safeguard occupants from illness or injury while evacuating a building during a fire and facilitate the activities of emergency services personnel. How this is achieved is specified as part of a performance based design and is typically done by keeping smoke away from escape routes during the evacuation phase. The design acceptance criteria are listed below and, as this work has been carried out in Australia, it is in accordance with the Building Code of Australia (BCA) (5).

1.1.2 Acceptance Criteria

In accordance with the International Fire Safety Engineering Guidelines (6), the following general acceptance criteria can be used to evaluate the performance of the fire engineering smoke control design:

Smoke Layer Height > 2.0m

The risk of inhalation of potentially toxic combustion gases is minimized when the smoke layer is above head height during occupant evacuation. For the purposes of building design, a safe smoke layer height of 2 m [BCA Clause 2 (a)(i)] above floor level is acceptable. Once the smoke layer height is below 2 m, the conditions are deemed no longer tenable when one or more of the following conditions is exceeded:

- The smoke temperature at head height (2 m) exceeds 100°C (57). The time to incapacitation due to elevated temperature is given by equation (1):

$$t_1[\text{min}] = \exp(5.1849 - 0.0273T^{\circ\text{C}}) \quad \text{Equation 1}$$

Where

T = temperature of smoke °C

t_1 = time to incapacitation in minutes

Using equation (1), the time to untenable conditions for an exposure temperature of 100°C is about ten minutes.

- Smoke Optical Density

Untenable visibility in a small enclosure occurs when the visibility is less than 5 m (0.2 optical density/m), which, for irritant smoke, is that level at which people move as if in darkness. In large enclosures, occupants require much greater visibility to orient themselves and therefore a minimum visibility is 10 m (0.1 optical density/m) (8). This visibility corresponds to an optical density of 1.3 dB/m for light reflecting signs and 3.4 dB/m for light emitting signs (ref SFPE).

- Exposure to toxic gases of combustion

It has been observed in several studies that Carbon Monoxide (CO) concentration is critical in determining the tenability in a smoky fire environment. The International Fire Engineering Guidelines (6) recommends the use of CO concentration as one of the acceptance criteria. However, it has been observed that the mixture of asphyxiant gases (CO, CO₂, low O₂ and HCN) is approximately additive and the tenability for total inhalation of an asphyxiant can be related to the optical density of smoke. It

has been recommended that the level of toxic products (asphyxiants and irritants), are unlikely to reach limiting levels for up to 30 min in situations where the smoke optical density does not exceed 0.1/m (or 10m visibility) (8).

To show the acceptance criteria have been achieved one of many smoke movement computer models are used. The models must be able to calculate the parameters set as the acceptance criteria and to do so within the limitations of the model. Two main types of models are in use by the engineering community: zones models and field models. Zone models model each enclosure as two homogeneous zones, a hot layer and a cold layer. Empirical relationships are used to calculate the exchange between the two layers most of which occurs in the fire plume.

Field models (CFD) divide the domain into many cells (100,000 or more) and the exchange between all these cells is modelled based on first principles physics.

2 HOT SMOKE TEST IN AUSTRALIA

The tests discussed and modelled in this paper were conducted in accordance with the Australian Standard AS 4391 – 1999 (54). The HST provides a means by which a specified quantity of smoke is generated by a test fire to assist in the assessment of the performance characteristics of a building's smoke management system. Methylated spirit is burnt in a tray to provide a clean, safe, dynamic buoyant plume and layer of smoke representative of a real fire. Artificial smoke is introduced into the plume as a tracer to identify the location of the smoke plume and hot gas layer.

2.1 Definitions from AS 4391-1999

Definitions from the standard AS 4391-1999 used in this report are:

Design fire – a quantitative description of assumed fire characteristics within a specific fire scenario on which a fire engineering analysis will be conducted. Typically, the design is a description of the variation with time of important fire variables such as heat release rate, smoke and toxics species yield.

Smoke – is the visible suspension in air of solid or liquid particles or gases resulting from combustion or pyrolysis, including the plume from the test fire and the tracer smoke. (Note: This varies from ASTM definition by inclusion of the word visible).

Smoke generator – a device for emitting a constant volume stream of smoke, also called smoke candles or smoke canisters.

Test fire – an actual fire size used to test smoke management systems without damage to the system or the building being protected.

Tracer smoke – the vapour emitted by the smoke generator and entrained in the hot plume for identification purposes.

2.2 Test Apparatus

Figure 1 shows a test in process with four test fires located around the smoke generator. Each fire tray is placed on a non-combustible board to protect flooring material underneath. The fire trays are made from welded 1.6mm steel, watertight and braced. The fuel tray sizes are standardized and based on ISO international metric paper sizes. An A1 size has a fuel surface area of 0.5 m², A2 0.25 m² etc which provides an easy standard for SI calculations. The fuel trays are placed in water bath to stabilise burning rates and to prevent sudden thermal bucking of the steel trays splashing burning fluid. The tracer smoke mixes with the heated air plume, rises to the ceiling and creates a hot smoke layer.



Figure 1. Typical Hot Smoke Test Layout using smoke canister.

The fire size is selected from an array of tray sizes that corresponds with a certain fire size that will, however, limit plume temperatures to a level that will not damage the building, linings fittings or activate sprinkler bulbs. This is achieved by selecting an array of tray sizes that corresponds with a particular fire size. For example, a single A4 size tray results in a net heat output of 26 kW (56), sufficient to provide the required buoyancy to the smoke in a relatively small compartment. The approximate net heat flux provided by four A1 trays is 1.4 MW, and if placed apart from each other provides the entrained smoke volume (mass flow rate) corresponding to a 3.5 MW fire. The artificial smoke used for these tests is a glycol based “disco” fog (a smoke generating firework is another option for more robust buildings and tunnels as shown in Figure 1), which is introduced into the centre of the array of fire plumes. Sufficient fuel is supplied to allow a test to run for at least 10 minutes.

Hot smoke tests are ideally applicable for buildings with special geometry and complex smoke control systems which includes atria, factories, warehouses, department stores, shopping and other complexes, multistorey office buildings or sporting and entertainment centres. The test is intended to verify the correct performance of a smoke management system including operation, sequence of control and, where practical, specified smoke layer depths.

2.3 Accuracy of hot smoke tests

The accuracy of the data measured in hot smoke tests is controlled by the requirements specified within the test standard. The heat sensors are required to have an accuracy of $\pm 3^{\circ}\text{C}$. A Type K thermocouple is used in accordance with EN 60584.1, with elements 0.6mm nominal diameter.

The standard does not specify a tolerance on the tray sizes. Each tray buckles due to heat during the test and therefore the area of each tray differs slightly.

Data supplied in Appendix A of AS 4391 (reproduced as Figure 3 in Section 5.1) is for denatured industrial grade methylated spirit (Grade 95). The data for the figure, heat release rate output per area, was gathered from 20 test fires in which the fuel mass loss was measured. The cubic polynomial presented in AS 4391 is a best fit curve for a correlation of 97% of the average values of all tray sizes obtained from the 20 experimental test and on-site tests. Oxygen consumption calorimetry measurements of the burning trays would provide additional verification of heat release rate, however, these have not been made. The standard recommends fuel quantities, which provide three minutes fire growth, ten minutes steady state burning and three minutes decay.

2.4 Limitations of hot smoke tests

Limitations of the test method are:

1. The temperatures must be limited so that no damage occurs to the building. Temperatures in the ceiling jet above the fire must be limited to less than 55°C to ensure sprinklers aren't activated. The temperatures are therefore much lower than would be expected by a real fire, even for a fire plume cooled by sprinkler spray fire where temperatures are typically still in the vicinity of 100°C or more.
2. The fire growth is close to instantaneous, which does not simulate a typical growing fire. Smoke exhaust systems activated by smoke detection designed for early occupant warning would typically activate at an early stage of a fire. In HST smoke

exhaust activation may occur in 30 seconds with a substantial smoke layer already moving through a space.

3. AHJs would like, and sometimes expect, the HST to assess tenability limits of the design, however, the standard clearly states that:

It is not intended as a means of establishing smoke obscuration levels or system integrity under real fire conditions.

The main reasons are the difference between real fires, as in points 1 and 2 above.

4. Repeatability – The repeatability of hot smoke tests is not as good as a standard test method because duplicate tests are really performed. The variables of the fire are only the trays, fuel and tracer smoke. The building spaces are generally complex which is an uncontrollable variability introduced into the test scenario.

2.5 Hot smoke tests internationally

Hot smoke test are carried out in many countries around the world. Consultants provide the service in New Zealand. NRC in Canada have carried out tests in the Montreal's Maurice-Richard Arena (31) where in-situ hot smoke tests were conducted using a clean-burning propane burner system developed at NRC. This system is capable of producing controlled fire sizes up to 5 MW. Video cameras were used for the visual monitoring of the smoke filling rate. Several laser beams were also used to trace the smoke. The time for the smoke layer to descend to different levels in the arena for different fire sizes was also predicted from the SFPE method.

LABEIN Technalia have carried out hot smoke tests in several Spanish tunnels and buildings. Their website (32) states

The test is based on a hot smoke generator and protocols for development, calibration and usage. The generator produces a flow of clean gases, the temperature of which is nevertheless sufficient to create stratification. This in-house technology is unique in Europe. Tests carried out to date include testing on tunnel P-11 on the Txorierra corridor (Bizkaia), the Lezarrri tunnel (Bergara) on the A-1 motorway (Eibar-Vitoria), tests on the Bilbao Exhibition Centre car parking facility, and on the Zubiarte shopping centre in Bilbao.

Hot smoke tests were carried out according to AS 4391 in a 60m high atrium in Langham Place in Hong Kong as the last part of a series of performance verification tests. The results were written up as an article presenting a case study of the use of air sampling detectors as part of the protection systems for the atrium (59).

Hughes Associates in the US have conducted tests including Atrium Smoke Control Performance Testing by constructing a smoke test apparatus for testing atrium smoke control systems that utilizes a cold smoke simulant using induced buoyancy (30).

The Land Transport Authority (LTA) of Singapore conducted a series of hot smoke tests in the Kallang/Paya Lebar (KPE) according to AS4391(33). The KPE is a 12-km expressway that stretches from East Coast Parkway (ECP) to Tampines Expressway (TPE). Nine kilometres of the expressway is constructed as an underground tunnel. To verify the operation and performance of the tunnel ventilation and other systems in a fire, hot smoke tests will be conducted in the tunnel.

17 of 19 of the tests carried out (60) in the PolyU/University of Science and Technology, China burn hall were done in accordance with AS 4391. The fires were methylated spirit A1 sized trays, using 6, 9, 12 or 15 trays at one time. The authors calculated the heat release rate of an A1 tray using oxygen consumption calorimetry and mass loss rate, demonstrating an average 386 kW and 0.0117 kgs⁻¹ once the steady state burn was achieved ($t > 60$ s). The test data was compared with equations from NFPA 92B (46) and a model developed by the authors.

The same authors have carried out other tests on the natural filling of atrium spaces with similar fire sources (9).

There are many other fire tests within buildings and other infrastructure spaces that have been performed, however the list above is limited to tests according to AS 4391 or tests that use a clean burning fuel and introduce a fake smoke as a tracer. Tests carried out in Australia with published papers are discussed in Section 2.6, and other fire experiments are discussed in Section 3.12.

2.6 Hot smoke tests in Australia

Papers on HSTs have been presented at conferences (3) and in journals (1;2). Allan's paper (1) described the hot smoke tests in a shopping atrium containing a heritage building. He also listed the significant problems that HSTs had identified during the commissioning of systems. These included:

- Exhaust duct inlets blocked by temporary construction which had not been removed.
- Dampers not operating.
- Fans not working at design capacity.
- Control interface not able to handle smoke detected simultaneously in more than one zone.
- Smoke flowing through a ceiling space not being able to reach exhaust points due to congested ceiling plenum space.
- Faulty logic control.
- Penetrations in risers shafts.
- Badly designed make up air supply.

Some of the deficiencies may/should have been detected at design or early commissioning stage, however some could only have been detected by a hot smoke test.

A HST in an uncompartmented shopping mall 110m long and 15m wide, in which the smoke exhaust fans were located 3m below the highest point of a curved roof, was carried out as part of a computer model verification (3). The computer model was Firecalc (15).

A series of twenty HSTs were carried out in the Melbourne Citylink road tunnels (2). Citylink consists of two tunnels, Burnley 3.4km and Domain 1.8km. The tunnel bores are each three lane, one way with jet fans, smoke extraction at 80m intervals and deluge zones. The tests purpose was:

- To investigate the movement of smoke “uphill” from the test locations in zero air velocity scenarios.
- To examine smoke back layering upstream from the fires in the optimum extraction configurations.

- To demonstrate the accessibility of a fire incident by emergency services.
- To test the performance of the pressurisation systems for the safe havens.
- To examine the impact of various numbers of jet fan operating upstream of the fires, creating various air velocities within the tunnels.
- To demonstrate the effect of the deluge on the smoke movement.

Over 200 hundred tests have been performed in Australia however not many have resulted in data published in the public domain.

3 FIRE DYNAMICS SIMULATOR (FDS)

This Chapter outlines the main assumptions and equations behind the FDS. The details covered in this Chapter are mainly referenced from Floyd et al. (20), SFPE handbook (14) and the FDS Technical Reference Guide (40).

Fire Dynamics Simulator (FDS) is a computational fluid dynamics (CFD) computer model of smoke flow from a fire. The software numerically solves a form of the Navier-Stokes equations appropriate for low mach number (low-speed), thermal buoyancy driven flow, with a focus on smoke and heat transport from fires. The equations and the numerical algorithm are described below in Section 3.2 to 3.6 (40). A visualization program called Smokeview may be used to display the results of a FDS simulation (21).

3.1 Comparison of methods of treatment of turbulence

Prior to the more recent evolution of Large Eddy Simulation (LES), most CFD work was based on the concept provided by the Reynolds-averaged form of the Navier-Stokes equations (RANS), in particular the k– ϵ turbulence model (51). However, this technique has a fundamental limitation for fire. RANS models' equations are a time-averaged approximation to the conservation equations of fluid dynamics. The averaging time is long enough to require the introduction of large eddy transport coefficients to describe the unresolved fluxes of mass, momentum and energy. This causes smoothing of the results. The smallest resolvable length scales are determined by the local velocity and the averaging time rather than the resolution of the grid. This property of RANS models is useful as it enables the ability to take large time steps.

Unfortunately, with this approach, large eddy structures characteristic of most fire plumes and the prediction of small swift events is lost. Increasingly fast computing power enables the LES technique to extract greater time and spatial resolution from more finely meshed grids.

The main assumption in the LES technique is that the eddies that account for most of the mixing are large enough to be calculated with reasonable accuracy from the equations of fluid dynamics, and that small-scale eddy motion can either be crudely accounted for or ignored.

A useful analogy is that presented by Cox and Kumar of the fine wire thermocouple within a fire, with the results of temperature measure graphed in Figure 2 (14). The RANS model solves the time-averaged properties. Complex turbulence sub models deal with the important factors of turbulence over the whole length scale, which are time averaged. The analogy would be a large gauge thermocouple with a long time constant.

LES avoids time averaging of fluctuations of larger than grid scale so these are rigorously represented. Below mesh size (typically the scale of chemical reaction) the sub-grid scale dissipative processes are modelled. The analogy would be a medium gauge thermocouple with a time constant that can follow most fluctuations but not the small-scale detail.

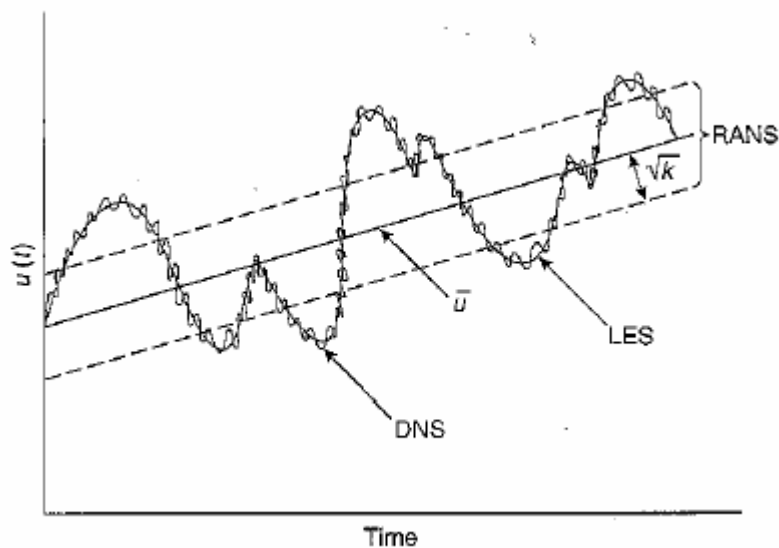


Figure 2. Schematic representation of different treatments for turbulence.

Direct numerical simulation (DNS) requires very fine mesh sizes ($< 1\text{mm}$) to be able to use the diffusive parameters directly to model combustion, species behavior, species viscosity

and conductivity. The analogy of a very fine thermocouple with a near zero time constant is used, but with such fine grids the domain size is restricted by computing power.

The equations describing the transport of mass, momentum, and energy by the fire-induced flows must be simplified so that they can be efficiently solved for the parameters of interest. The calculation of relevant high-speed flow and shock waves etc can also be ignored in fire simulation. The simplified equations, developed by Rehm and Baum (52), describe the low speed motion of a gas driven by chemical heat release and buoyancy forces.

The low speed (low Mach number) equations are solved numerically by dividing the physical space where the fire is to be simulated into a large number of rectangular cells. Within each cell the gas velocity, temperature, etc., are assumed to be uniform, changing only with time.

The accuracy with which the fire dynamics can be simulated depends on the number of cells, limited by the computing power. Currently the ratio of the largest to smallest eddy length scales that can be resolved is in the order of 100. Combustion processes take place at length scales of 1 mm or less, while the length scales associated with building fires are 10-100 meters. The range of length scales needs to be 10^4 to 10^5 to catch all fire processes.

FDS can be used to model the following phenomena:

- Low speed transport of heat and combustion products from fire
- Radiative and convective heat transfer between the gas and solid surfaces
- Pyrolysis
- Flame spread and fire growth
- Sprinkler, heat detector, and smoke detector activation
- Sprinkler sprays and suppression by water

This work will focus only on the first element in the above list as the fire is clean burning with very low radiative fraction. The fire reaction will be simplified and will not directly model the fuel combustion but will utilize the HRPPUA variable. Sprinklers and sprinkler spray will not be modelled. The model algorithms are described in the following sections.

3.2 Hydrodynamic Model

FDS numerically solves a form of the Navier-Stokes equations appropriate for low speed, thermally-driven flow with an emphasis on smoke and heat transport from fires. The core algorithm is an explicit predictor-corrector scheme, second order accurate in space and time. Turbulence is treated by means of the Smagorinsky form of Large Eddy Simulation (LES). It is possible to perform a Direct Numerical Simulation (DNS) if the underlying numerical grid is fine enough. LES is the default mode of operation. In DNS the dissipative terms are computed directly. LES directly computes the large-scale eddies and the sub-grid scale dissipative processes are modelled.

The conservation equations for mass, momentum and energy for a Newtonian fluid are presented below in Table 1.

Table 1. Equations solved by FDS.

Conservation of mass

$$\frac{\partial \rho}{\partial t} + \nabla \cdot \rho \mathbf{u} = 0 \quad \text{Equation 2}$$

Conservation of Momentum (Newton's Second Law)

$$\rho \left(\frac{\partial \mathbf{u}}{\partial t} + (\mathbf{u} \cdot \nabla) \mathbf{u} \right) = -\nabla p + \nabla \cdot \boldsymbol{\tau} + \rho \mathbf{g} + \mathbf{f} \quad \text{Equation 3}$$

Conservation of Energy (First Law of thermodynamics)

$$\frac{\partial}{\partial t} (\rho h) + \nabla \cdot \rho h \mathbf{u} = \frac{Dp}{Dt} + \dot{q}''' - \nabla \cdot \mathbf{q} + \Phi \quad \text{Equation 4}$$

Equation of State for a perfect Gas

$$p = \frac{\rho R T}{M} \quad \text{Equation 5}$$

Conservation of mass in terms of the mass fractions of individual gas

$$\frac{\partial}{\partial t} (\rho Y_i) + \nabla \cdot \rho Y_i \mathbf{u} = \nabla \cdot \rho D_i \nabla Y_i + \dot{m}_i''' \quad \text{Equation 6}$$

See the Nomenclature, list of terms and the sections below for a explanation of terms.

3.2.1 Conservation of mass

The general conservation of mass equation states that the rate of mass storage within a given control volume, due to density changes, is balanced by the net rate of inflow of mass by convection. In the case of a steady flow situation, the conservation of mass equation states that what flows in must come out. Where the first term of Equation 2 describes the density changes with time, and the second term defines the mass convection (mass moving through a cell face). The vector \mathbf{u} describing the velocity in the u , v and w directions.

3.2.2 Conservation of species

In the presence of a vector \mathbf{u} , the conservation of mass fraction Y of a chemical species i is given by Equation 5. Where the first term on the left side represents the accumulation of species due to change in density with time, the second term is the inflow and outflow of species from the control volume due to convection. The right side gives the terms for the inflow or outflow of species from the control volume due to diffusion and the production/consumption rate of particular species within the control volume caused by chemical reaction.

The mass conservation mass equation is often written in terms of the mass fractions of the individual gaseous species as in Equation 6.

3.2.3 Conservation of momentum

The equation for the conservation of momentum (Equation 3) is derived by applying Newton's second law of motion, which states that the rate of momentum of a fluid element is equal to the sum of the forces acting on it (13).

Here the left hand side represents the increase in momentum and inertia forces, while the right hand side comprises forces acting on it. These forces include pressure \mathbf{p} , gravity \mathbf{g} , an external force vector \mathbf{f} (which represents the drag associated with sprinkler droplets that penetrate the control volume) and a measure of the viscous stress tensor $\boldsymbol{\tau}$ acting on the fluid within the control volume. Among these forces,

gravity is the most important because it represents the influence of buoyancy on the flow.

3.2.4 Conservation of energy

The equation for conservation of energy Equation 4 is the first law of thermodynamics which states that the increase in energy of the control volume is equal to the heat added minus the work done by expansion. Here the left side describes the net rate of energy accumulation, whereas the right side comprises of the various energy gain or loss terms that contribute to this energy accumulation.

Note the use of the material derivative, $D(\cdot)/Dt = \partial(\cdot)/\partial t + \mathbf{u} \cdot \nabla(\cdot)$. These include the pressure work term, energy driving the system, represented by HRR per unit volume \dot{q}''' .

$\nabla \cdot \mathbf{q}$ represents the conductive term $\nabla \cdot (k \nabla T)$ and radiative heat flux vector \mathbf{q}_{rad} .

The term Φ is known as the dissipation function, the rate at which kinetic energy is transferred to thermal energy due to the viscosity of the fluid. This term is usually neglected because it is very small relative to the heat release rate of the fire.

The energy equation is never explicitly solved, but its source terms are included in the expression for the flow divergence.

3.2.5 Equation of state

The conservation equations are supplemented by an equation of state relating the thermodynamic quantities (36). In FDS, due to the low Mach number assumption (Section 3.4) the equation of state can be expressed in the form of:

$$p = \rho T R \sum_i (Y_i / M_i)$$

Equation 7

3.3 Treatment of turbulence

In comparison with other CFD codes LES ignores (or crudely accounts for) aspects of the flow that are not relevant to fire flows, and increases the need for fine meshing and small time steps to add fidelity to the fire scale turbulence which gets smoothed in other codes.

The Smagorinski treatment (53) of viscosity is to implement a model viscosity (μ), thermal conductivity (k) and material diffusivity (ρD) dissipative processes that cannot be resolved at smaller than grid resolution. (k) and (ρD) are related to viscosity; Pr and Sc are assumed constant for a given scenario. The model of viscosity handily provides numerical stabilization as well as looking for all intents and purposes like the dissipation of kinetic energy.

If the grid is small enough ($<1\text{mm}$) μ , k and ρD can be modelled directly with the DNS solver.

3.4 Low Mach number assumption

High speed flow CFD codes involve compressibility effects and shock waves. Low speed solvers, however, explicitly eliminate compressibility effects that give rise to acoustic (sound) waves. As written above, the Navier-Stokes equations describe the propagation of information at speeds comparable to that of the fluid flow (for fire, 10-20 m/s), but also at speeds comparable to that of sound waves (for still air, 300 m/s).

Decomposing the pressure into a “background” component, a hydrostatic component, and a flow-induced perturbation:

$$p = p_0 - \rho_\infty g z + \tilde{p} \quad \text{Equation 8}$$

For most applications, p_0 is constant and the other two components are relatively small, leading to the approximation of the equation of state Equation 7.

The pressure p in the state and energy equations is replaced by the background pressure p_0 .

3.5 Combustion Model

In an LES calculation where the grid is not fine enough to resolve the diffusion of fuel and oxygen, a mixture fraction-based combustion model is used. The mixture fraction is defined as the fraction of gas that originated as fuel. The model assumes that combustion is mixing-controlled, and that the reaction of fuel and oxygen is infinitely fast. The mass fractions of all of the major reactants and products can be derived from the mixture fraction by means of “state relations,” empirical expressions arrived at by a combination of simplified analysis and measurement.

The state relation for the oxygen mass fraction provides the information needed to calculate the local oxygen mass consumption rate. Classical laminar diffusion flame theory and the requirement that fuel and oxygen simultaneously vanish when reacting leads to a “flame sheet” model. The local heat release rate assumes that the heat release rate is directly proportional to the oxygen consumption rate (at the flame surface), independent of the fuel involved.

The mixture fraction is defined as:

$$Z = \frac{sY_F - (Y_O - Y_O^\infty)}{sY_F^I + Y_O^\infty} \quad ; \quad s = \frac{\nu_O M_O}{\nu_F M_F} \quad \text{Equation 9}$$

Z varies from Z = 1 in a region containing only fuel to Z = 0 where the oxygen mass fraction is ambient value, Y_O^∞ . An ideal reaction of hydrocarbon fuel is used to derive the state relations.

A non-dimensional value D^* is the characteristic fire diameter, a measures how well the fire is resolved. For coarse grids an adjustment is made to smooth the energy release across the fire. The fires modelled in this paper have used multiple grids to ensure resolution around the fire is ample and the adjustment would not occur.

3.6 Radiation Transport

Radiative heat transfer is included in the model via the solution of the radiation transport equation for a non-scattering gray gas. Soot is the most important combustion product controlling the thermal radiation from the fire and hot smoke, closely followed by CO₂ and water.

In optically thin flames, where the amount of soot is small compared to the amount of CO₂ and water, the gray gas assumption may produce significant over-predictions of the emitted radiation. This may well be the case in the modelling of the methylated spirit fires, which burn very cleanly (FDS Database SOOT_YIELD=0.0).

In calculations of limited spatial resolution, the source term, I_b , in the RTE requires special treatment in the neighborhood of the flame sheet because the temperatures are averaged over a grid cell. The fire resolution in this work is expected to be fine enough to use the ideal value.

The equation is solved using a technique similar to finite volume methods for convective transport, thus the name Finite Volume Method (FVM).

Water droplets can absorb thermal radiation, important in cases involving sprinklers. The absorption coefficients are based on Mie theory. No sprinklers are modelled in this work, so this aspect of FDS will not influence the outcome.

3.7 Geometry

Input file for FDS requires the prescription of rectangular obstructions that are forced by the software to conform with the underlying grid. More than one rectangular mesh can be proscribed in a calculation, aka “Multiple Meshes”. This is usually done, as in this study, to handle cases where the domain is not easily embedded within a single mesh.

3.8 Boundary Conditions

All solid surfaces are assigned thermal boundary conditions. Where necessary, information about the burning behavior of the material is also included. In this study the only burning is the methylated spirit. Material properties can be drawn from the database provided. Heat and mass transfer to and from solid surfaces is handled with empirical correlations, the convective heat flux to the surface is obtained from a combination of natural and forced convection correlations. The characteristic length, L , is taken to be 1m for most calculations.

3.9 Other features.

FDS also has correlations to enable simulation of charring fuels, liquid fuels, thermoplastic fuels, activation of and suppression by sprinklers, and smoke detectors. As these are not used in this study these features will no longer be discussed.

3.10 Limitations

The FDS software numerically solves a form of the Navier-Stokes equations appropriate for low-speed, thermally driven flow with an emphasis on smoke and heat transport from fires. FDS cannot be used for high-speed flows, shock waves such as engine combustion, or pressurized jet fires where other CFD codes can be used. This is a limitation, but is also a benefit as the resources saved in not modelling these aspects have been turned to enhancing other features.

The elimination of compressible flows and high speeds (greater than the speed of sound) enables several assumptions and a simplification to the equation of state.

This limits the calculation method so that it is not appropriate for tightly sealed enclosures and fires at altitude. This is not a problem for this study and is a reason why reasonable openings to the outside must be provided in all FDS domains, otherwise the calculation can become unstable.

The treatment of momentum means that the vorticity generated in the fire itself is not resolved as the fire is generally not well enough resolved. However, the vorticity in the plume above the fire due to mixing with ambient air dominates.

The grid in FDS must be rectilinear which limits the modelling of curved and angled structures. FDS does have a sawtooth function which smoothes the effects on the flow field by to prevent vorticity from being generated at sharp corners, and limits extra drag at sharp corners. This is not a complete solution. This study has all right angle and straight line geometry and the sawtooth function is not implemented.

The solver has two modes of operation – a gray gas model (default) and a wide band model. The default mode of grey gas lumps the spectral dependence into one absorption coefficient and assumes a non-scattering gas. The wide band model can be used to calculate the spectral dependence lumped into up to ten bands.

Leakage can be modelled from a building, however this is only possible if three criteria are met: First, the boundary of the computational domain must coincide with the exterior walls of the compartment. Second, there must be no OPEN (passive) vents to the exterior. Third, only one mesh must be used. Specifying building leakage would have been useful in this project, however the domain did not satisfy the second and third criteria.

Treatment of liquid fuels – see Section 3.12.1.1 and section 5.7.3 of user guide (41).

FDS is demonstrated to predict thermal conditions resulting from a fire in an enclosure within 5% to 20 % of experimental measurements (See Section 3.11).

3.11 Model Sensitivity

All computational techniques are susceptible to changes in input parameters. A sensitivity analysis considers the extent to which uncertainty in model inputs influences model output. FDS solves the fundamental conservation equations, and is much less susceptible to errors resulting from input parameters that stray beyond the limits of simpler

empirical models. The programmers have not put any limitations on the inputs (unlike many zone models that limit inputs to validated values) because applications often push beyond the range for which the model has been validated.

The user must be responsible for the prescription of all parameters. The grid size is the most important numerical parameter in the model, as it dictates the spatial and temporal accuracy of the discretized partial differential equations. The heat release rate is the most important physical parameter, as it is the source term in the energy equation. Both of these items are subjected to a sensitivity study in Section 5. Property data, like the thermal conductivity, density, ought to be assessed in terms of their influence on the heat release rate. Validation studies (see Section 3.12) have shown that FDS predicts well the transport of heat and smoke when the HRR is properly prescribed.

3.12 Validation and verification

For any model to be applicable to real life scenarios there must be a means of calibration, to ensure that the degree of difference between measured and predicted quantities results are within acceptable limits of uncertainty. FDS is now up to version 4, and there have been many years of development, starting with the formulation of the low Mach number form of the Navier-Stokes equations and the development of the basic numerical algorithm. The complex nature of fire creates the daunting task of confirming the accuracy of the FDS model. The actual process of model validation attempts to simulate a controlled experiment and analyze the difference between the predicted and experimental results (41). The input parameters, mathematical formulation, and interpretation of the results are all areas that require evaluation. Experiments must be simplified and well controlled otherwise it is difficult to locate specific errors associated with the assessment of the model. Most fire experiments, however, are not meant to validate FDS models but are devised for other purposes (41). This is indeed the case for most hot smoke test that are designed for fire safety system commissioning and approval.

The efforts to validate FDS have come from comparisons with full-scale tests for specific evaluation, previously released publications, with standard tests, with documented fire experiences and with engineering correlations. Collectively, these attempts provide useful calibration of the model. Formal methods of confirming accuracy are expensive and

time consuming. Early attempts at calibration involved salt water plume experiments (7), and fire plumes (7). FDS was compared to Steckler's highly instrumented room fire test (39). Large fire experiments were performed by NIST at the FRI test facility in Japan, and at US Naval aircraft hangars in Hawaii and Iceland (16). Room airflow applications were considered by Emmerich and McGrattan (18;19). This report falls into the category somewhere between a standard test and a document fire experience.

Since the World Trade Center catastrophe however, many official tests were conducted to validate FDS (23). Calculations performed before the experiments were given to the researchers conducting the tests so that comparison with the measurements could take place immediately upon completion. Known as blind predictions, these calculations are used to ensure the predictions are not reverse engineered. To improve the accuracy of the predictions, the measured and predicted gas temperatures of the upper layer were compared for each test.

...An analysis was performed to assess how sensitive the measured temperatures were to changes in the HRR... the 5 % uncertainty in the HRR corresponds to a $2/3 \times 5 \% = 3.3 \%$ uncertainty in the temperature rise. For upper layer temperatures of approximately 600°C C, this translates to roughly 20°C. The difference in measured and predicted upper layer temperatures ranged from 5°C to 20°C meaning that the predictions were within the uncertainty range of the HRR. (41).

FDS was applied to a series of benchmark fire tests performed as part of the "International Collaborative Project to Evaluate Fire Models for Nuclear Power Plant Applications" (17). Benchmark Exercise #2 was analysed by Floyd (20;22). The FDS model predicted the layer height and temperature of the space to within 10 % of the experimental values.

3.12.1.1 Verification of model aspects relevant to HST

Colt International and the Building Research Establishment (BRE) carried out a series of tests in a simulated car park to demonstrate the effectiveness of smoke control using impulse fans (10;12). A further objective of the tests was to prove the effectiveness of CFD in predicting the spread of smoke in a car park fitted with impulse fans . They found that the

conditions during the tests were very similar to those predicted by the computational fluid dynamics (CFD) modelling approach as used by Colt for system design. The test rig, set up in a simulated car park at a Middlesborough test facility, was 35m x 30m x 3m. The two opposing ends of the rig were open, but protected as far as possible from wind effects, and ventilation was provided by two Colt Cyclone 100 fans running at 80% full speed (64% thrust). These were located to limit the smoke to one side of the test rig, keeping the other side substantially free of smoke. A car shell containing a tray of diesel fuel was ignited to create a 1MW fire size.

Test were also carried in an existing underground car park in Bristol to assess the ability of systems to clear a smoke logged car park (11). The car park was smoke logged by operating 4 smoke generators for a period of 4 minutes. Smoke distribution was aided by entraining the smoke into the airstream of 4 portable propane heaters.

Pool fires

Several authors have published works on comparison of FDS prediction relating to pool fires experimental results. FDS was (61) used to model a 1 m diameter methane pool fire in a computational domain 2 m by 2 m by 4 m with a uniform grid size of 2.5 cm. The predicted results were compared to experimental data and found to qualitatively and quantitatively reproduce the velocity field.

Work by VTT and NIST (29) on FDS modelling of methanol fires concluded

The prediction of liquid pool burning rate, starting for first principles, is an extremely challenging task. Individual numerical and physical errors are difficult to separate due to the strong coupling between the pool burning rate, gas phase heat release, gas temperatures and gas to solid heat transfer. Further validation should be carried out by trying to separate different sources of errors.

The predicted burning rate was lower for the smallest pool (10mm) and 37 to 100% too high for the 100, 300 and 1000mm fires. The errors were larger than the uncertainty of the experiment and therefore significant. Due to the over estimation of the burning rate for the three larger pools the plume temperatures were also over estimated in the simulations. The study repeated the simulation using a fixed burning rate of 14 g/m²/s, which resulted in a better agreement with the measure flame temperature profiles. The difficulties in modelling

liquid pool burning rates have resulted in this study prescribing a fixed burning rate by setting the HRRPUA.

FDS simulation of several materials and scenarios include modelling of heptane pool fires (28). The aim of the study was to establish the prerequisites for modelling of a pool fire on the basis of heat transfer mechanisms only. The results obtained with FDS showed the dependence of the burning rate on the heptane pool fire diameter, and reproduced the data well. The concluded prerequisite was at least 20 computation grid cells within the diameter of the pool.

The cell numbers needed to define a fire (28) suggest roughly twice as fine a grid is required for reliable prediction of burning rates of liquid fuels to predict velocities and temperatures. The reason for this is the prediction of the heat feedback to the burning surface necessary to predict rather than to prescribe the burning rate.

4 METHODOLOGY

The methodology for this thesis can be set out in the following steps.

1. Calibrate FDS for the prediction of one pool tray fire plume. This work is described in Section 5 by modelling a single A3 tray.
2. Calibrate FDS qualitatively for a hot smoke tests in a simple geometry. This work is described in Section 6 by modelling a hot smoke test in a cinema auditorium.
3. Calibrate FDS qualitatively for a hot smoke tests in a complex geometry. This work is described in Section 8 by modelling a hot smoke test in an airport concourse.
4. Conduct a study of scaling work in the cinema auditorium as described in Section 7.

5 FDS CALCULATIONS OF THE PLUME

The first stage of this investigation is to assess the ability of FDS to simulate the engine of the test method, namely the methylated spirit fire and plume. FDS calculations were carried out to verify that the plume profile and temperatures of a methylated spirit fire could be predicted by FDS. The conclusions were then applied to the modelling of a hot smoke test in building spaces.

5.1 Single tray fire correlation

The first step in the modelling process was to use FDS to predict a single A3 methylated spirit tray fire. The results were compared to the temperature profiles in AS 4391 – 1999 Appendix A. The basis of the temperatures in the Appendix of the standard was many tests carried out in the development of the standard. The reports of the development test have not been published and are therefore unavailable for comment, however indication from an author (34) of the standard involved with the testing indicated that the temperatures measured were consistent over many tests in still air. The results of the FDS modelling demonstrated that FDS provided a reasonable prediction of the average plume temperatures (Refer Figure 4). A sensitivity study was carried out to assess the impact of three parameters: radiant heat fraction, grid size and the heat release rate per unit area (HRRPUA). The sensitivity to the grid size and the solver were also investigated.

5.1.1 Sensitivity to radiant fraction and Heat Release Rate per unit area

The value of the radiant fraction was varied from the default value in the FDS database of 0.0 to 0.20. The calculated results were not sensitive to the value selected as shown in Figure 4. The most appropriate value from literature was concluded to be 0.15 (58). The input value of the HRRPUA was varied from 471kW/m² (56) to 377 kW/m². The heat output per unit area is calculated from literature sources and graphed in the Appendix of AS 4391 (See

Figure 3). The calculated values were fairly insensitive, as expected, (see Figure 5) and improved the plume temperature profile as shown in Figure 4.

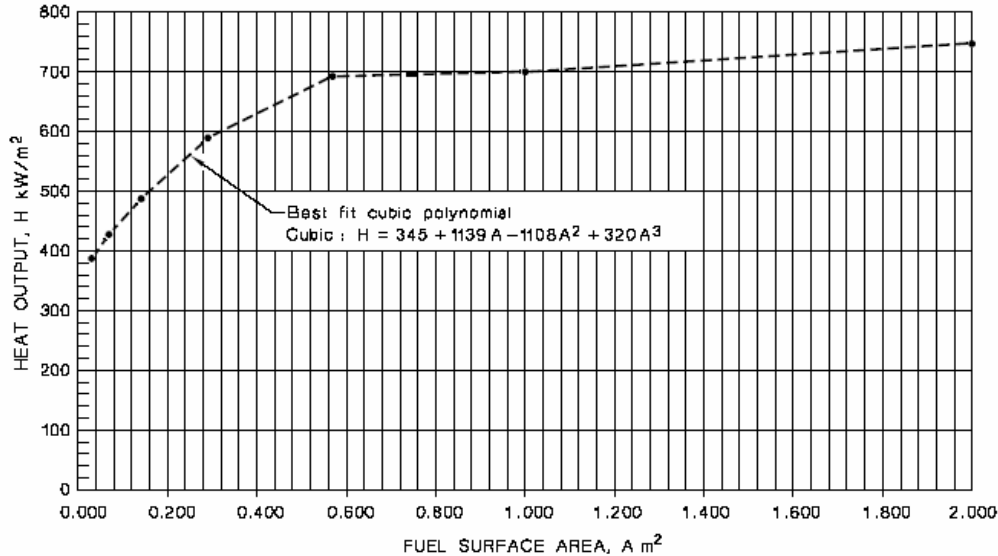


FIGURE D1 TOTAL HEAT OUTPUT

Figure 3 Heat output for methylated spirit from AS 4391.

5.1.2 Sensitivity to grid resolution

The plume temperature profile showed sensitivity to the grid size and the solver. FDS has two solvers that may be selected: the Large Eddy Simulation (LES) or the Direct Numerical Simulation (DNS). As expected, the DNS solver provide better correlation of temperatures near the fire, however a large number of cells are required leading to long calculation times. The cell sizes for the DNS modelling were 0.037 x 0.035 x 0.007 m, which is on the larger size for DNS calculations (37). The LES solver provided good agreement at distances of 4m from the plume, however it over-estimated the plume temperature close to the fire (Refer Figure 6). A cell size of 40mm around the plume was required to get the temperature calculation to within 30% at 4m from the fire.

The runs carried out and the change in parameters are listed in Table 2.

Table 2. Sensitivity analysis of methylated spirit pool fire.

Run ID	Number of cells (thousands)	Radiant fraction	HRRPUA	Solver
methoplume4	111	5%	471	LES
methoplume5	111	15%	471	LES
methoplume6	885	15%	471	LES
methoplume7	111	10%	471	LES
methoplume8	885	20%	471	LES
methoplume9	885	5%	471	LES
methoplume10	1327	15%	471	LES
methoplume11	111	10%	471	LES
methoplume12	111	20%	471	LES
methoplume13	111	15%	447	LES
methoplume14	111	15%	424	LES
methoplume15	111	15%	400	LES
methoplume16	111	15%	377	LES
methoplume17	111	15%	236	LES
methoplume18	1327	15%	471	DNS
methoplume19	1673	15%	471	DNS

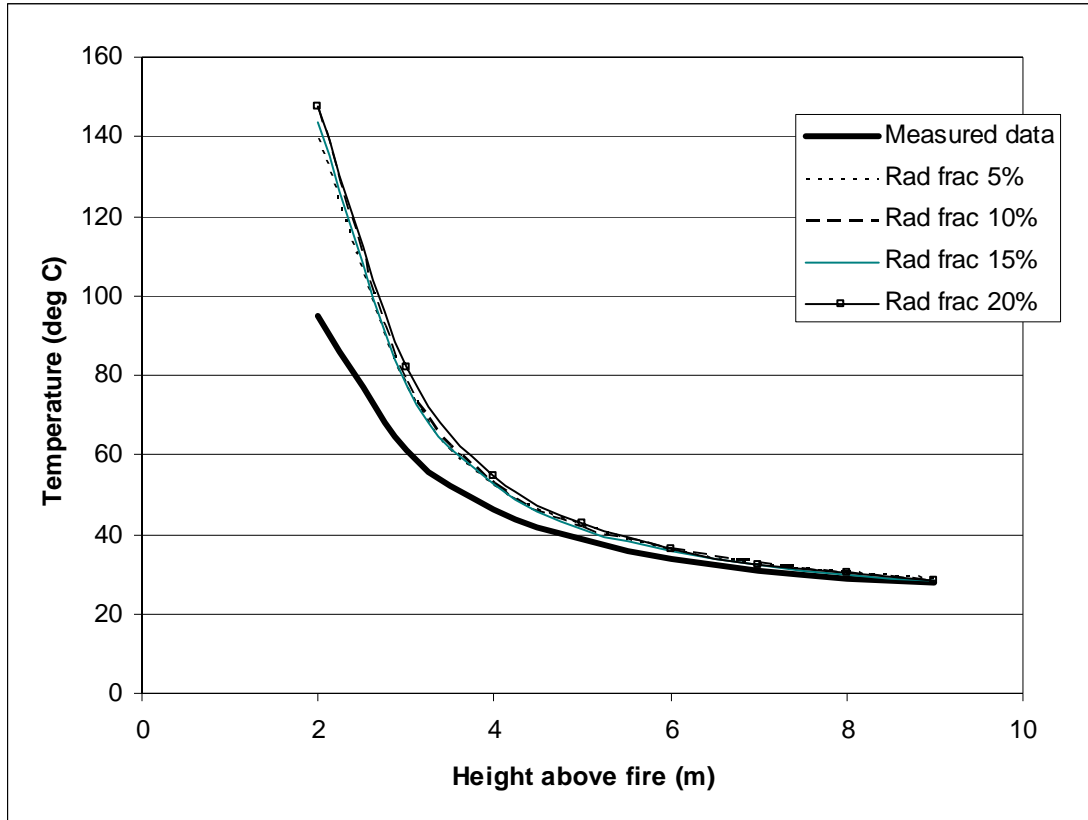


Figure 4. Variation in plume temperature calculations due to radiative fraction.

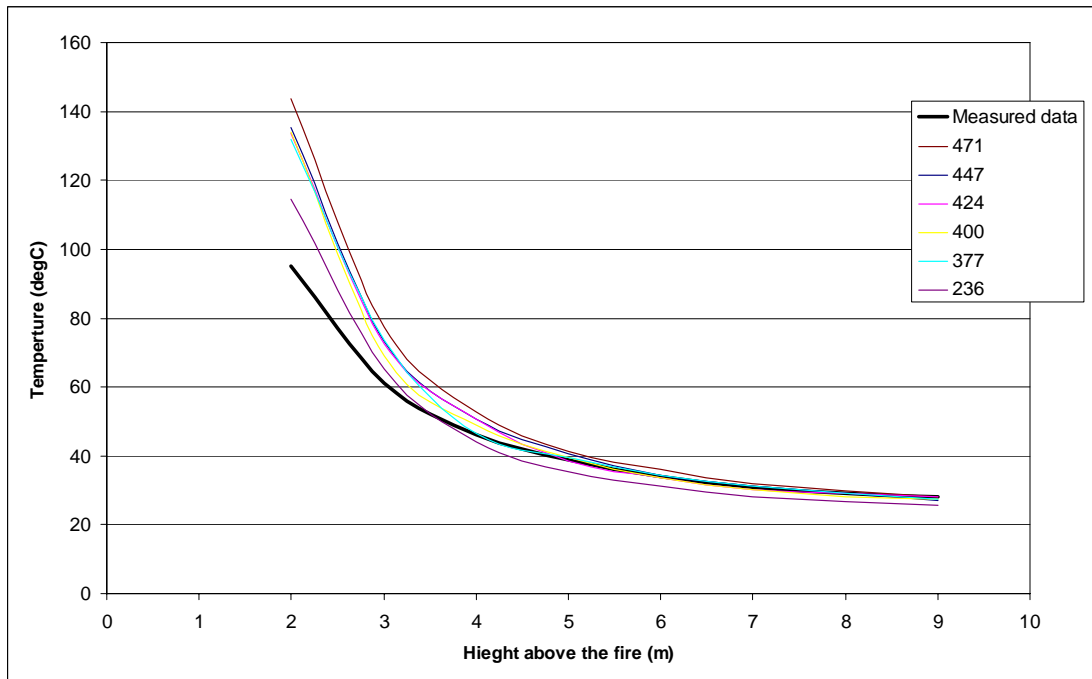


Figure 5 Variation in plume temperature calculations as a function of HRRPUA.

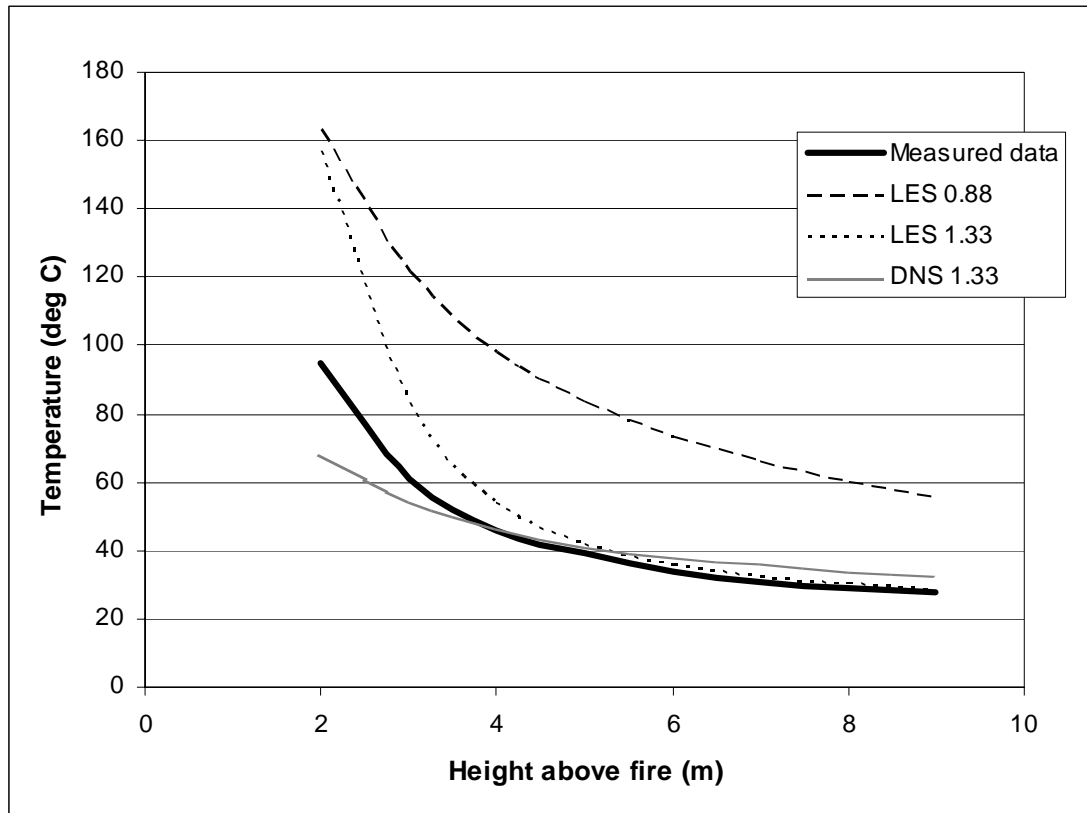


Figure 6. Variation in plume temperature calculations due to solver and number of cells (number in the legend denotes millions of cells).

A sensitivity analysis of the soot yield was carried out by changing the value until a reasonable match of the visibility output was observed when compared with the observations and video footage. The most appropriate fuel input data for FDS concluded from the sensitivity analysis and applied throughout the modelling of hot smoke tests was:

&REAC ID='METHANOL'	Parameter to define a fuel type
FYI='Methyl Alcohol, C H ₄ O'	Description of the fuel
MW_FUEL=32.	Molecular weight of the fuel
NU_O2=1.5	Ideal stoichiometric coefficients
NU_H2O=2.	for the reaction of a hydrocarbon
NU_CO2=1.	fuel.
EPUMO2=13290.	Energy Per Unit Mass Oxygen,
	kJ/kg
SOOT_YIELD=0.02,	The fraction of fuel mass converted into

RADIATIVE_FRACTION=0.15 /

HRRPUA=471.0

smoke particulate,
The fraction of energy released
from the flame as thermal radiation.
Heat Release Rate per Unit Area

5.1.3 Ethanol and Methanol

An error in the specification of the fuel was noted after the completion of all the modelling in the following sections. The author was informed that methylated spirit was 90% ethanol, not methanol. The two fuels are very similar in composition so instead of rerunning all the modelling a selected run was repeated using the input data for ethanol (ethyl alcohol). The input values for the two fuels are compared in Table 3.

Table 3. Comparison of Methanol and Ethanol FDS input values.

	Methyl Alcohol	Ethyl Alcohol
Chemical formula	C H ₄ O	C ₂ H ₆ O
MW_FUEL	32	46
NU_O2	1.5	3
NU_H2O	2	3
NU_CO2	1.	2
EPUMO2	13290.	12842
SOOT_YIELD	0.0	0.008
RADIATIVE_FRACTION	0.0	0.2

The computer run repeated was the run with ID “*methoplume8*”. This was rerun twice. *ethoplume8* used the input data listed in Table 3. *ethoplume81* was run with the input data listed in Table 3 however the SOOT_YIELD = 0.0. The results are graphed in Figure 7 which show the use of the incorrect fuel input values resulted in an increased prediction of temperature of about 6% at 2 above the fire. This correction of fuel input data improves the prediction slightly.

The most appropriate input data for any future modelling is therefore the data for ethanol and a soot yield value determined from a smoke meter located at the fire source.

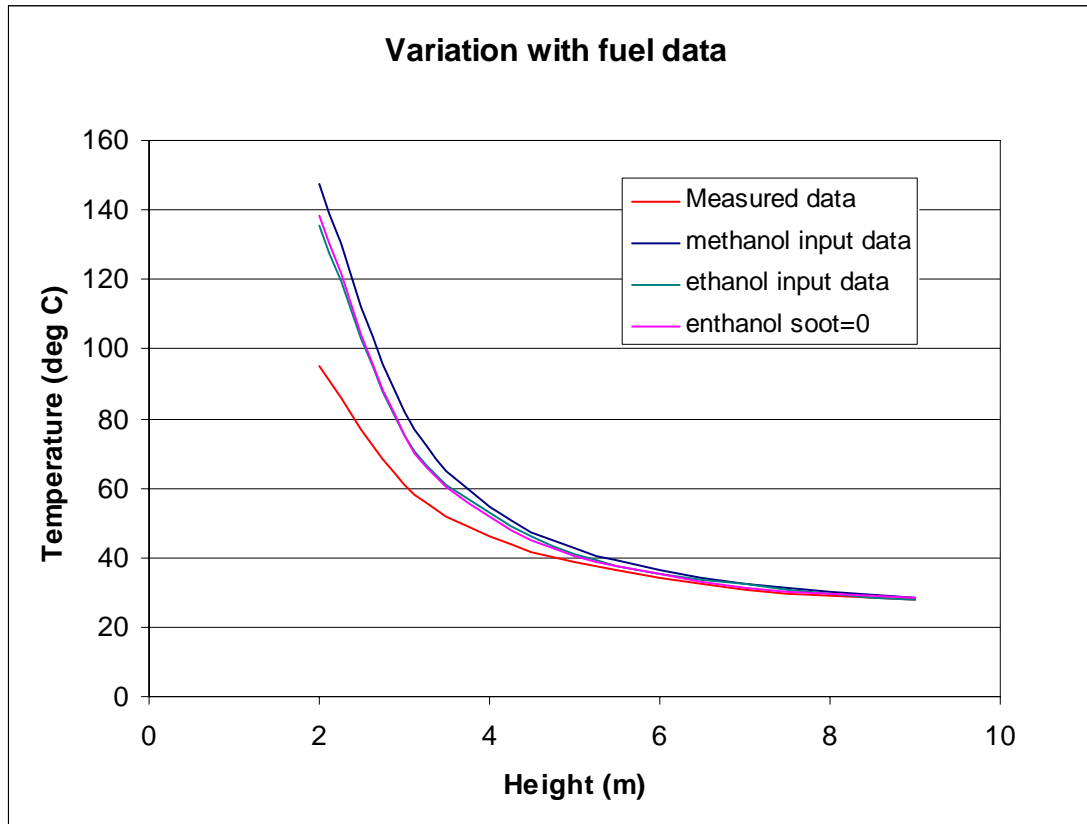


Figure 7. Variation in plume temperature calculations due to fuel input data.

6 HST IN A CINEMA AUDITORIUM

The cinema complex is located on the uppermost level of a multilevel shopping mall. There are individual cinemas connected to the main shopping centre atrium via the foyer. The auditoriums for each cinema are separate fire compartments, with the exception of the projection room's ports and metal duct penetrations, which don't have fire dampers. The smaller 280 seat auditorium was being refurbished and had an existing smoke exhaust located at the centre of the ceiling capable of extracting smoke at the rate of 20 m³/s. This design was not ideal, as the high flow rate through one grille created a potential plug flow situation. Unfortunately, modification of the exhaust point grille was not desirable, due to the implications on external roof profile, sound attenuation requirements, auditorium lining modifications etc.

Two exits are provided from each cinema auditorium. One of these exits connects the cinemas to the foyer and the other exits out of the cinema complex into the open car park of the shopping centre. Make-up air is provided through the two exits doors.

6.1 Testing and Commissioning

Four A3 trays spaced 1 m apart were used to simulate the design fire which was sufficient to provide an entrained smoke volume corresponding to 2.5 MW design fire. In accordance with the standard, the artificial smoke used for the tests was a glycol based fog, which was introduced into the centre of the fire plumes. Sufficient fuel was supplied to allow the test to run for at least ten minutes. For the purposes of assessing the tenability criteria the start of test is taken as the time at which the smoke production commences. The tests were recorded on video.

Temperatures were not recorded in the cinema. These fires were located between the front row of seats and the cinema screen. This represents the scenario that entrains the maximum

amount of smoke given that the distance from the fire to the ceiling is a maximum fire at this location.

The input value for the fuel that provides a reasonable correlation to the single plume was used in the FDS modelling of the cinema hot smoke test. The graphic of the auditorium configuration and test fire set up is shown in Figure 8. The four trays of liquid fuel are seen bottom left. Two mesh sizes were used: a coarse mesh for the majority of the space and a finer mesh around the fires.

The results of the modelling are presented as plots of visibility along the long axis of the room. Figure 9 shows a temperature “slice” at 100 seconds and Figure 10 at 300 seconds. The smoke filling can be seen with the plume filling towards the back of the room, where the raked seating rises up near the ceiling. These were compared with the video of the hot smoke test at various times and the observed results described below. Several runs were performed; only one run has been plotted.

A case with no external wind effects was assessed. External wind effects were modelled to assess a wind of 2.5m/s entering the exit connecting to the car park. This was estimated to represent the wind on the day of the test, however there was little difference in the two cases, as the air velocity through the exit was similar in both cases.

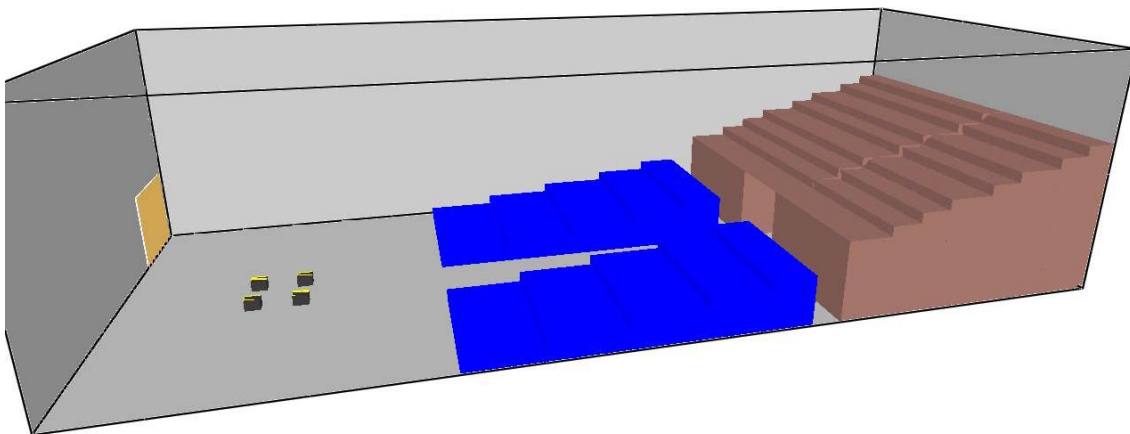


Figure 8. Small auditorium FDS model .

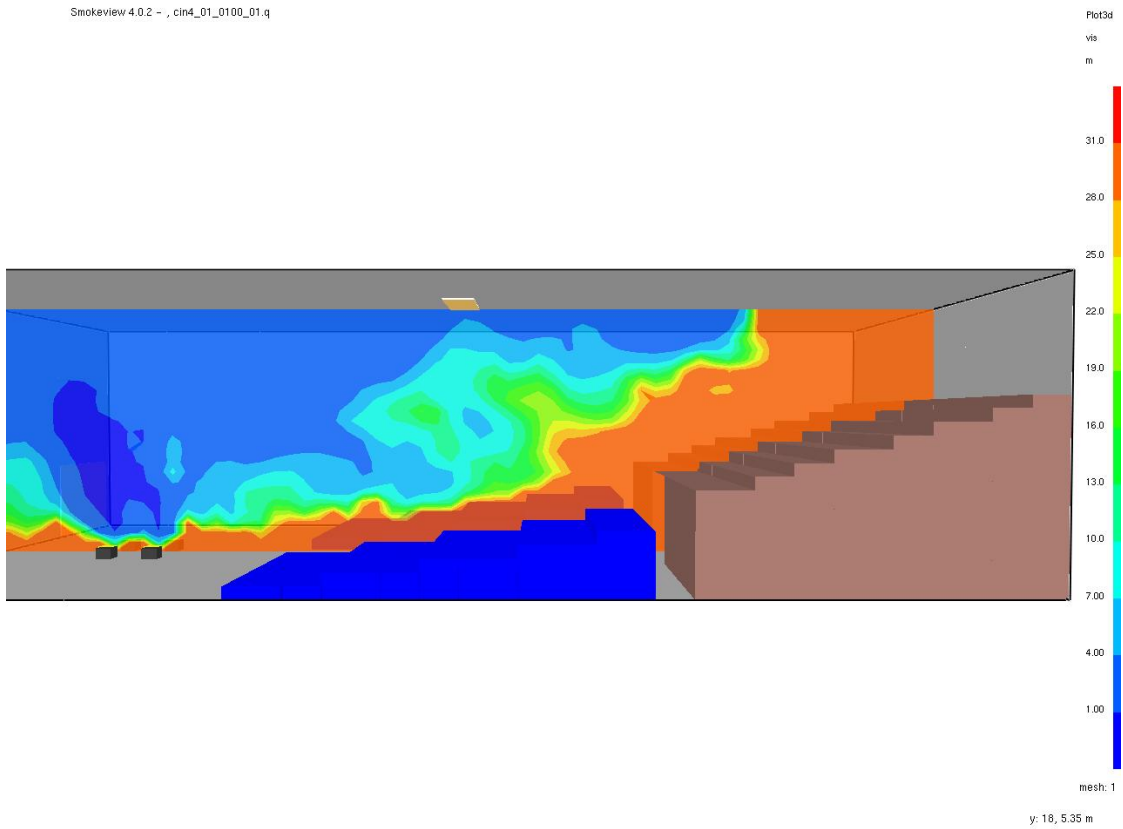


Figure 9. Small auditorium FDS model results - visibility slice at 100 seconds.

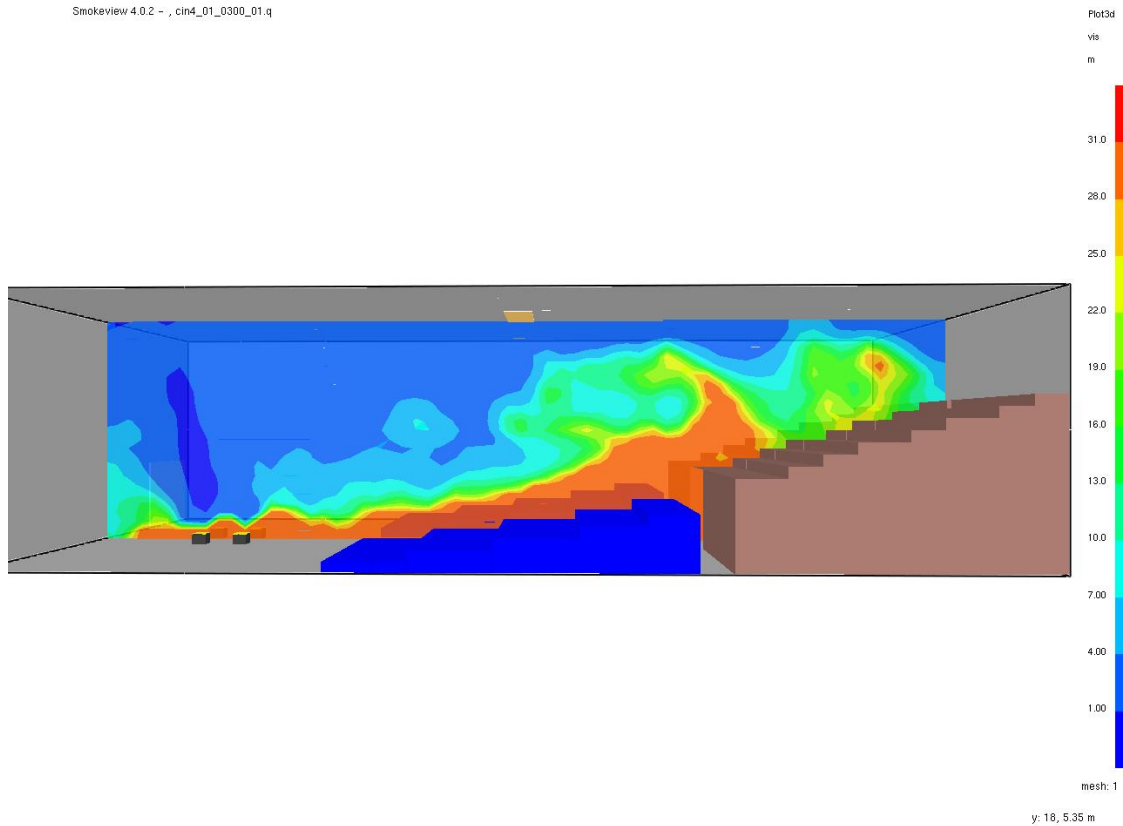


Figure 10. Small auditorium FDS model results - visibility slice at 300 seconds.

6.2 Observations

Table 4 provides a summary of the observations during the test as noted by the CSIRO observer and from video footage.

Table 4. Hot smoke test event times and comments.

Time from commencement of smoke	Comments
Min:sec	
0:00	Ignition of the fuel in the trays.
0:10	Generation of smoke commenced.
0:30	Smoke reaches the ceiling above the fires.
0:45	Alarm sounds and some visible smoke spill into the rear of the cinema. The front exit doors open to simulate escape of the first occupants from the cinema. The exhaust starts operating and draws smoke in the central part of cinema out of the enclosure.

1:00	Alarm sounds
1:30	The smoke starts to descend in the rear section of the cinema. All exit signs are clear of smoke and visible. The egress routes from the rear and front sections of the cinema are clear of smoke.
2:00	Smoke layer descends to approximately 2m height from floor level in the back section (approximately 3 rows of seating). Some smoke has started to diffuse into the rear section of the cinema.
3:00	The smoke diffuses into the egress paths at the rear of cinema but the path with emergency lighting is clear of smoke, being at a lower height.
4:00	The exit signs at the front and at the centre of cinema are clear of smoke, being approximately 3m below ceiling level. The foyer is clear of smoke. The front area of the cinema has very little smoke at or below the head height.
5:00	Significant amount of smoke has diffused into the rear section of the cinema. Egress routes from the front and the central section of cinema are clear of smoke.
6:00	The cinema foyer is still clear of smoke. The exhaust is observed to draw significant amount of smoke. However, there is little change in the level of smoke logging in the rear section of the cinema.
7:00	The conditions are tenable in the front section of the cinema. There is significant amount of smoke logging in the rear of the cinema.
8:00	No significant change in the smoke distribution throughout the cinema.
10:00	Test completed.

The wind on the day of the test made comparison with the modelled data difficult. The smoke test verified the operation of the smoke detection and smoke handling systems to assist in commissioning within a building. The smoke produced during the test was contained within the cinema and did not migrate to the foyer or to the other cinemas. All fire safety systems in the cinema operated satisfactorily as designed. The observations during the tests show that smoke detection and handling systems operated satisfactorily and tenable conditions were maintained during the time required for occupant evacuation.

It was observed that some movement of smoke occurred towards the rear part of the cinema after the first two minutes of the test and significant smoke logging was observed during the later part of the test.

6.3 Comparison between FDS and test observations

The comparison between the FDS model and the test observation is qualitative only; no physical measurements were made during the test. The FDS predicted the smoke movement acceptably well. The plume shape and tilting, smoke layer nose progression across the ceiling, smoke layer shape and clear air layer all match the observed results well. As discussed in the section above addressing input parameter, the soot yield used as input to FDS was estimated based on the smoke generator fuel mass loss rate and typical fuel data properties for polyurethane and wood. A sensitivity analysis was performed by changing the soot yield value until a reasonable match was observed between the computed plots of visibility and the observed test results.

7 SCALING

The tray selection process for the tests discussed above was done according to the test standard AS 4391. Since this test an alternative method of specifying the test configuration has been investigated. A recent paper by Morgan discussing the setting up of hot smoke tests based on scaling relationships (43) was applied to the small cinema auditorium test. Morgan concluded that a hot smoke test not based on scaling can give potentially misleading results when assessed on parameters such as smoke layer depth.

Scaling laws use fundamental relationships to extrapolate from one condition to another. This can be applied to SCS and hot smoke tests to ensure a hot smoke test fire is designed to simulate the design appropriately.

Assuming the design fire for the auditorium consisted of convective heat release rate of $Q_1=2500\text{kW}$, fire perimeter $P_1=8.8\text{m}$, and an initial clear height of 7.0m , then the hot smoke

test parameters of number and size of trays can be calculated using the dimensional analysis approach as shown in Figure 11.

Parameter analysis		
Inputs		
HRR	Q_1	2500 kW
Fire Perimeter	P_1	5 m
Clear height to ceiling	Y_1	7 m
Entrainment constant	C_e	$0.21 \text{ kgs}^{-1}\text{m}^{-3/2}$
Max Temperature at ceiling	θ_2	30 degC
ambient temp	T_{amb}	20 degC
HRR methyl alcohol		700 kW/m ²
Tray type	A2	
Tray area		0.25 m ²
Tray perimeter		1.434 m
Tray HRR		140 kW
Calculated values		
Area of fire	A_2	1.5625 m ²
	$3Af^{0.5}$	3.75
Mass flow rate	M	19.4 kgs ⁻¹
Temp above ambient	θ_1	130 deg C
HRR test fire	Q_2	369 kW
Number of trays of type	A2	2.6
Test Fire Perimeter	P2	3 m
Number of trays of type	A2	2.2
Spacing of trays		2.2
Subscripts		
Design fire		1
Smoke test		2

Figure 11. Calculation of hot smoke test parameters

The calculation concludes that with two A2 and one A3 trays arranged in the well-dispersed “footprint” of the design fire, the layer depths observed in the test should correspond to those specified in the design. An anomaly between the calculation method and AS4391 is the temperature at the ceiling. The calculated temperatures at the ceiling using Morgan’s method (See Figure 11) are lower than those specified in the Appendix A of the test Standard. Use of the Morgan relationship may underestimate the ceiling temperatures which may lead to activation of sprinklers. Alternatively FDS may be used to show that ceiling temperatures are not so low.

8 AIRPORT CONCOURSE INTRODUCTION

Five hot smoke tests were carried out at an airport terminal in accordance with the Australian Standard 4391 -1999 [1]. The tests were conducted between 1am and 5am Friday 27th of May 2005. The purpose of these hot smoke tests was to verify the operation of the smoke hazard management systems in the terminal as part of the commissioning process for building. These tests were the second phase of testing following tests carried out in September 2003.

8.1 Test Method

The tests were conducted in accordance with the Australian Standard AS 4391 - 1999. The test fire size was selected according to the ceiling height to ensure no damage.

The artificial smoke used for the tests was a glycol based fog produced by a “disco” smoke machine. The smoke was introduced into the centre of the fire plumes and directed toward the ceiling using a metal duct elbow.

The heat source was four A4 size trays positioned in water baths to cool the trays. Sufficient fuel was supplied to allow the test to run for at least 10 min. For the purposes of assessing the smoke conditions, the start of test is taken as the time at which the smoke production commences. The tests were recorded on video and still photography.

The test fires were located remote from smoke exhaust grilles, between sprinkler heads and smoke detectors. The test fires are chosen to ensure temperatures at ceiling were sufficiently low to ensure no damage occurred.

The EWIS system was disabled during the tests because members of the public were in the building during the test.

8.1.1 Instrumentation

Instrumentation was installed for *Tests 1* and *Test 2* in locations as shown in Figure 14. Smoke meters and thermocouples were installed at three locations. An anemometer was installed at one location.

The temperatures were monitored with type K, 2mm mineral insulated metal sheathed (MIMS) unearthed tip thermocouples 300mm down from the ceiling. The thermocouples were of a greater diameter than that suggested by the tests standard, 0.6mm.

The smoke obscuration was measured with smoke meters built at CSIRO. These meters had a path length of 1m, a red LED source, a photo detector receiver and were calibrated with neutral density filters (see Figure 12).

One video was recorded by a stationary camera located east of the fire.

A hot wire anemometer was installed at instrumentation station 2 near the fire, 1.5 from the floor. The Air Velocity Transducer was made by TSI, Model number 8475-075. The transducer was not directional so flow direction is taken from visual observations of smoke movement.

All instrumentation was logged at 5 second intervals using a Datataker 505 datalogger.

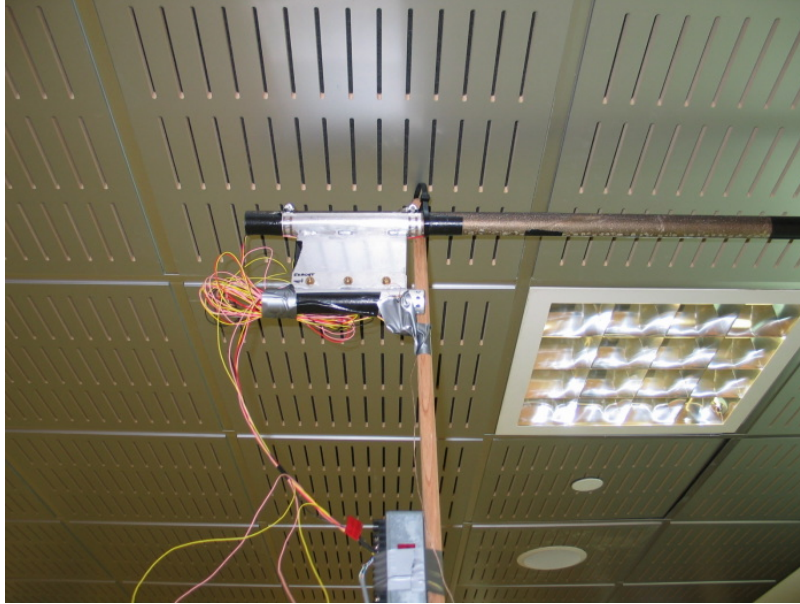


Figure 12. Smoke meter and thermocouple located 300mm from the ceiling.

8.2 Description of the test site

The tests were carried out in five locations within the terminal building, however only one test location is covered by this report as identified in Table 5 and in Figure 13.

Table 5 Test location and details

Test number	Location	Ceiling height	Test fire
1 and 2	ITB Departures Concourse	2.9	4 x A4

The test in the departures concourse was a repeat of a test carried out in September 2003.

The test site at the commencement of the tests is pictured in Figure 13. The photograph is taken from the east looking along the concourse to the test fire. Behind the test fire is a kiosk in the centre of the concourse and beyond that the concourse leads to the satellite and gate lounges.

A plan of the site is included as Figure 14. The plan shows the concourse running east -west. The satellite and gate lounges are located to the west (left of the page). The passport control and main terminal is located to the east (right) of the page. Small tenancy shops are located

along the concourse. During the test the majority of tenancies were closed with security doors closed as the test were carried out between 1am and 5am.

Gate 1 and gate 2 are located off the concourse to the east of the test fire. The entrance to gate lounge 1 is 12m east of the test fire location to the north of the concourse. Gate lounge 2's entrance is 20m east of the test fire location to the south of the concourse. A duty free store is located east of Gate lounge 1 and 2's entries.

The instrumentation locations were:

Instrumentation 1: 12 m east of the centerline of the test fire. 2m from the north wall of the concourse. This station was very close to the entry to gate lounge 1.

Instrumentation 2: 1 m west of the centerline of the test fire. 1.0m north of the test fire centre line. This station was very close to the test fire.

Instrumentation 3: 12 m west of the centerline of the test fire. 2m from the north wall of the concourse. This station was toward the satellite.

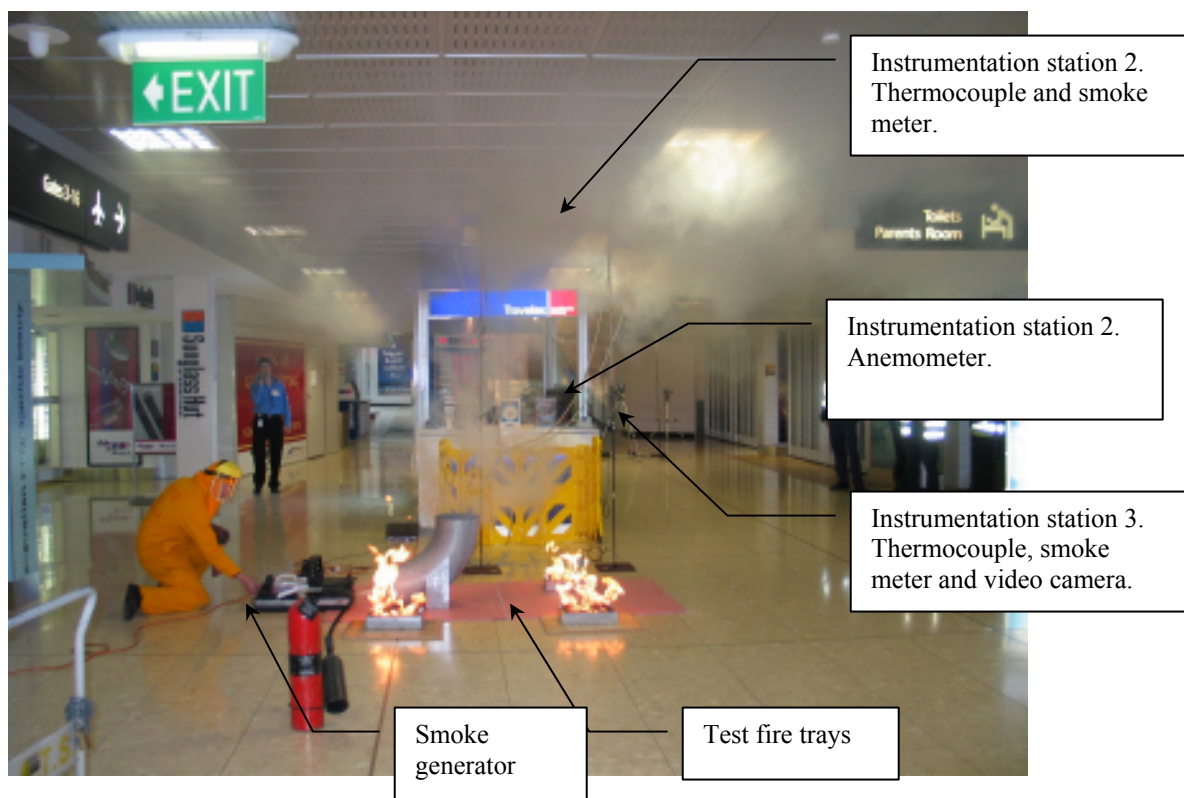


Figure 13 Test 1 and 2. Departures concourse

8.2.1 *Smoke exhaust locations*

The smoke hazard management systems in each smoke zone are described below and the detail of grille location is included in Figure 14.

The building area included four smoke zones.

Zone 1: Concourse

The concourse has three exhaust points in the ceiling; the test fire was located in the smoke zone in this area.

1. SEF 07: Centre concourse near terminal building 5,500l/s.
2. SEF 08: Centre concourse in duty free store 7,700l/s.
3. SEF 09: Centre concourse near satellite building 11,000l/s.

Each of the above points draw from horizontal ceiling grilles located near the centre of the concourse.

Zone 2: Gate 2.

1. SEF01: Gate lounge 2 ceiling 3,000l/s
2. SEF02: Gate lounge 2 ceiling 3,000l/s
3. SEF03: Gate lounge 2 ceiling 3,000l/s

Each of the smoke exhaust fans in zone 2 were ducted to draw from 2 grilles. A total of 6 grilles were located in the ceiling of Gate 2.

Zone 3: Gate 1

1. SEF04: Gate lounge 1 ceiling 3,000l/s
2. SEF05: Gate lounge 1 ceiling 3,000l/s
3. SEF06: Gate lounge 1 ceiling 3,000l/s

Each of the smoke exhaust fans in zone 3 were ducted to draw from 2 grilles. A total of 6 grilles were located in the ceiling of Gate 1.

Zone 4: Satellite

The smoke exhaust in the satellite was not included in this analysis or modelling.

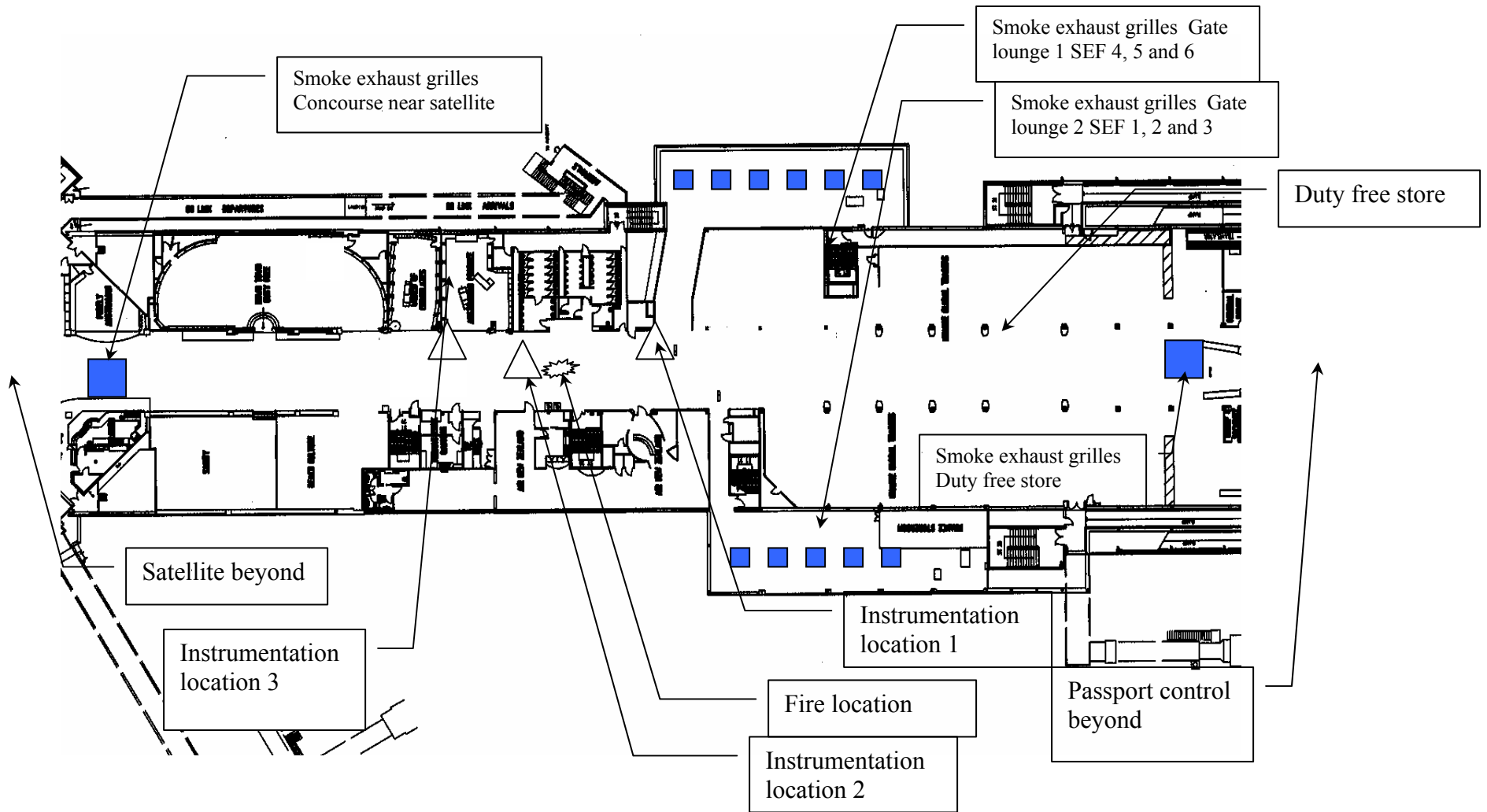


Figure 14 Location of test 1 and repeat showing instrumentation

8.3 Observations and discussion

The smoke filling and movement was recorded for each test. The timing of the activation of the smoke exhaust operation was also noted.

The air flow rate was noticeable at some grilles, however the smoke exhaust in some zones did not operate when expected. The smoke exhaust system of the Departures Concourse did not operate during the first test.

The test in the International Departures concourse is a repeat of the hot smoke test carried out in Phase I in September 2003, described in CSIRO report CMIT(C)-2003-199 titled “Hot smoke test in the airport terminal.”

Two tests were carried out in the international departures concourse. In Test 1 upon fire detection:

- The smoke exhaust did not automatically operate, and
- the HVAC system did not shut down.

CSIRO was informed that this was due to an override switch locking out the systems.

A repeat test was then performed with the override switch in the automatic position and the systems performed as required, namely:

- The smoke exhaust did automatically operate, and
- the HVAC system did shut down.

8.3.1 Test 1 –Departures Concourse

8.3.1.1 Observations Test 1

Table 6. Test 1: Hot smoke test event- times and comments.

Time from commencement of smoke		Comments
Minutes:seconds	seconds	
		Air movement is from the main building toward the satellite measured at the centre of the cross section of the concourse at 0.4 m/s. Air was noticeable moving from gate lounge 1 and 2 into the concourse.
-0:10	-10	Ignition of the trays.
0:00	0	Generation of smoke commenced.
0:20	20	Plume tilted so that the top of instrument location 1 is in the plume. Smoke layer reaches 16m from test fire west.
0:40	40	Smoke reaches slope section of the concourse 26m from fire
0:47	47	Smoke detection registered at the FIP but smoke exhaust does not activate and HVAC still operational.
0:51	51	Smoke 34m from fire west down concourse.
1:30	90	Smoke below smoke baffle (48m from fire) and moves into the satellite zone.
2:00	120	Smoke 64m from fire and 16m into satellite
2:45	165	Smoke layer diffuse and to the floor at the satellite/concourse boundary
4:00	240	Smoke reaches into satellite 90 m from fire. Smoke 8m east of fire. No smoke near gate 1 and 2.
4:40	280	Smoke exhaust fans SEF 7, 8 and 9 manually activated. HVAC still operating
4:53	297	Smoke reaches into satellite 100 m from fire.
6:00	360	Smoke exhaust fans in satellite running. Activation not known.
7:00	420	Smoke layer height 1.8m at 12m from fire west.
8:00	480	Smoke is above fire and to the west. No smoke east of fire.
9:15	555	Smoke in west end of concourse clearing slightly but diffuse smoke to floor level.
11:00	660	Test ended.
11:30	690	Building systems shut down and reset.

8.3.1.2 Discussion of visual observations Test 1

The air velocity at the start of the test, due to the building air conditioning systems and external wind conditions, caused air to flow east to west along the corridor at a velocity of 0.4m/s.

Smoke production from the smoke machine was not steady as is typical when tests are carried out with CSIRO's machine. A rented machine was used in these tests: Smoke production ran for approximately 20 seconds and then production stopped for 2 to 5 seconds before quickly ramping up to full production again. This made the data analysis more difficult as average and assumptions implemented as modelling the cycle was not done.

Initially the plume tilted to the west, the smoke layer flowed along the concourse away from the fire towards the satellite due to the air movement induced by the HVAC systems. The plume tilt touched the top of the nearest instrument station. The plume smoke was at some points directly moving through the smoke meter beam near the ceiling. However, it appeared that the plume did not flow directly onto the anemometer, which was located 1.5m from the floor. Upon activation of the fire detection system the airflow did not change, as the smoke exhaust did not operate and the HVAC systems did not shut down. CSIRO were informed that this was due to an override switch in a lower level control being switched on.

Smoke flowed under the smoke baffles separating the concourse from the satellite, activating the exhaust in the satellite smoke zone. As a result, high air volumes were drawn into the satellite, disturbing the smoke layer. This was ineffective smoke exhaust because the smoke was not contained in the smoke zone of origin and caused smoke logging in the satellite area.

The manual activation of the smoke exhaust near the end of the test drew some smoke from the concourse and less smoke flowed towards the satellite. The HVAC systems were not shut down; the satellite smoke exhaust was still operational and so there was still airflow from the east to west along the concourse.

8.3.1.3 Results Test 1

The results of instrumentation for the test are illustrated in Figure 15 to Figure 37.

For the duration of the test the smoke plume tilted toward the west.

8.3.1.3.1 Results for location 1 - Test 1.

Location 1 is 12 m east of the test fire. The location of the instrumentation in regard to the test fire can be seen in Figure 17. The air movement from east to west kept smoke away from instrumentation station 1. The air movement prevented any back layering until near the end of the test. After the test shut down, the reset of the systems allowed some smoke to move to the station.

The smoke obscuration was very low, (Figure 15) as was the temperature rise (Figure 16) during the test. The prevention of the back layering can be seen in Figure 18, where the smoke layer was clearly held 2m from the instrumentation station for the duration of the test. The obscuration is a gradual trend upward during the test with a more noticeable increase, but still low obscuration, toward the end of the test and post test (>660s).

The average temperature prior to the test is 24 °C, which does not change during the test. Late and post test there is some temperature variation, but no noticeable temperature rise.

The prevention of back layering and critical velocity could be assessed based on calculation techniques used in tunnel design (4).

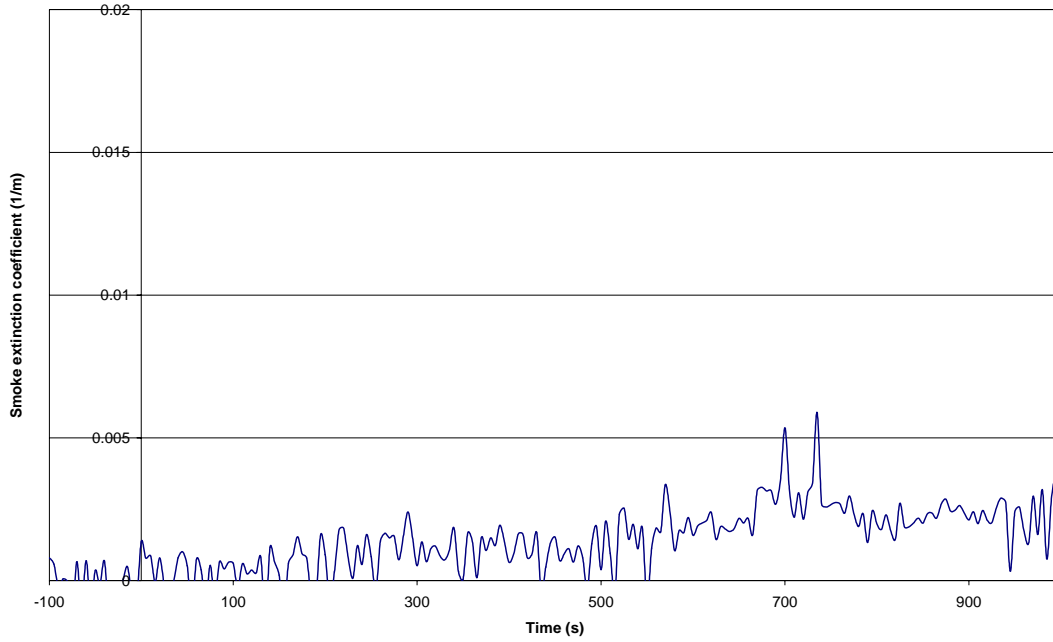


Figure 15. Smoke extinction coefficient station 1

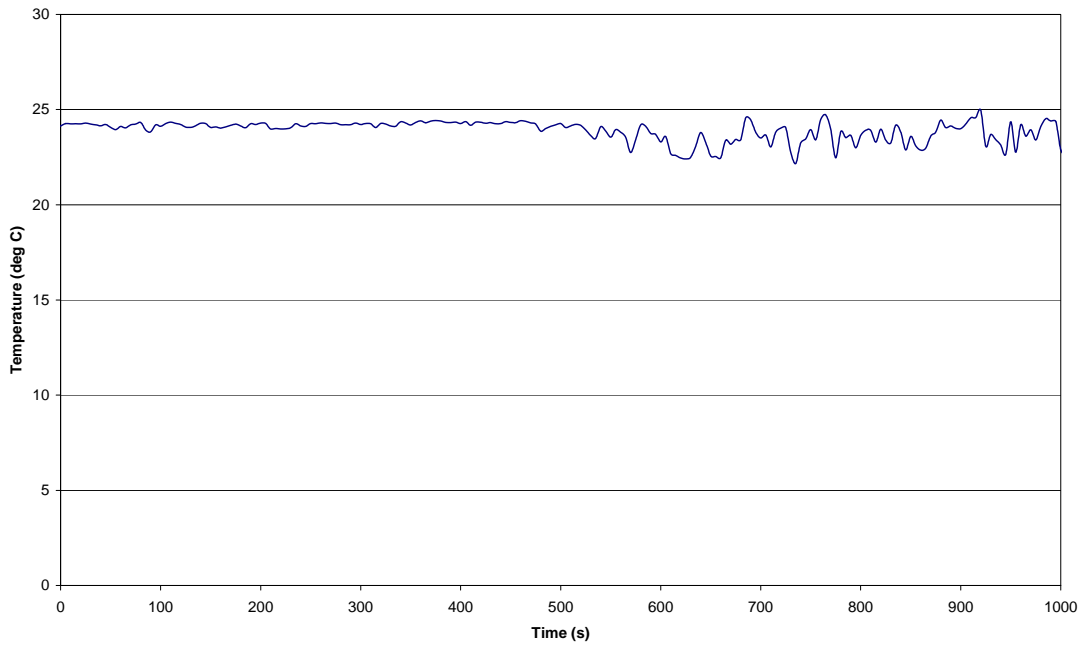


Figure 16. Temperature station 1

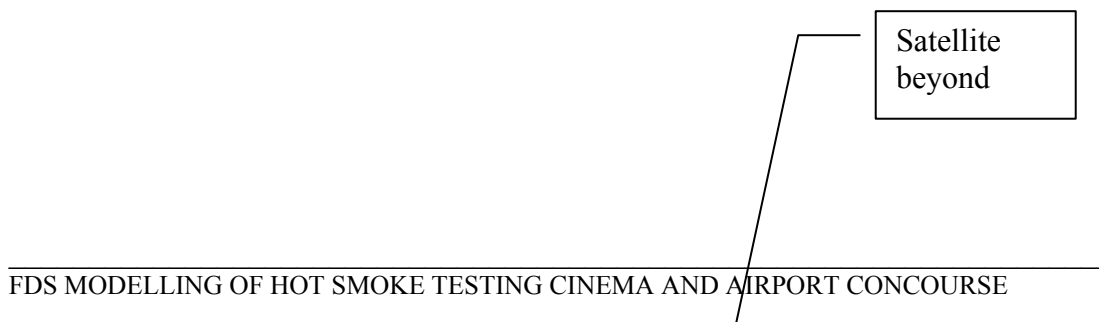




Figure 17. Location of instrumentation station 1 in regard to the test fire looking east to west.



Figure 18. Location of instrumentation station 1 in regard to the smoke layer during test 1.

8.3.1.3.2 Results for location 2 - Test 1.

Instrumentation station 2 is 1.0 m west and 1.0 north of the centreline the test fire. The location of the instrumentation in regard to the test fire can be seen in . The air movement from east to west tilted the plume so that for the majority of the test the plume toward the instrumentation station as seen in Figure 23. The smoke meter at this station was therefore measuring the obscuration at the top of the plume and not the ceiling jet, which was the intention of the location selected.

The smoke obscuration shows a consistent 20 cycle which matches the cycle of the smoke meter which would stop smoke production for 2 seconds every 20 seconds. The smoke obscuration has been average for two obvious time intervals for the test. The two intervals are prior to and after manual activation of the smoke exhaust system in the concourse. The low obscuration in the interval 250 – 300 relates to a event of air movement that pushed the smoke plume to the floor and appeared not to be drawn into the heated air plume and hot layer. There is no obvious reason for the tilting of the plume at this time. The “flat spot” in the obscuration can also be noted in the station 3 obscuration graph Figure 24.

The average smoke extinction coefficients for these times are noted in Figure 19

Air speed

The average air speed prior to the commencement of the test was 0.4m/s east to west. The velocity increases within 30 seconds of the commencement. Visual observation concluded that the plume did not directly impinge on the anemometer. No building systems have been activated in this time so the change in air speed is due to the indirect influence of the test, fire plumes and smoke machine induced air turbulence. There is a small cyclical feature in the air speed graph consistent with the timing of the smoke generation cycle. The influence on magnitude is estimated to be 25 – 50% of the magnitude of the air velocity change due to the test fires.

Temperature

The average temperature prior to the test is 24.1°C. The temperature initially increases and then settles down a stable temperature, with an average of 32.3 °C from two minutes until the end of the test.

The air speed and temperature was plotted against the smoke obscuration coefficient (Figure 22) to assess any affect the smoke generator cycling had on the station 2 recorded data. The graph shows points of similarity; however in general there is no direct correlation between the peaks and troughs of the obscuration and the variation in the temperature and air velocity.

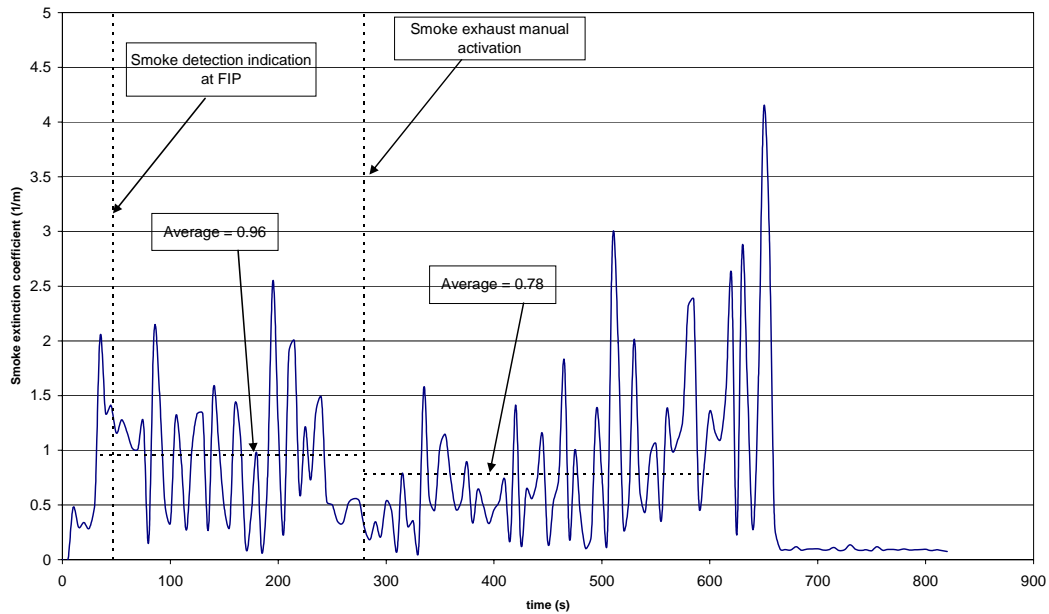


Figure 19. Smoke extinction coefficient station 2

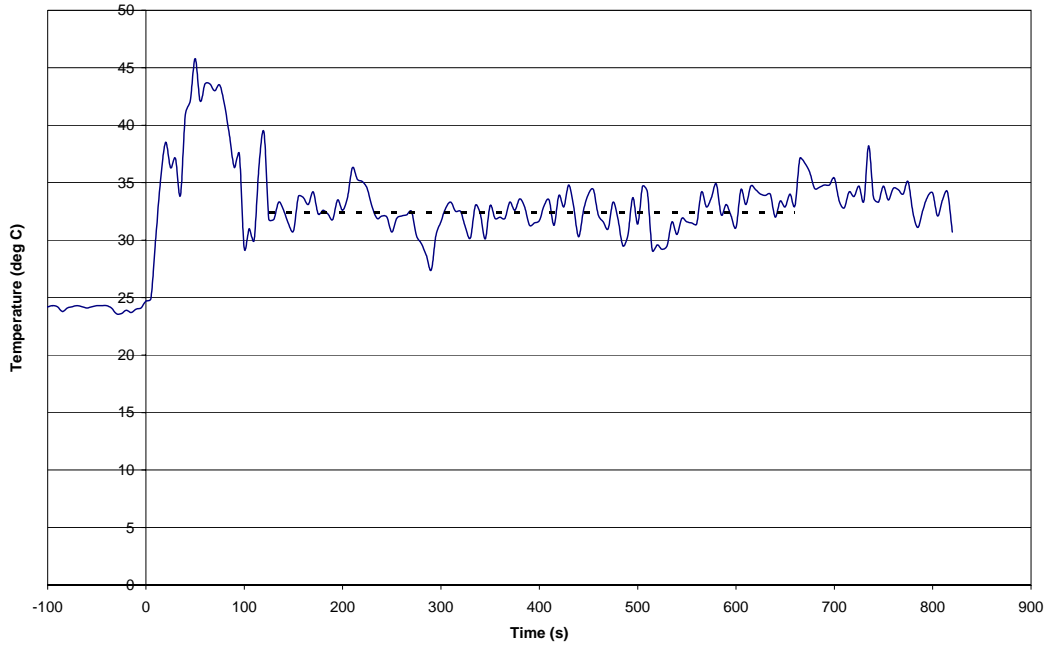


Figure 20. Temperature station 2

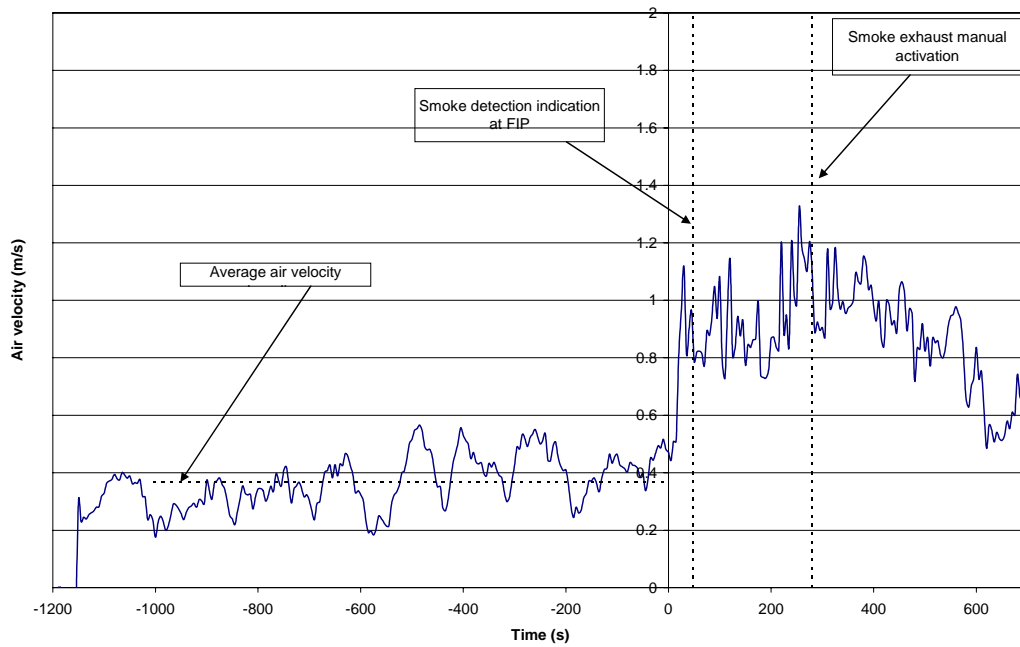


Figure 21. Air velocity station 2

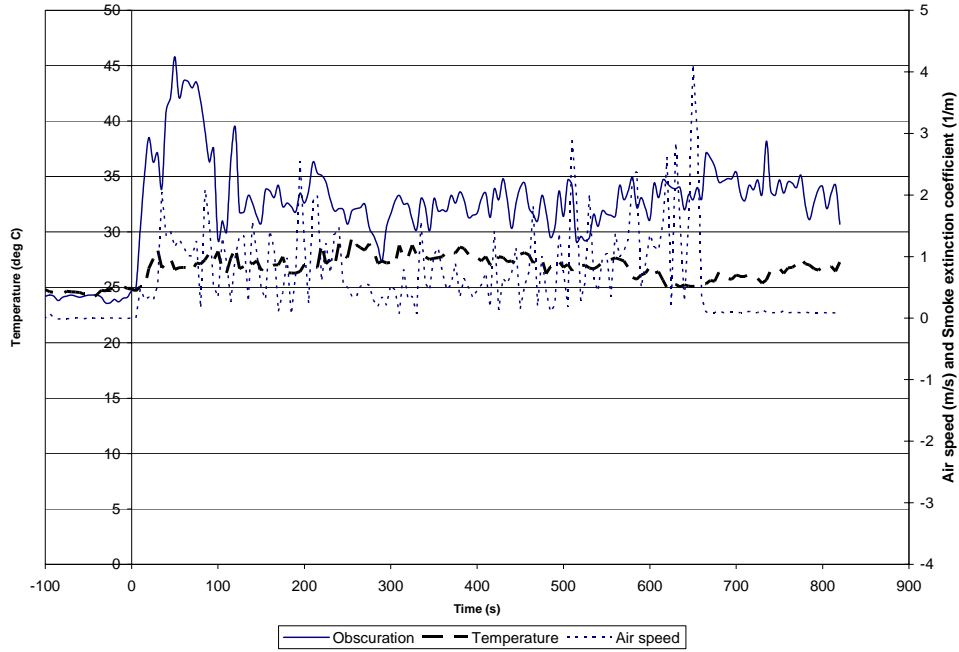


Figure 22. Comparison of air speed, temperature and smoke extinction coefficient station 2



Figure 23. Test fires and instrumentation station 2 during the test.

8.3.1.3.3 Results for location 3 - Test 1.

Location 1 is 12 m west of the test fire. The location of the instrumentation in regard to the test fire can be seen in Figure 26. The air movement from east to west quickly swept smoke towards instrumentation station 3. The smoke layer was visually tracked as it moved down the concourse and the times to distances west of the fire are noted in Table 6. The visual smoke front reached instrumentation station 20 seconds after the start of test. A smoke layer was moving past the instrumentation station from this time until the end of the test.

The smoke obscuration (Figure 24) increase was recorded by the smoke meter at 30s, as was the temperature rise (Figure 25). The temperature rise above ambient was steady for the duration of the test. The obscuration has more variation than the temperature, which may be attributed to the cycling of the smoke generator, although with less amplitude than that measured at station 2. The “flat spot” in the obscuration appears to correlate with the smoke plume wafting to the floor, as discussed in Section 8.3.1.3.2.

The average temperature prior to the test is 24 °C the rise is about 5°C.

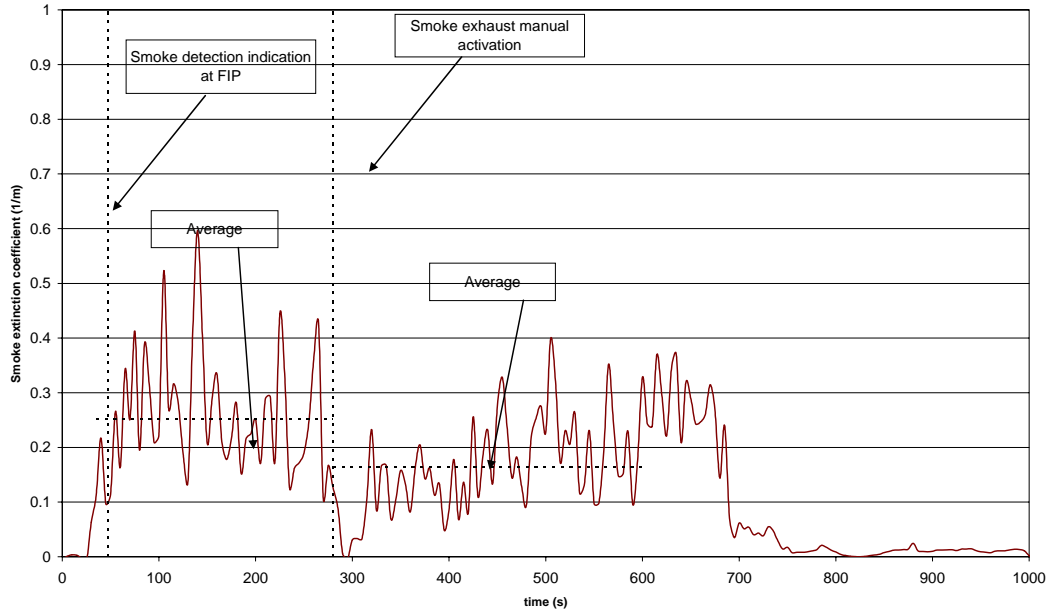


Figure 24. Smoke extinction coefficient station 3

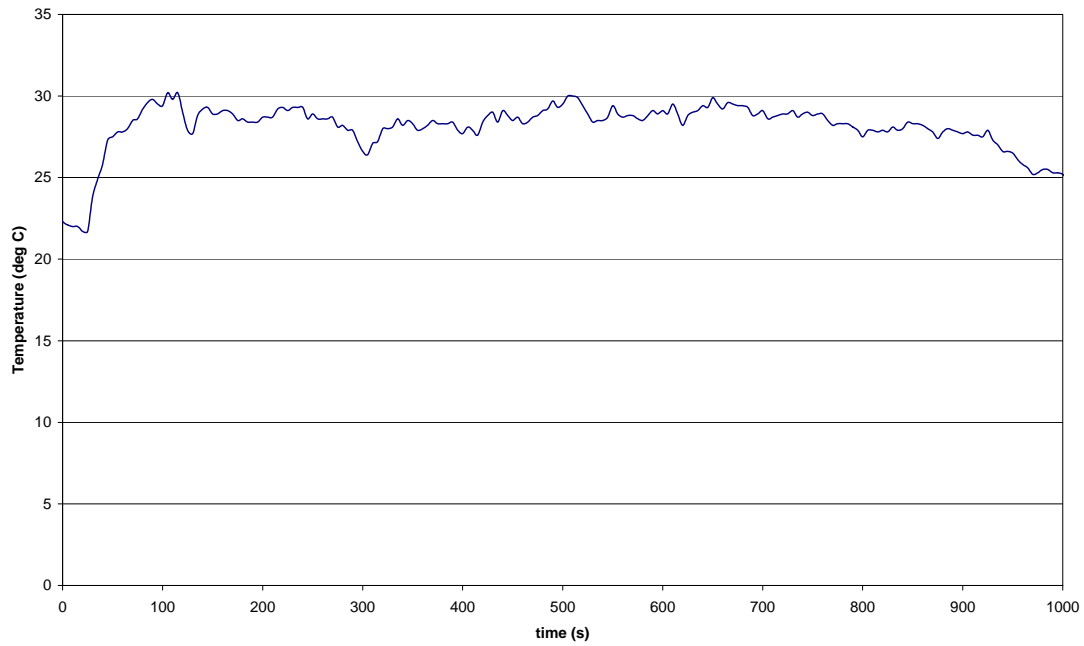


Figure 25. Temperature station 3



Figure 26. Location of instrumentation station 3 in regard to the test fire looking west to east.

8.3.1.3.4 Comparison of results for all locations - Test 1.

Figure 27 and Figure 28 plot the temperature and smoke obscuration for points for comparative purposes. The data matches the visual observations and expectations with the ranking of temperature and obscuration from highest to lowest, being Station 2, Station 3 and Station 1.

Turbulence as the smoke layer moves west along the concourse both cools and mixes the smoke layer, reducing the temperature and obscuration and making the layer more homogeneous.

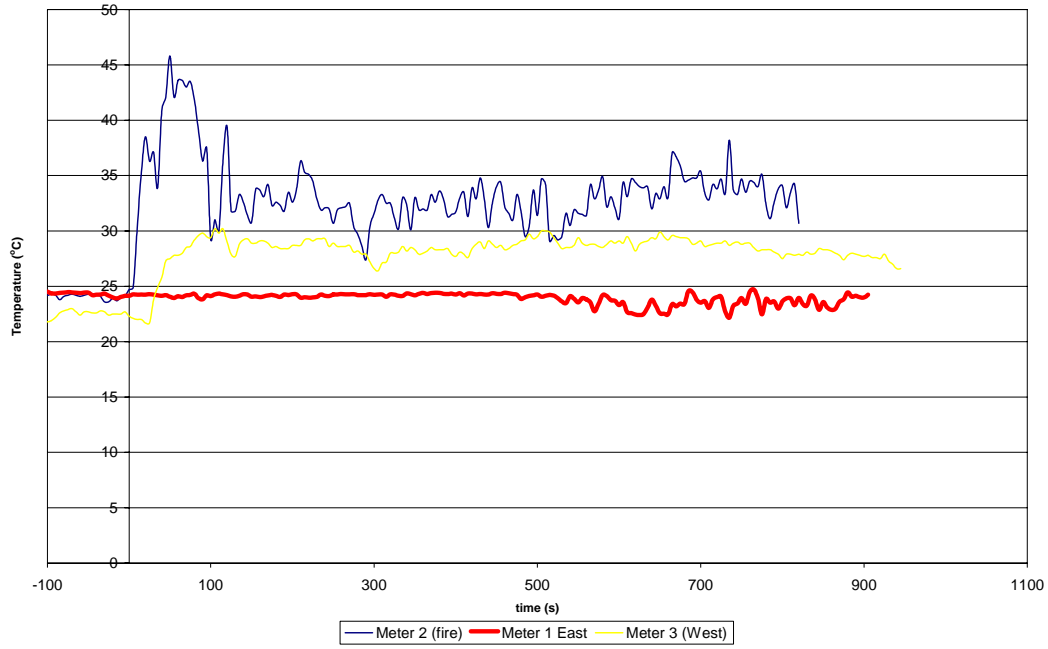


Figure 27. Temperature comparison for all stations

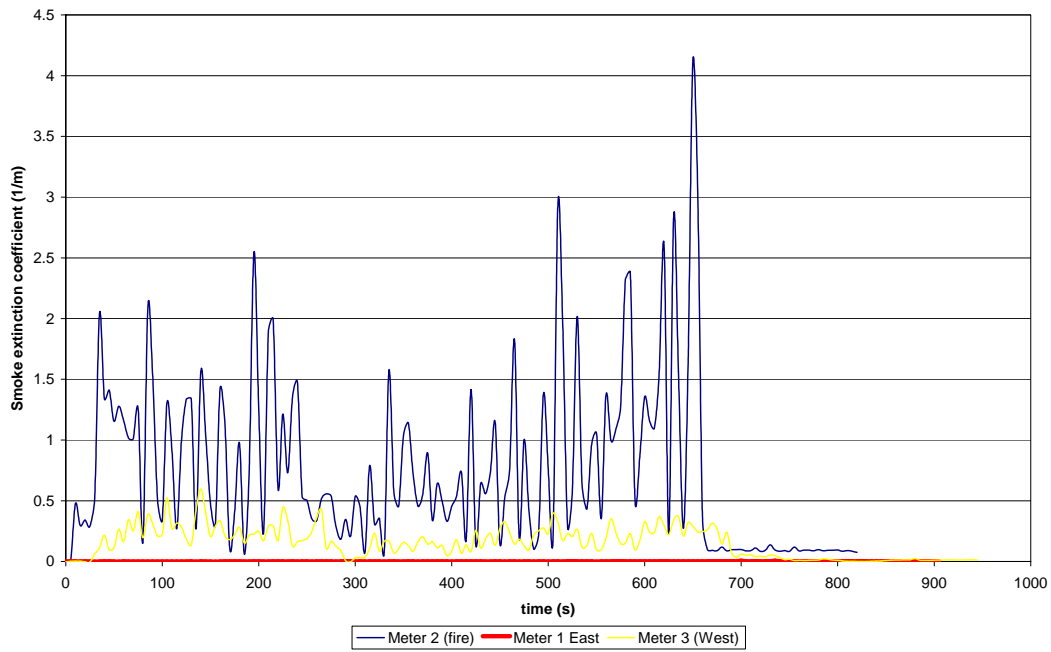


Figure 28. Smoke extinction coefficient comparison for all stations

8.3.2 Test 2 – Departures Concourse repeat test

Due to the smoke exhaust fans not activating during the first test, the fire safety systems were reset and the test repeated.

8.3.2.1 Observations Test 2

Table 7. Test 2 - Hot smoke test event times and comments.

Time from commencement of smoke		Comments
Minutes:seconds	seconds	
		Air movement is from the main building toward the satellite measured at the centre of the cross section of the concourse at 0.4 m/s. Air was noticeable moving from gate lounge 1 and 2 into the concourse.
-0:10	-10	Ignition of the trays.
0:00	0	Generation of smoke commenced.
0:15	15	Smoke to smoke meter 16m west of fire. Layer 1 m deep at the fire.
0:31	31	Activation of smoke detection and SEF 7, 8 and 9 and HVAC shut down. Smoke to 26m west of fire. Activation of burglar alarm by fire brigade member. Layer down to 1.6m just west of the fire.
0:44	44	Smoke to 34m west of fire
1:03	63	Smoke reaches the smoke meter 12 m east from the fire. Smoke layer now above head height (2m from floor)
2:15	135	Smoke reaches gate lounge 2 baffle.
3:00	180	Smoke layer above head height; formed layer between satellite baffle, duty free security door and gate lounge baffles.
3:35	205	Activation of SEF 4,5,6 in gate lounge 2. Smoke reach smoke baffle between concourse and satellite at 48m from fire.
5:53	353	Activation of SEF 1,2 and 3 gate lounge 1. Smoke logging in gate lounge 2 due to high air velocities into the gate lounge drawing smoke from the concourse. Smoke plug with smoke to 0.5m from the floor moves from the satellite moving along the concourse from the west.
7:00	420	Smoke layer in concourse 1.5m from floor. Smoke logging in gate lounge 1 due to high air velocities into the gate lounge drawing smoke from the concourse. West end of concourse clear of smoke up to 12m from fire.
10:00	600	Test terminated.

8.3.2.2 Discussion of visual observations – Test 2

Initially the smoke layer flowed along the concourse away from the fire towards the satellite due to the air movement induced by the HVAC systems. Upon fire detection activation at 30 seconds the smoke exhaust activated and the shut down of the HVAC occurred. The smoke had not reached the smoke baffle that separates the satellite from the concourse zone. The

airflow east to west dropped to near zero (See further discussion of this in Section 8.3.2.3.2). Smoke at the fire now flowed in both east and west from the fire. Smoke flowing west was effectively exhausted from the concourse at the westerly grille. Smoke flowing east filled the reservoir toward the duty free store and the Gate 1 and 2 lounges.

The smoke flowed under the smoke baffles separating the concourse from Gates 1 and 2 lounges activating the exhaust in these smoke zones at 205 (Gates 1) and 350 seconds (Gates 2). As a result of the exhaust activation high air volumes and smoke was drawn into the gate lounges, disturbing the smoke layer. This event provided effective smoke exhaust from the concourse as the smoke was contained between the fire and the easterly exhaust grille in the duty free store. However, the event caused smoke logging in the lounges.

8.3.2.3 Results – Test 2

The results for the three instrumentation stations are included as graphs in the following sections and each is discussed. Each graph has the following major events marked and identified:

- Smoke detector activation in the concourse resulting in HVAC shut down and concourse smoke exhaust fans SEF 7, 8 and 9.
- Smoke detector activation in the gate lounge 2 resulting in HVAC shut down and concourse smoke exhaust fans SEF 4, 5 and 6.
- Smoke detector activation in the gate lounge 1 resulting in HVAC shut down and concourse smoke exhaust fans SEF 1, 2 and 3.

8.3.2.3.1 Results for Station 1 – Test 2.

Location 1 is 12 m east of the test fire. The location of the instrumentation in regard to the test fire can be seen in Figure 28. The initial air movement from east to west kept smoke away from instrumentation station 1. The air movement prevented any back layering until the HVAC shut down allowing the smoke layer to move east to station 1. Evidence of the arrival of smoke layer at station 2 at 60 seconds is the increase of obscuration and temperature in Figure 29 and Figure 30. Activation of the gate lounges smoke exhaust further changed the air movement in the concourse, increasing the air flow west to east (Figure 33).

The initial ceiling jet plume passing the station was thicker (higher obscuration) than the following flowing smoke, which may be due to a build up of smoke in the prevented back layer.

The smoke obscuration (Figure 29) was noticeable once the HVAC system shut down and varies during the test due to:

- Changes in exhaust volumes
- The movement of a smoke plug from the satellite to the east upon reversal of the air flow direction.

The average temperature prior to the test is 24 °C, which increases 10°C during the test (Figure 30) during the test..

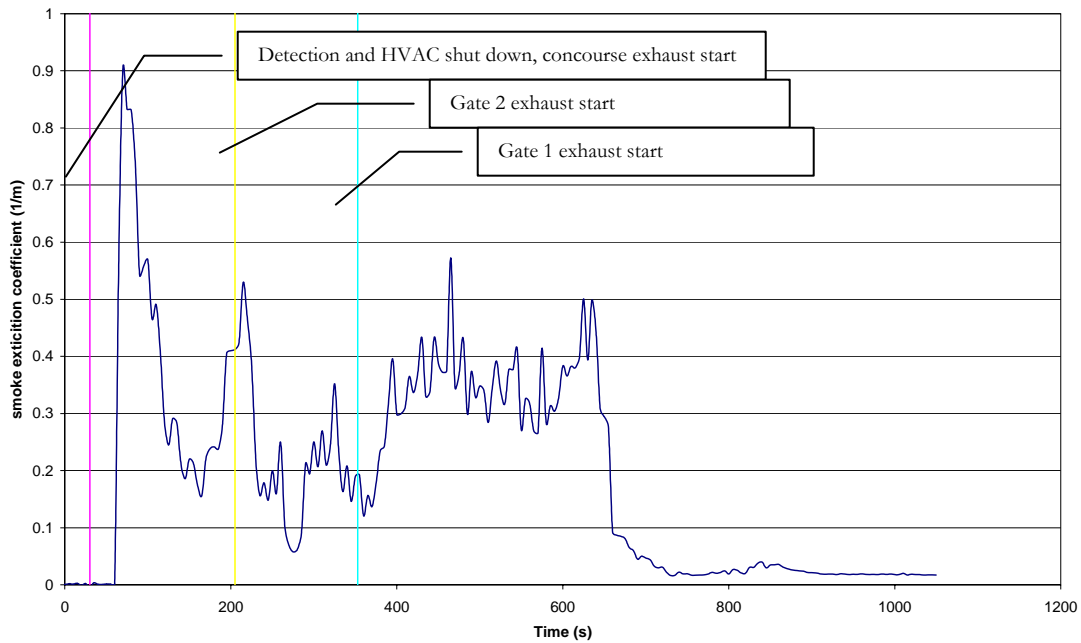


Figure 29. Smoke extinction coefficient station 1

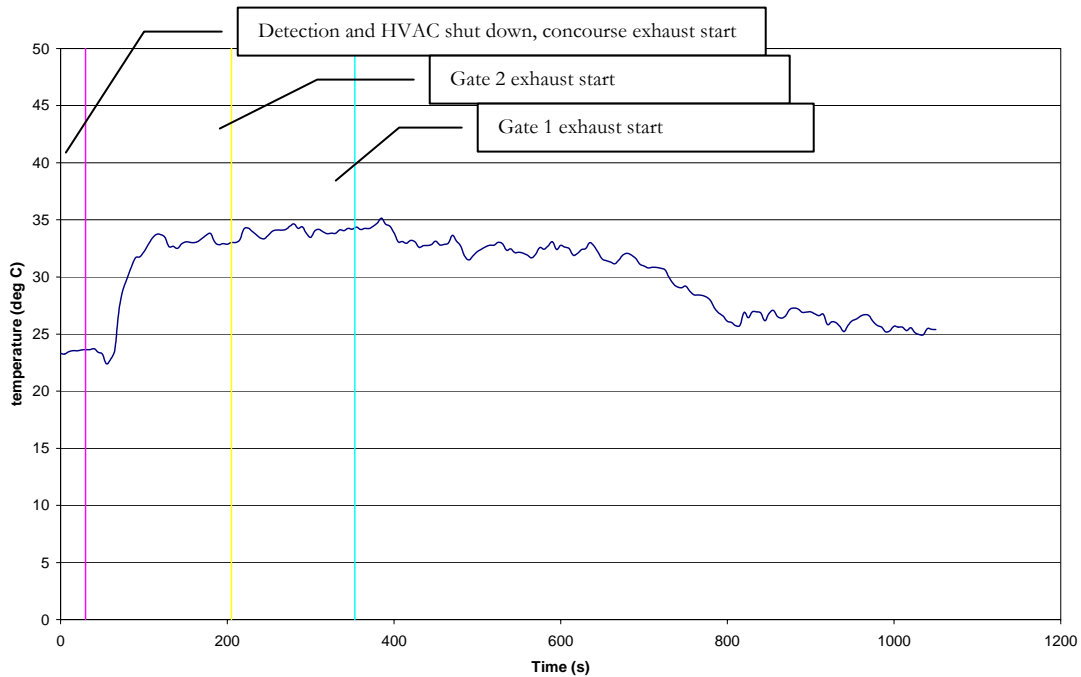


Figure 30. Temperature station 1

8.3.2.3.2 Results for Station 2 – Test 2.

Instrumentation station 2 is 1.0 m west and 1.0 north of the centreline the test fire. The location of the instrumentation in regard to the test fire can be seen in . The air movement from east to west at the start of the test tilted the plume toward the instrumentation station. In this stage of the test the measure obscuration is high, up to 3 m^{-1} (Figure 31). Upon shut down of the HVAC the plume resumed a vertical axis symmetric shape. Consequently, the smoke meter at this station began to measure the ceiling jet, which was the intention of the location selected. The plume tilted slightly to the south. The obscuration dropped to less than 0.5 m^{-1} until a change in the airflow around the 280 second mark when the plume was noticeable more turbulent and tilted a little more toward the instrument station.

The smoke obscuration shows a consistent approximate 20 cycle consistent with test 1 (See section 8.3.1.3.2). The generation cycling of the smoke meter would stop smoke production for 2 seconds every 20 seconds.

Air speed

The average air speed prior to the commencement of the test was 0.4m/s east to west as for test 1. The velocity increases at the start of the test (due to plume turbulence) however drops upon HVAC shut down. The air velocity increase during the course of the test is most likely due to the activation of smoke exhaust drawing more air from the satellite to the gate lounges.

Temperature

The average temperature prior to the test is 24.1°C. The temperature increase immediately following ignition of the fires and after some initial variability remains between 43 and 35 °C during the test.

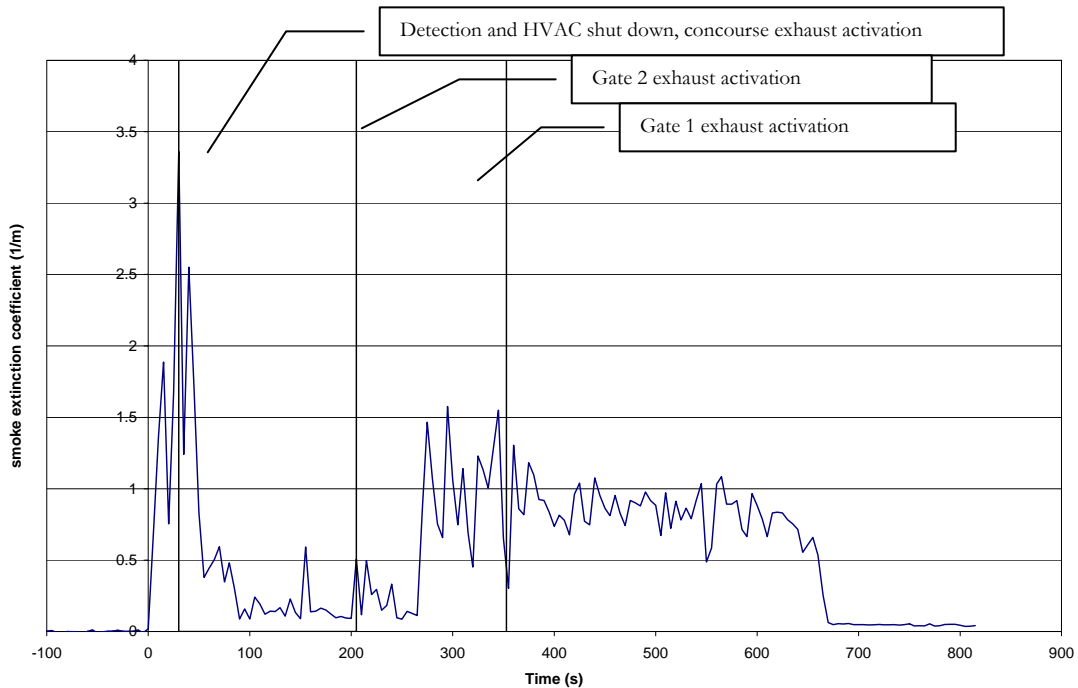


Figure 31. Smoke extinction coefficient station 2

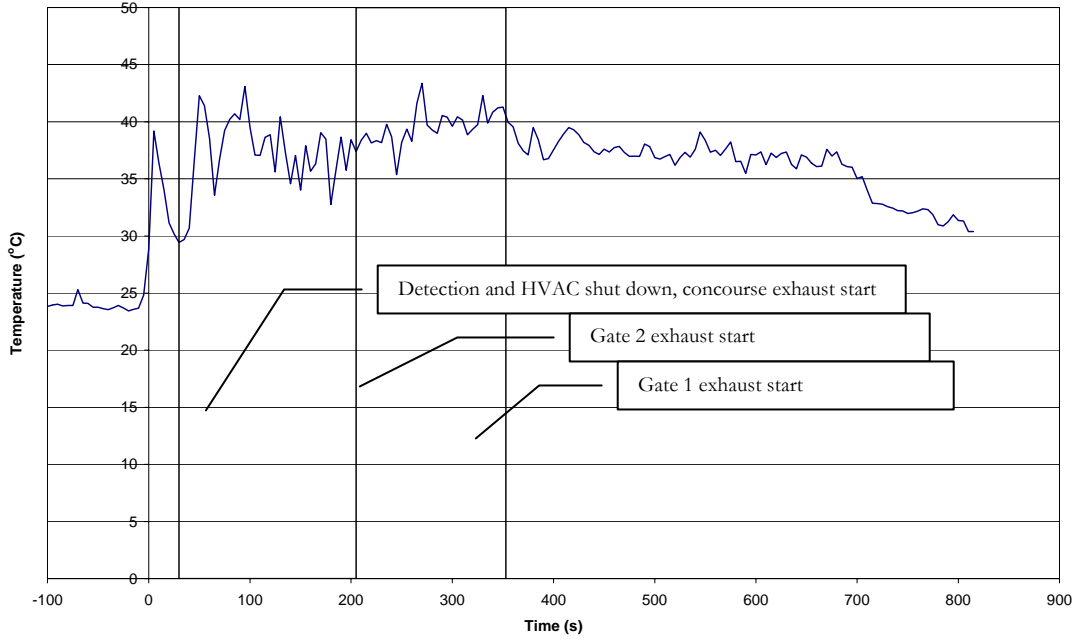


Figure 32. Temperature station 2

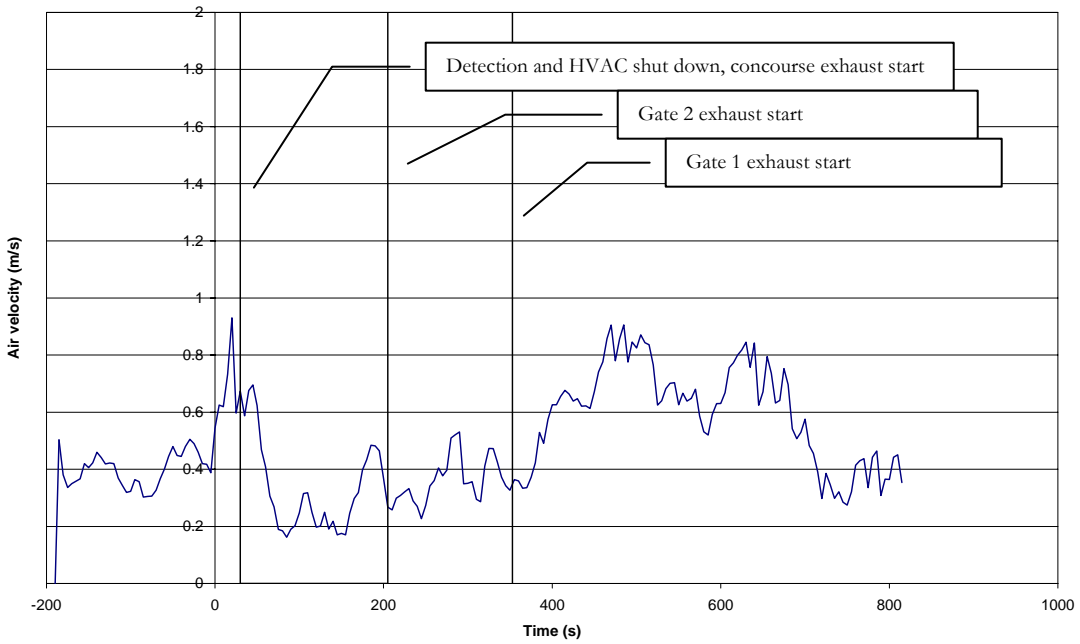


Figure 33. Air speed station 2

8.3.2.3.3 Results for Station 3 – Test 2.

Location 1 is 12 m west of the test fire. The air movement from east to west quickly swept smoke towards the instrumentation station 3. The smoke layer was visually tracked as it moved down the concourse and the times to distances west of the fire are noted in Table 6. The visual smoke front reached instrumentation station 20 seconds after the start of test, similar to test 1. A smoke layer was moving past the instrumentation station from this time until the shut down of HVAC systems, at which point whereby the similarities with test 1 ceased. The smoke layer progression slowed greatly and was contained within the smoke zone. No smoke entered the satellite zone.

The smoke obscuration (Figure 34) increase was recorded by the smoke meter at 30s, as was the temperature rise (Figure 35).

The temperature rise above ambient stabilised at about 100 seconds, at 32 degrees. This is significantly higher than in test 1 due to the lower air speed reducing turbulence and therefore hot layer mixing. After activation of the second gate lounge exhaust the temperature began to reduce to 25°C at the end of the test.

The obscuration has more variation than the temperature, which may be attributed to the cycling of the smoke generator, however with less amplitude than that measured at station 2. The reversal of the flow in the concourse may be indicated by the increase in obscuration after the activation of the fans in gate lounge 2.

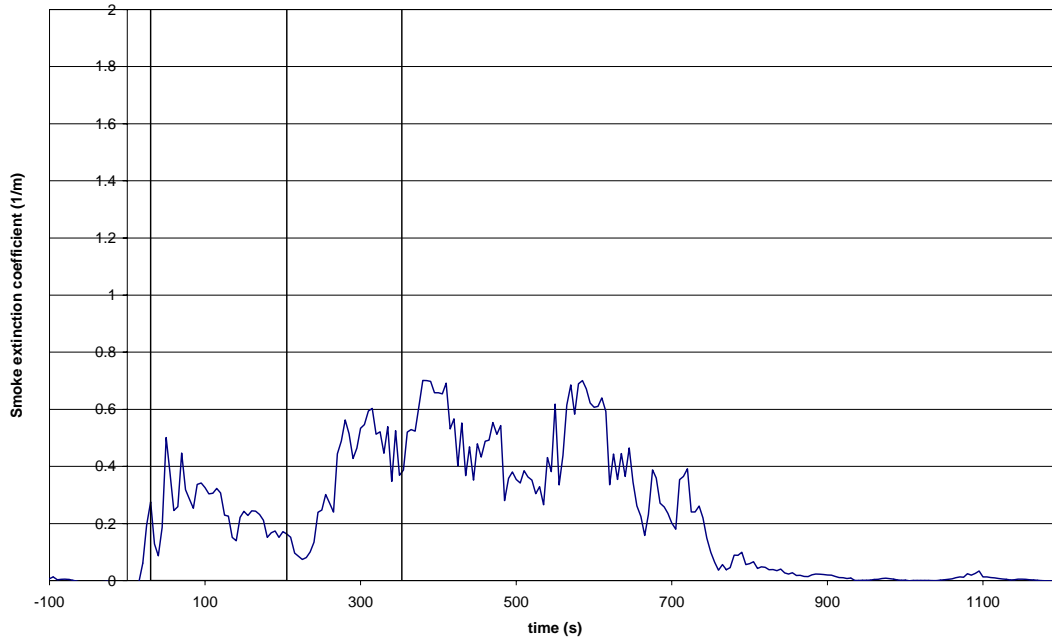


Figure 34. Smoke extinction coefficient station 3

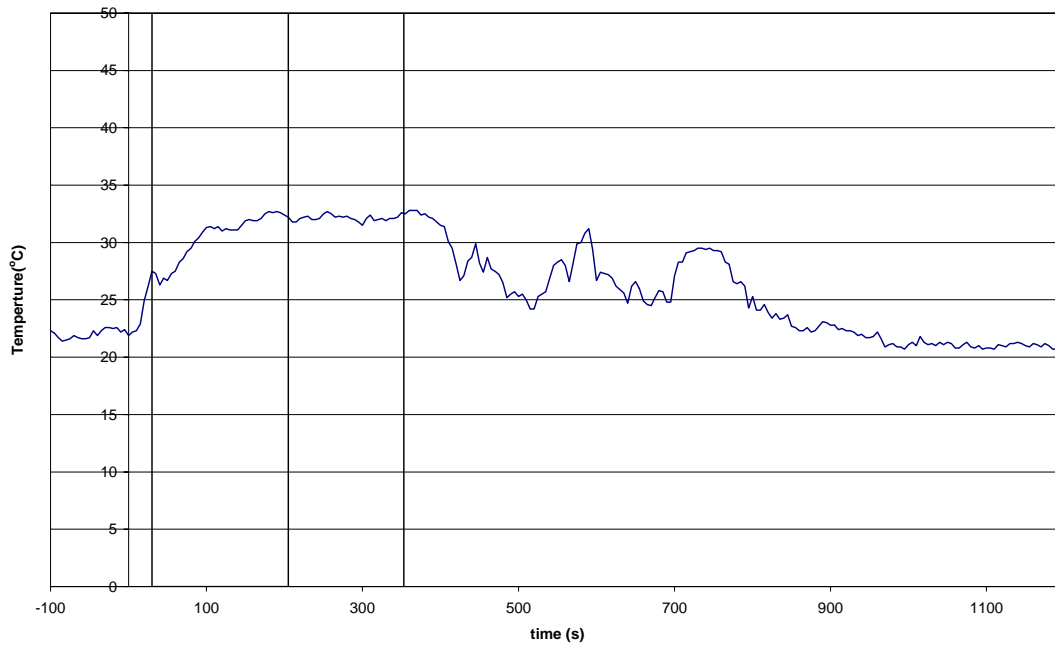


Figure 35. Temperature station 3

8.3.2.3.4 Comparison of results for all locations – Test 2.

Figure 27 and Figure 28 plot the temperature and smoke obscuration measurements, for comparative purposes. The data matches the visual observations and expectations, with the ranking of temperature and obscuration from highest to lowest being Station 2, Station 3 and Station 1.

Turbulence as the smoke layer moves west along the concourse both cools and mixes the smoke layer, reducing the temperature and obscuration and making the layer more homogeneous.

The similarity of obscuration at all stations between 100 and 250 seconds indicates a well-formed hot layer that is not being disturbed by non-fire generated air movement.

Prior to HVAC shut down the airflow is clearly pushing the smoke plume into the station 2 meter. From the 250-second mark until the end of the test Station 1 and 3 are surprisingly similar, with station 2 experiencing density smoke due to the proximity to the fire.

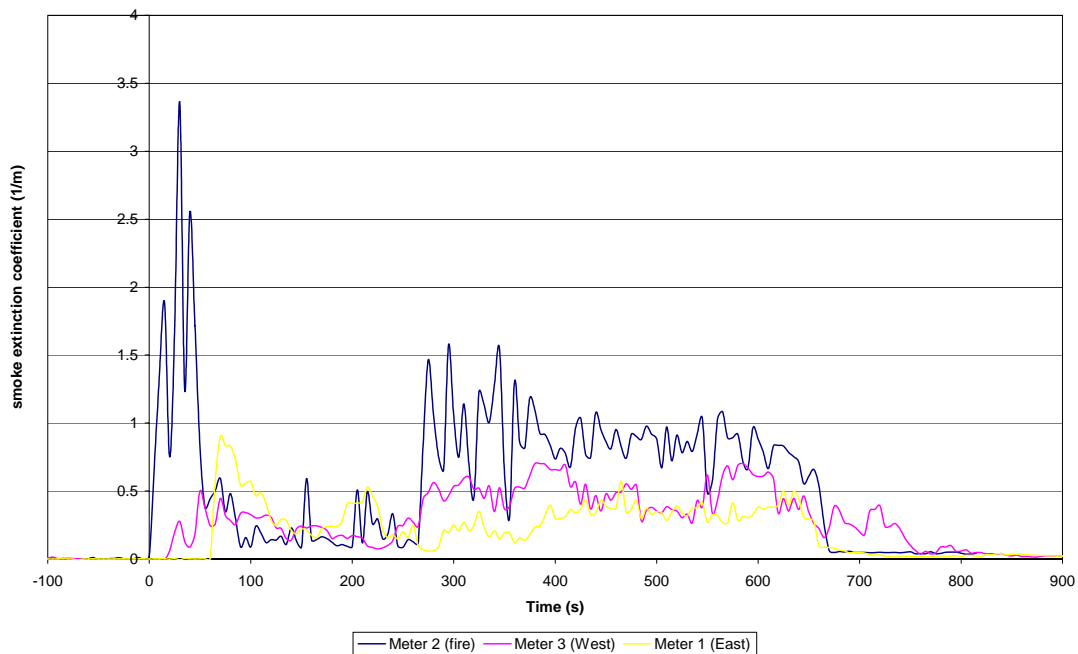


Figure 36. Smoke extinction coefficient comparison for all stations

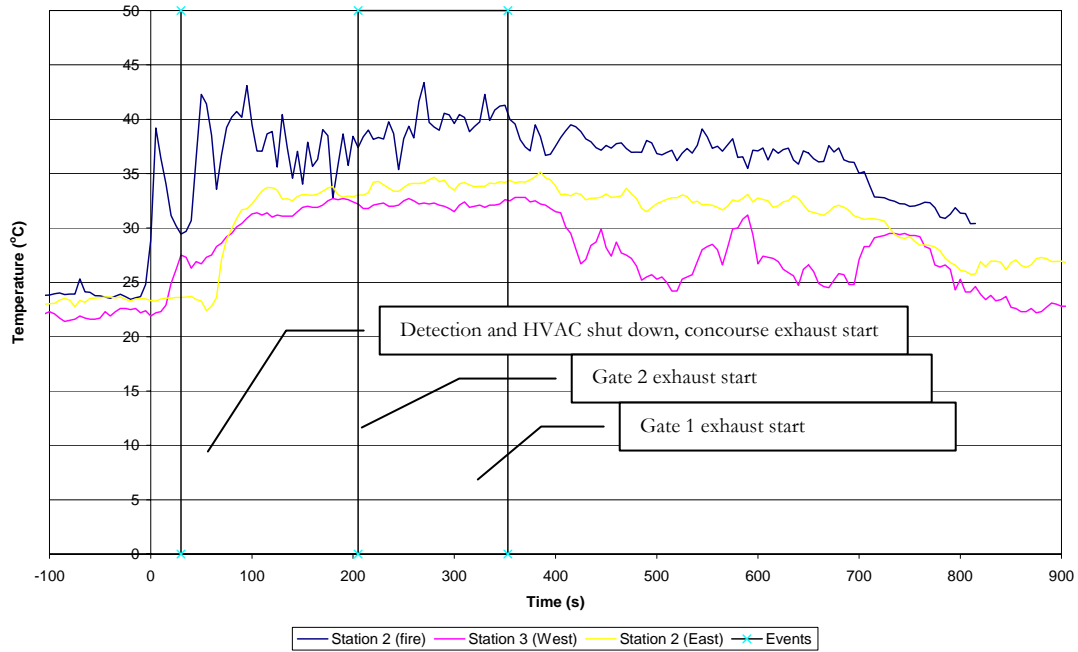


Figure 37. Temperature comparison for all stations

8.4 Experiment Conclusions

Hot smoke tests were carried out in an airport terminal building, in accordance with the Australian Standard 4391 -1999. The hot smoke tests verified some aspects of the operation of the smoke hazard management systems in the buildings and gathered data on temperature, obscuration and air speed for computer modelling purposes.

A detailed analysis of the Fire Indicator Panel, Building Management System and visual graphics display was not carried out.

Input values for FDS modelling were determined.

Air velocity prior to AHU shut down is assumed to be a steady 0.4 m/s from the east to west (terminal towards the satellite). During test 1 the AHU did not shut down, so the air velocity is sustained for the duration of the test. In test 2 the air velocity is 0.4 m/s from the east to

west (terminal towards the satellite) and is reduced to zero upon smoke detection and AHU shut down.

The pulsing of the smoke generator in cycles of 20 seconds on, 4 seconds off, results in an oscillation in the obscuration data that may be difficult to simulate.

9 FDS MODELLING OF AIRPORT CONCOURSE HOT SMOKE TEST

CFD modelling of the hot smoke tests was carried out. The CFD model used was FDS. The first test was used to calibrate the model to vary the supply air rate, ventilation locations and fuel soot yield. The parameters concluded from Test 1 were then used as input to predict the more complex conditions experienced in Test 2.

The computer simulations were carried out on three computers, depending on the number of nodes required:

1. Dell Notebook D610 with a Intel Pentium processor 2.00Ghz, 1.00 GB of RAM running Windows XP Professional 2002.
2. Desktop with a Intel Pentium processor 3.20Ghz, 0.99 GB of RAM running Windows XP Professional 2002.
3. CSIRO high speed computing centre operating a NEC SX-6 is a 28 node system with 224 parallel vector processors providing 1.8 TFLOPS (trillions of floating point operations per second) peak performance, and an aggregate 1.8 TB (trillion bytes) of main memory running Linux / HP-X 11i v. 16.

9.1 Input file

An increase in the soot production parameter for the combustion of methylated spirit was implemented to simulate the artificial smoke and obscuration. The methanol default value was $SOOT_YIELD=0.02$ (g/g), however this was increased to 0.06 to simulate the fake smoke generated by the smoke generator. The value of the $SOOT_YIELD$ parameter was determined by trial and error simulation of test 1 to achieve reasonable agreement with the experimental results.

A sensitivity study was carried out into the radiative fraction through use of the `RADIATION=.FALSE` term. This study added the statement `RADIATION=.FALSE.` to the `MISC` line which turns off the radiation transport solver (saving roughly 20 % in CPU time). The default `RADIATIVE FRACTION` for methanol is 0.0 because it is such a clean burning fuel, virtually no soot was produced (`SOOT_YIELD=0.02`), hence there is not a great deal of point modelling radiation. Indeed, the increase in soot fraction to simulate the fake smoke will increase the radiation from the plume. Turning off the radiation counter balances the increase. If burning is taking place and radiation is turned off, then the total heat release rate is reduced by the `RADIATIVE FRACTION`. This radiated energy completely disappears from the calculation.

The temperatures were modelled using the “`THERMOCOUPLE`” parameter in FDS, which models the response of a thermocouple as opposed to the actual temperature at a point. The temperature of the thermocouple itself is usually close to the gas temperature (but not always).

9.2 Geometry

The concourse geometry was drawn from the floor plan provided by the facility and by measurements at the site. Ceiling heights were measured with a laser measure.

The area modelled included a 137m length of concourse and two gate lounges. Figure 38 to Figure 40 show the perspectives views of the domain from several directions.

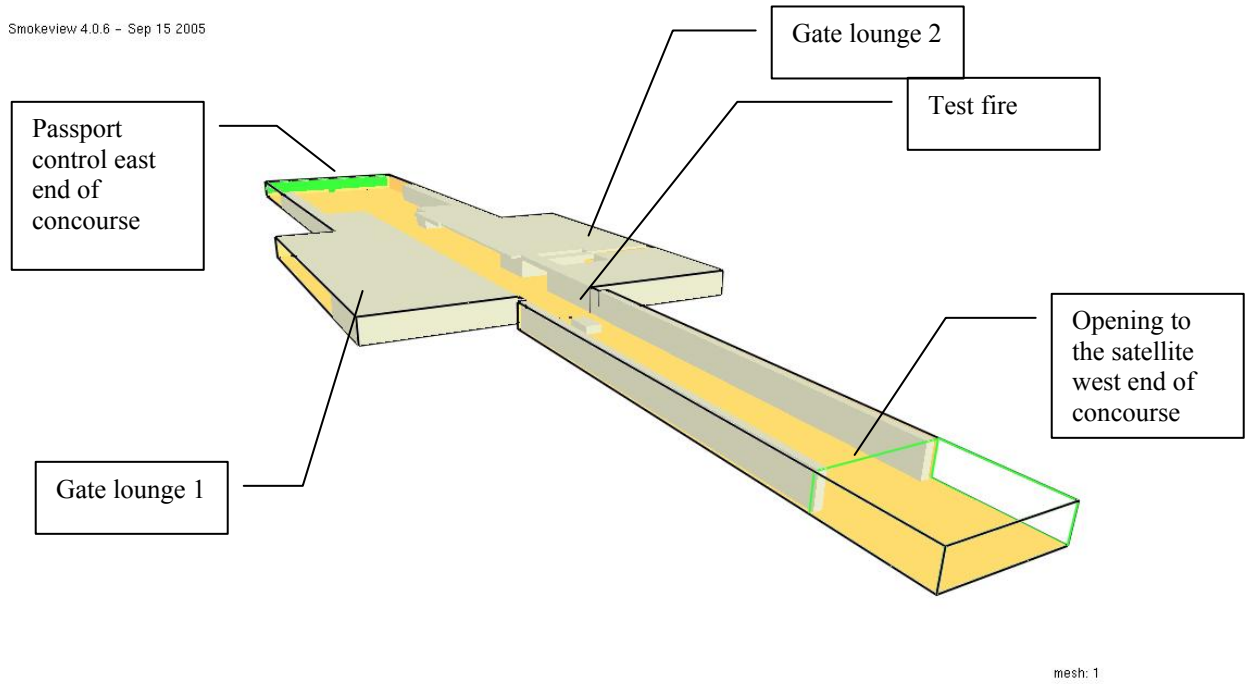


Figure 38. Perspective view of the building from above

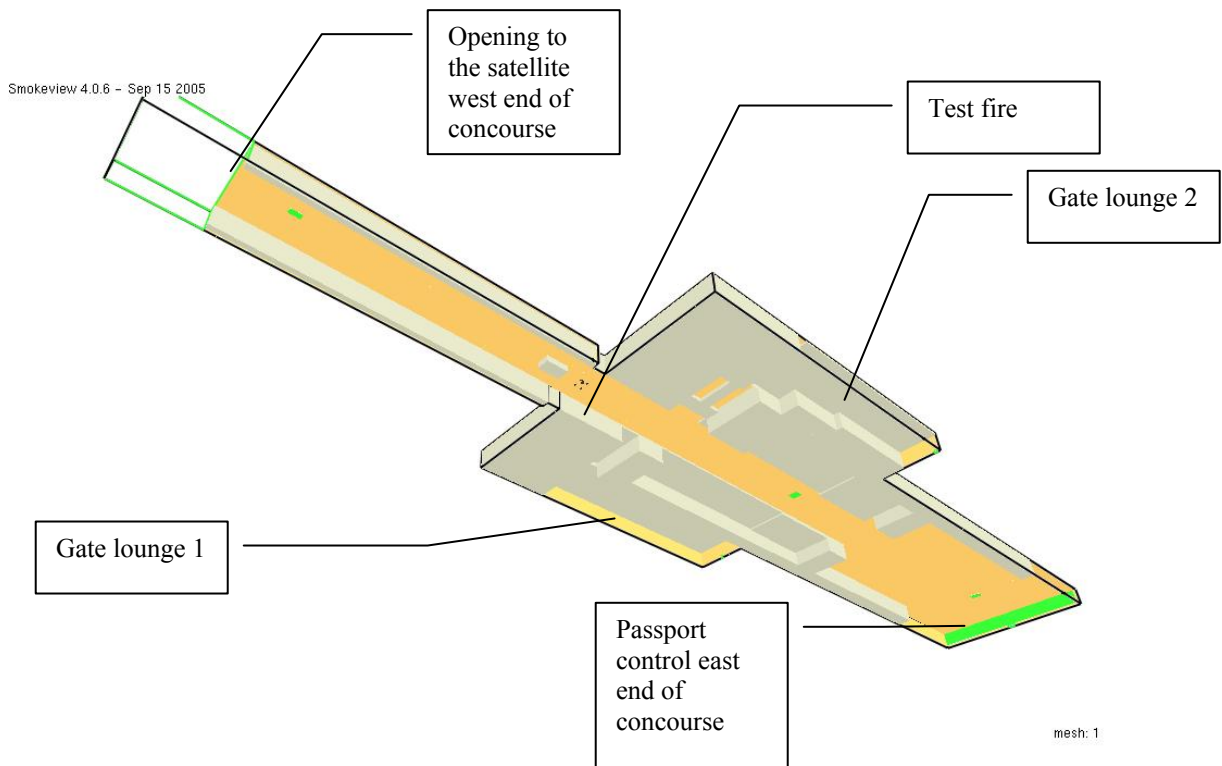


Figure 39. Perspective view of the building from below (Reflected ceiling plan view)

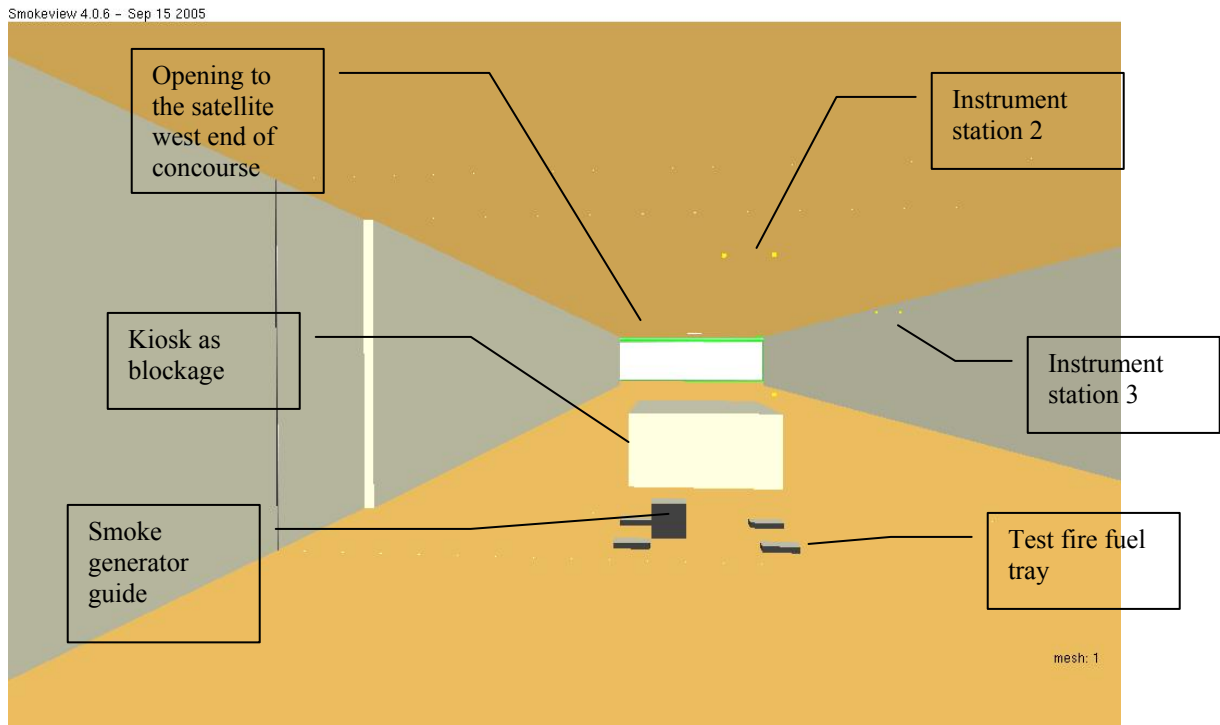


Figure 40. Perspective view of the test fire location from east, looking toward the satellite (compare to showing the test site)

9.2.1 Grids

The domain was set up as four grids:

Grid 1 was the region around the fire divided into a uniform grid using a 50mm x 50mm x 50mm grid distribution:

- 2m wide (x direction);
- 9 m long (the width of the concourse in the y direction); and
- 3 m high (the ceiling height of the concourse in the z direction).

Grids 2, 3 and 4 were divided into a uniform grid 300mm x 300mm x 300mm.

Grid 2 was the concourse west of the fire including open air:

- 51.5m wide (x direction with the concourse 41.5 long with 10m open air simulating the large scale of the satellite)
- 11 m long (the width of the concourse in the y direction plus 1m either side), and
- 3 m high (the ceiling height of the concourse in the z direction).

Grid 3 was the gate lounges and concourse east of the fire:

- 47.m wide (x direction from the fire to the end of gate lounge 2)
- 44 m long (the width of the concourse and gate lounge 1 and 2, y direction), and
- 3 m high (the ceiling height of the concourse in the z direction).

Grid 4 was the concourse east of the gate lounges:

- 47.m wide (x direction from the fire to the end of gate lounge 2)
- 44 m long (the width of the concourse and gate lounge 1 and 2, y direction), and
- 3 m high (the ceiling height of the concourse in the z direction).

Figure 41 shows the extent of each grid in the X direction.

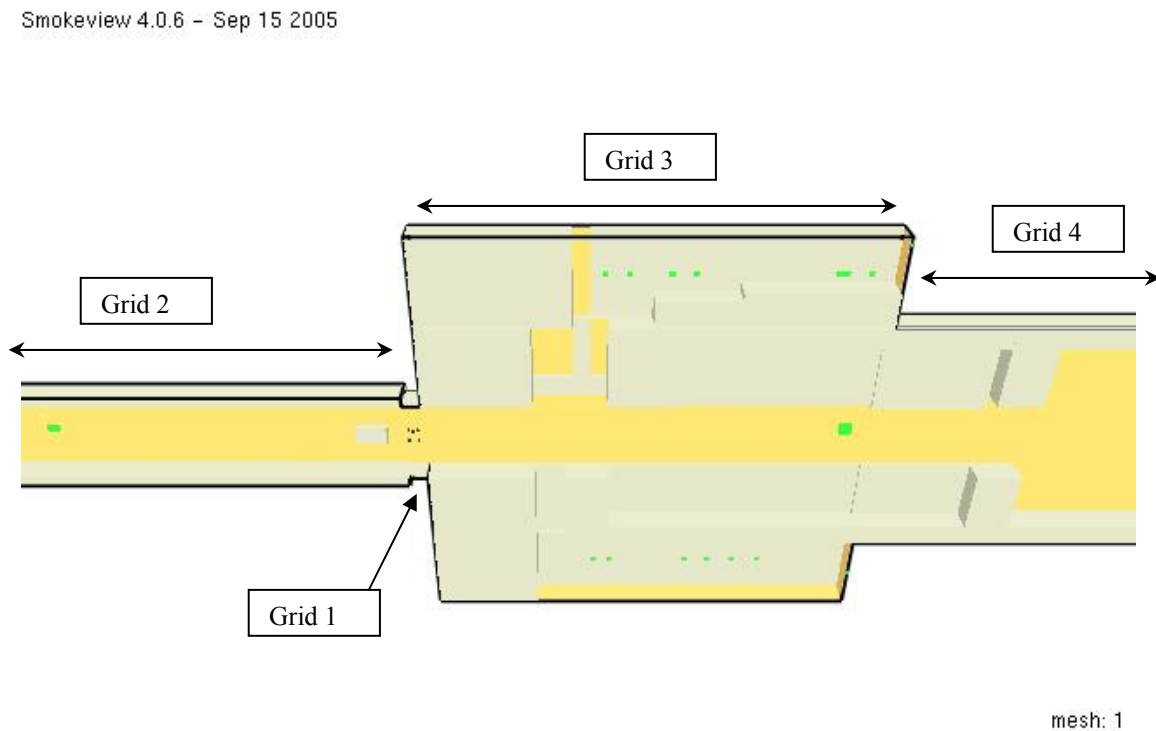


Figure 41. Perspective view of the domain grids from below (Reflected ceiling plan view)

9.2.2 *Sensitivity analysis of node number.*

A study of the sensitivity to number of nodes was carried out by decreasing the cell dimensions, with a subsequent increase in number of cells (See Section 9.9).

9.2.3 *Ventilation Openings*

The opening from the concourse to the satellite was treated as an opening to the outside air. The satellite area is a reasonably open space with a diameter of 45m and ceiling height varying between 3 to 7m. Several doors lead to air bridges and stairs to pavement level.

An opening in each gate lounge one cell wide and long in the wall to outside was simulated to model building leakage from the façade and door to the air bridge.

An opening was added at the east end of the concourse to simulate door leakage to the main airport building.

The above openings were sized at one cell in each multi grid domain. Multiple openings to the “outside” assisted in ensuring that the pressure did not increase within each grid network, creating computational stability.

The details of the experimental supply air were not obtained. A supply air vent was modelled at the east end of the concourse with a volume flow rate of $18\text{m}^3/\text{s}$, which provided an airflow of $4\text{m}/\text{s}$ at the anemometer at instrument station 2.

9.2.4 *Mechanical Smoke Exhaust*

The smoke exhaust grilles for the concourse, gate 1 and gate 2 were included in the simulation as shown in Figure 42 and Figure 43. See Section 8.2.1 for the smoke exhaust fan designation and flow rate.

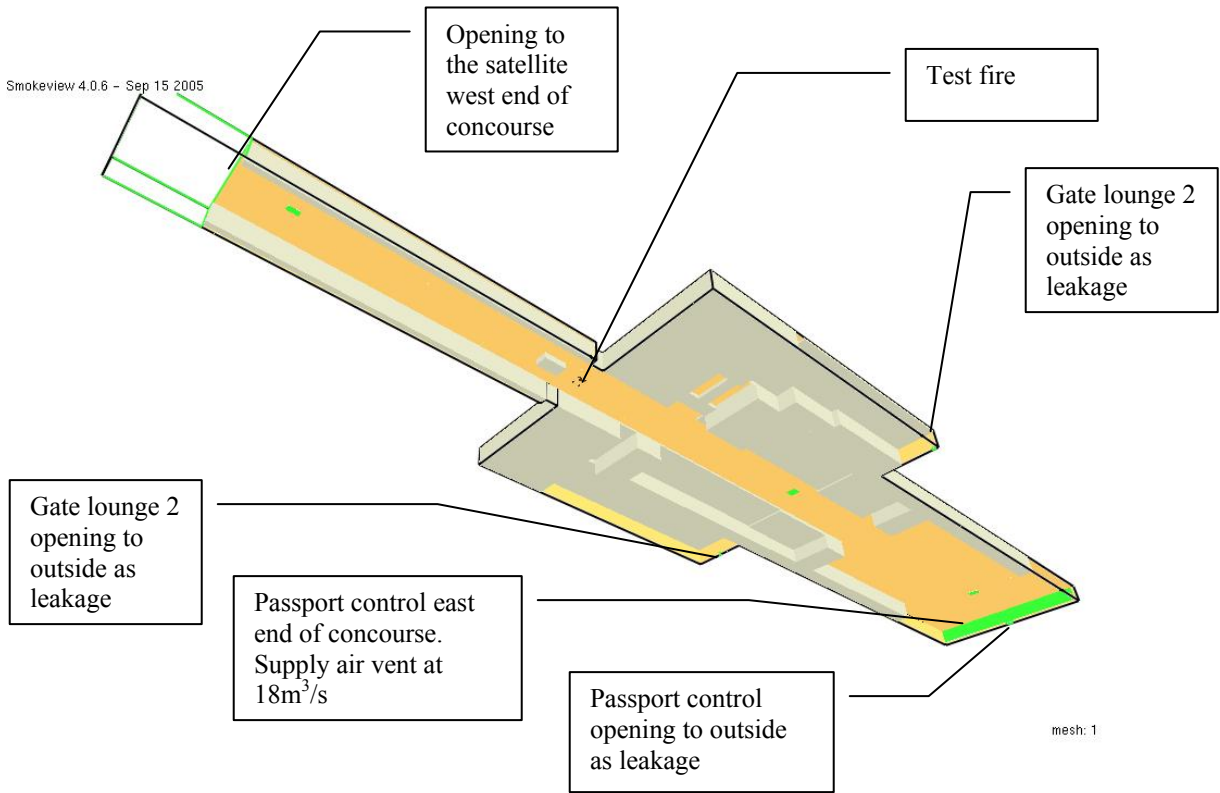


Figure 42. Perspective view of the building from below (Reflected ceiling plan view)

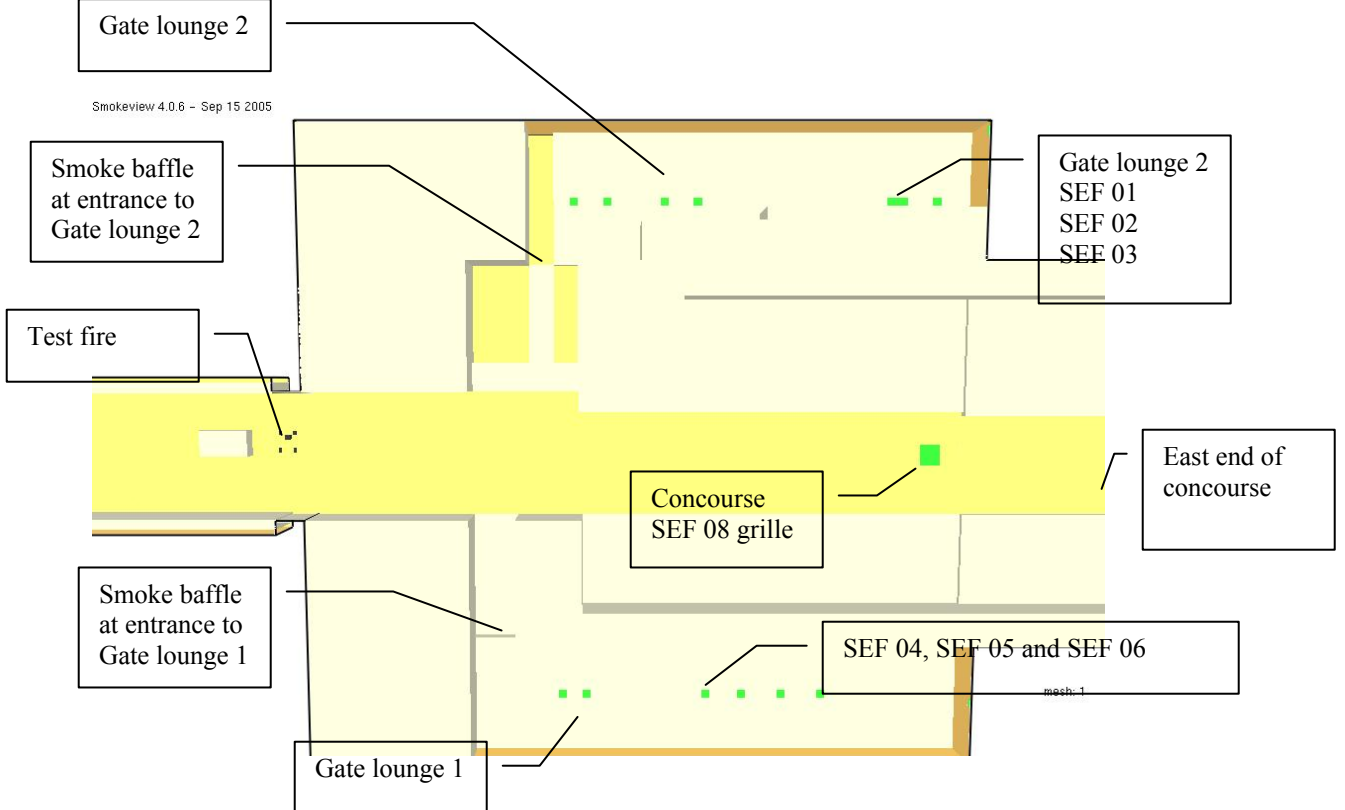


Figure 43. Perspective view of the exhaust fans in gate lounges from below (Reflected ceiling plan view)

9.2.5 *Smoke detection*

The concourse has a smoke detection system installed that complies AS 1670.1. (55). The smoke detection has not been modelled as part of the investigation.

9.3 Simulation of test 1 events

The timing of events during the test were modelled using the following parameters as input. The activation of the smoke exhaust systems was based on the activation times experienced in the testing, and not on a FDS modelled activation time of smoke detection.

Table 8. Simulation of Test 1 – FDS Hot smoke test event times and comments.

Time from commencement of smoke		Simulation time	Input event
Minutes:seconds	seconds	seconds	
-0:30	-30	0	Supply air (18m ³ /s) from passport control (east end) creates air movement from the main building toward the satellite.
-0:10	-10	30	Ignition of the trays.
0:00	0	30	Generation of smoke commenced.
0:20	20		Plume tilted so that the top of instrument location 1 is in the plume. Smoke layer reaches 16m from test fire west.
4:40	280	310	Smoke exhaust fans SEF 7, 8 and 9 manually activated. HVAC still operating.
11:00	660	690	Test ended.
			Events that do not occur: Shutdown of supply air. Activation of SEF 4, 5 and 6 in gate lounge 2. Activation of SEF 1, 2 and 3 in gate lounge 1.

9.4 Simulation of test 2 events

Table 9. Simulation of Test 2 – FDS Hot smoke test event times and comments.

Time from commencement of smoke		Simulation time	Input Event
Minutes:seconds	seconds	seconds	
-0:30	-30	0	Supply air (18m ³ /s) from passport control (east end) creates air movement from the main building toward the satellite.
-0:10	-10	30	Ignition of the trays.
0:00	0	30	Generation of smoke commenced.
0:31	31	61	Activation of smoke detection and SEF 7, 8 and 9 and supply air shut down.
3:35	205	235	Activation of SEF 4,5,6 in gate lounge 2.
5:53	353	385	Activation of SEF 1,2 and 3 in gate lounge 1.
10:00	600	630	Test terminated.

9.5 Results of test 1 model and comparison with test data.

The results of the FDS run, Input file *melbairtest1b.data* (model run b of Test 1) are plotted below showing the comparison with the experimental data gathered. The results from the FDS simulation have all been time shifted 30 seconds so that the first 30 seconds of computation used to stabilize the ambient air movement have been shifted to -30 to 0 seconds.

9.5.1 Air velocity – test 1

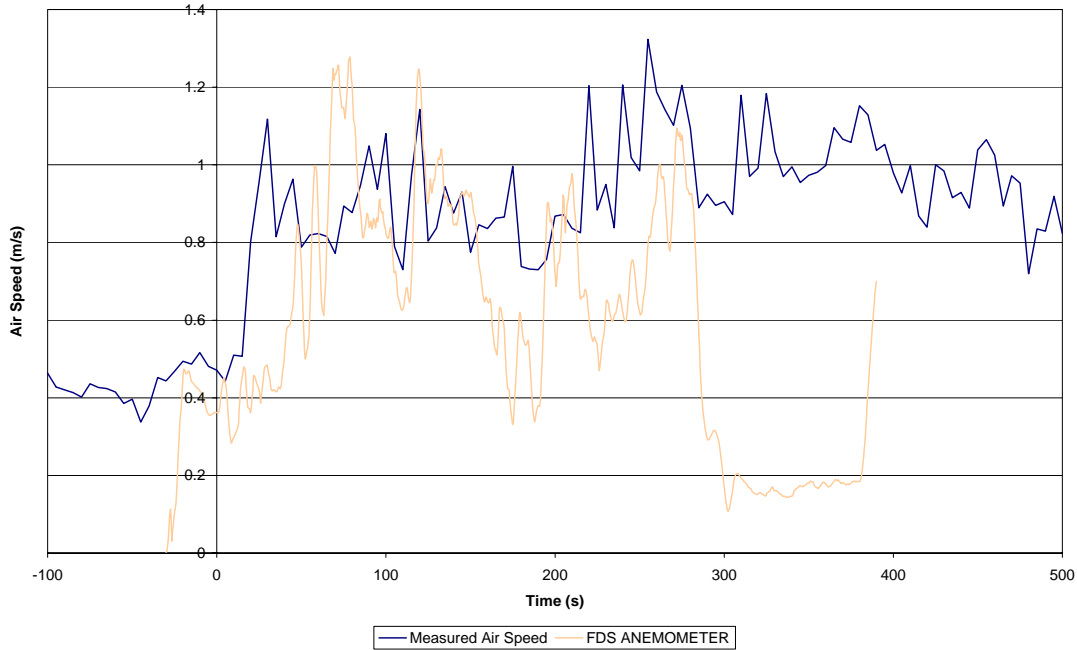


Figure 44. Air velocity station 2 – Comparison of Test 1 simulation and measured data

The supply air set-up simulates well the initial air speed of 0.4m/s at station 2 as seen in the -30 to 0 seconds of the simulation results in Figure 44. The increase in air speed due to the influence of the hot air plume is reasonably well matched for the 0 to 280 seconds period, considering the proximity to the fire tray and the turbulence in the area. In future tests it would be better to locate the anemometer further from the test fire, to measure ambient air flow field without the influence of the local plume turbulence. At 280 seconds the activation of the concourse smoke exhaust causes a drop in velocity at the location of the anemometer. The air velocity did not change following the activation of the smoke exhaust in the test. This highlights the simulation deficiency in modelling the supply air and building leakage.

9.5.2 Temperature – test 1

The simulation of the temperature at the Station 2 location, both near the fire and (at times) in the plume when the plume tilted significantly towards the satellite, was surprisingly

satisfying for the first 140 seconds. After that time the temperature settled into an oscillation between 30 and 34 degrees. The predicted temperatures are about 5 degrees above this value. When viewed in conjunction with the under-prediction of air velocity during this time the higher temperature would be expected because high air speeds would lead to an increase in mixing and cooling of plume gases.

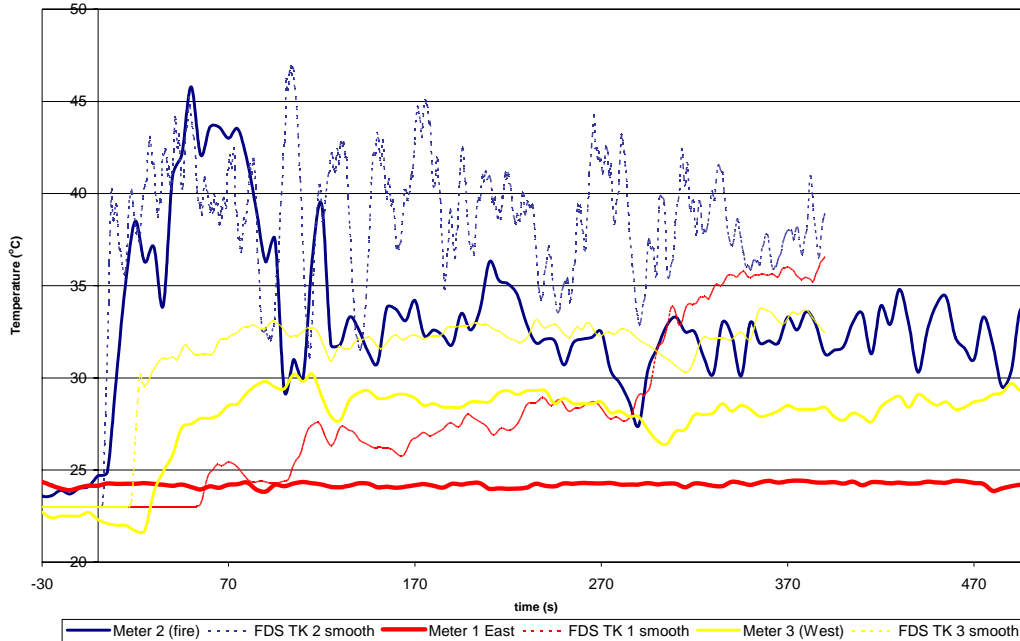


Figure 45. Temperature all stations

The temperature at station 3 is also over-predicted by 3 to 4 degrees. This however could be reduced to 1-2 degrees considering that the measured temperature at Station 3 is 2 degrees lower than at the other stations and the assumed ambient temperature for the simulation. This shift could be attributed to local air conditioning or thermocouple drift; considering this consideration the simulation result is satisfactory.

The temperature at station 1 did not increase at all in test 1 because the air velocity was high enough to prevent “back layering”. The simulation however predicted that the smoke plume would proceed up-stream to reach Station 1 and beyond. The temperature increase of about 3 to 4 °C was modelled in the period prior to the activation of the smoke exhaust in the concourse.

9.5.3 *Smoke – test 1*

The pulsing of the smoke meter in the test was unfortunate as this created impressive amplitude in the obscuration data. Two graphs are provided below, the first Figure 46 with the raw data showing the full oscillation of the recorded smoke obscuration. The second, Figure 47, has the station 2 data smoothed over 20 seconds to make comparison with the simulated data less unacceptable.

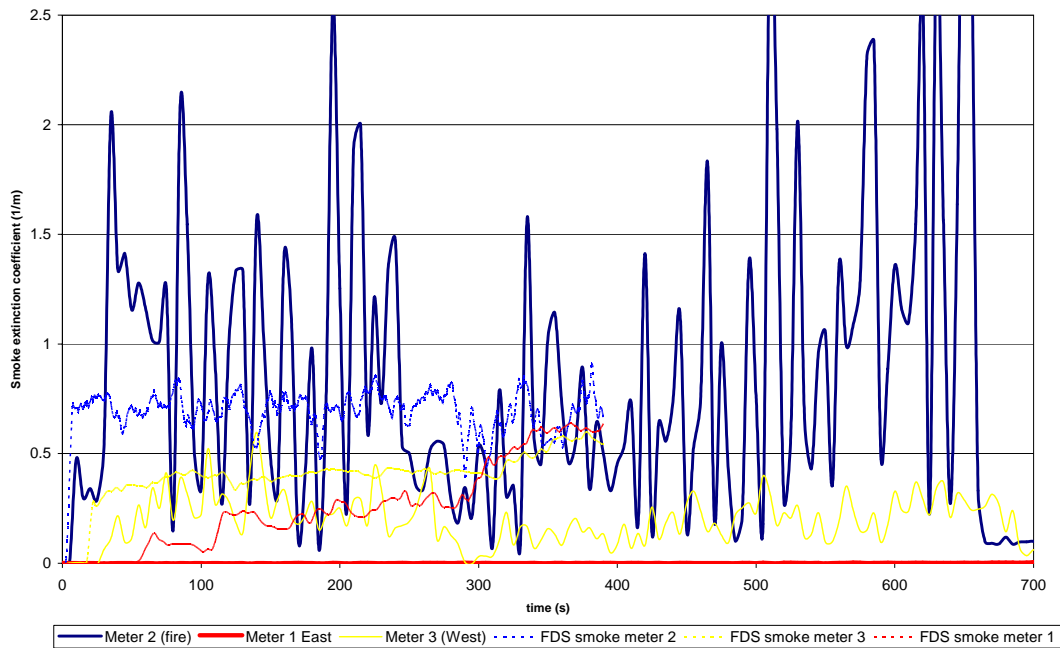


Figure 46. Smoke extinction coefficient all stations

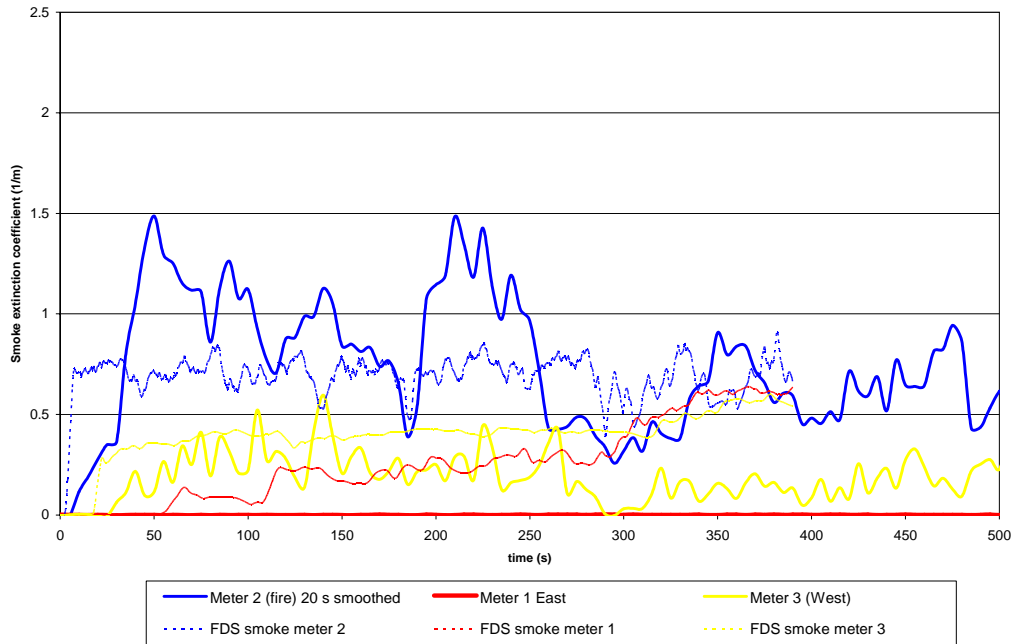


Figure 47. Smoke extinction coefficient all stations – station 2 smoothed

The obscuration at station 2 is slightly under-predicted and station 3 is over-predicted. Station 1 is over-predicted because the plume was predicted to reach the station in contradiction to the witnessed prevention of the smoke layer flowing to the station in the test. The “flat spot” in obscuration noted during the test due to plume tilt, and discussed in 8.3.1.3.3, was not predicted by FDS.

9.6 Results of test 2 model and comparison with test data.

The results of the FDS run, Input file *melbairtest2a.data* are plotted below, showing the comparison with the experimental data gathered.

9.6.1 Air velocity – test 2

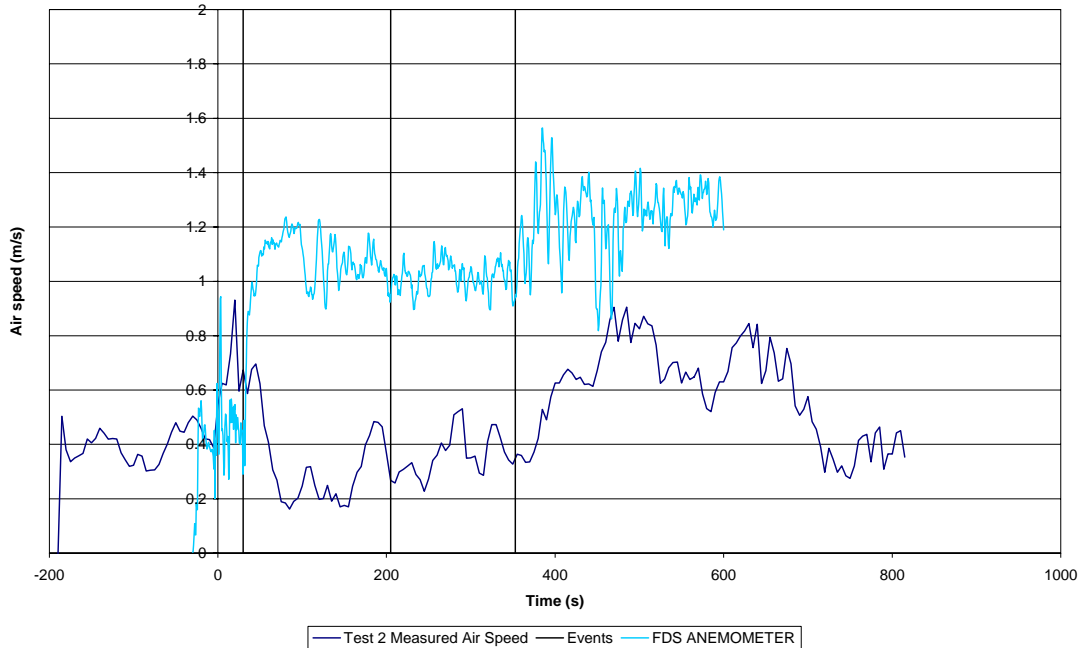


Figure 48. Air velocity station 2 – Comparison of Test 2 simulation and measured data

The supply air set-up simulates well the initial air speed at station 2 of 0.4m/s, as seen in the -30 to 0 seconds of the simulation results in Figure 48. The increase in air speed due to the influence of the hot air plume is not modelled by the simulation in the 0 to 30 s period; considering the proximity to the fire tray and the turbulence in the area this could be been expected. However, the air speed is not well simulated after the activation of the smoke exhaust fans due to the lack of information on the make up air locations, the building leakage and modelling the satellite area as an “open space”. After the activation of the smoke exhaust the error in the simulation of the air velocity has a greater impact on some aspects of the temperature and smoke, discussed below.

The FDS simulation clearly is over-estimating the air velocities within the concourse. Figure 49 shows a plot of air speed across the concourse and the entrance to gate lounge 1. The air speed of 0.6 to 1.2m/s is much higher than those measured and witnessed. The air speeds across the entrance to gate lounge 1 may be more realistic as the witnessed air speed in that location is noticeable higher.

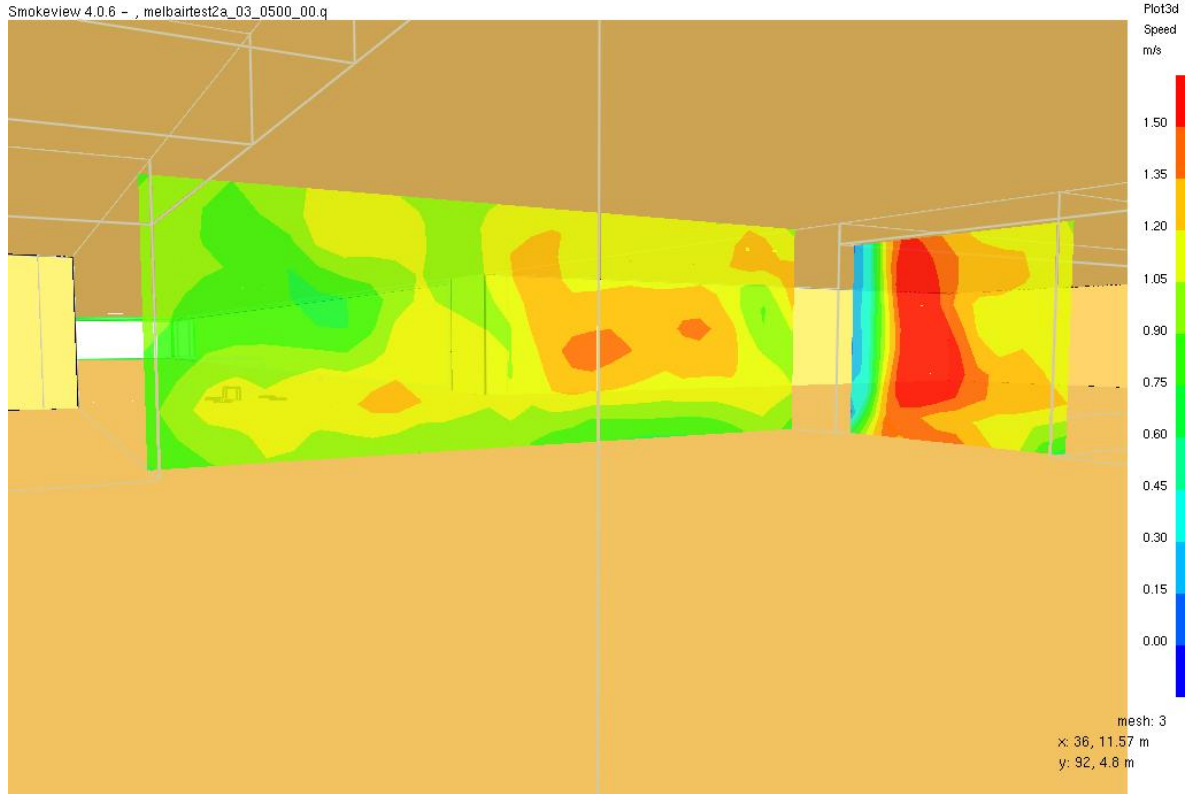


Figure 49. Air speed - Test 2 in the concourse and entrance to gate 1.

9.6.2 Temperature – test 2

The simulation of the temperature at the Station 2 location, near the fire and at times in the plume when the plume tilted significantly towards the satellite, was satisfying for the first 30 seconds prior to the activation of the concourse smoke exhaust. After 30 seconds the simulation of station 2 and 3 were not as accurate because the simulation did not have smoke west of the fire and hence the modelled temperatures and smoke obscuration were ambient conditions. At Station 1, however, the temperature was predicted satisfactorily. The measured temperature settled to 34 degrees. The predicted temperatures are about 3 degrees less than this value. When viewed in conjunction with the over-prediction of air velocity during this time the lower temperatures are expected, as high air speeds would lead to an increase in mixing and cooling of plume gases.

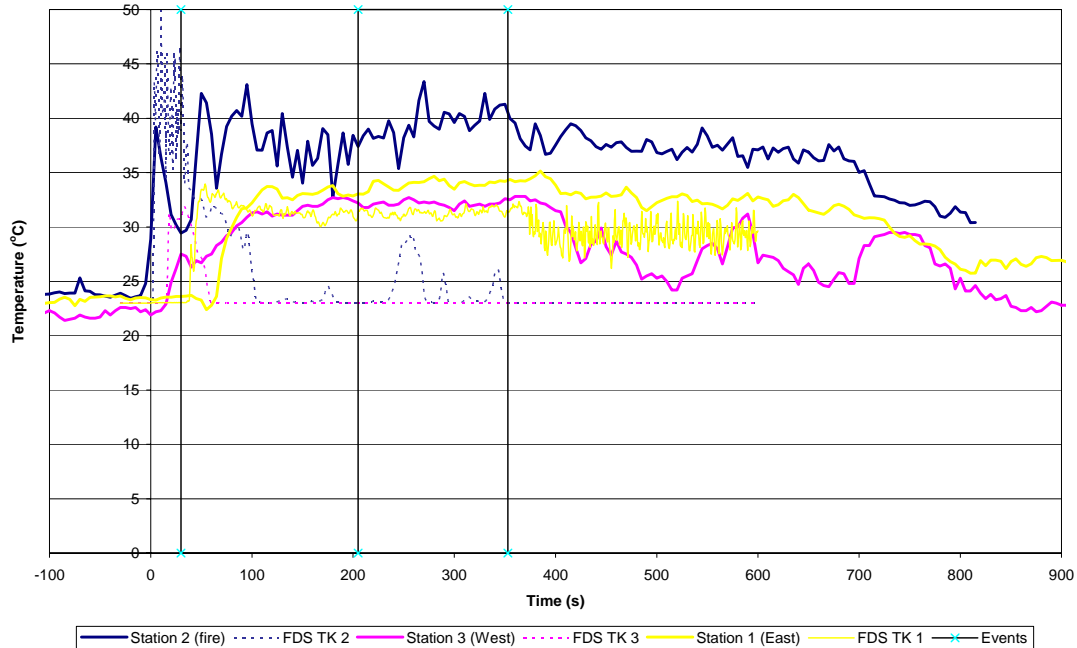


Figure 50. Temperature all stations – test 2

The temperature at station 3 was predicted accurately in the first 30 seconds, and especially the time to the start of the increase of temperature showing that FDS modelled the transport of the plume along the concourse well. FDS also predicted the rise to 32 degrees, however the timing of the rise was incorrect. The test data had a slow rise to 32°C at about 120 seconds, remaining there until the activation of the final gate lounge exhaust at 350 seconds, at which point the temperature gradually dropped away over the next 300 seconds. FDS modelled the temperature as an abrupt occurrence at 17 seconds, but dropping back to ambient by 60 seconds.

9.6.3 Smoke – test 2

The pulsing of the smoke meter in the test was unfortunate as this created considerable amplitude in the obscuration data for test 2 as well as for test 1.

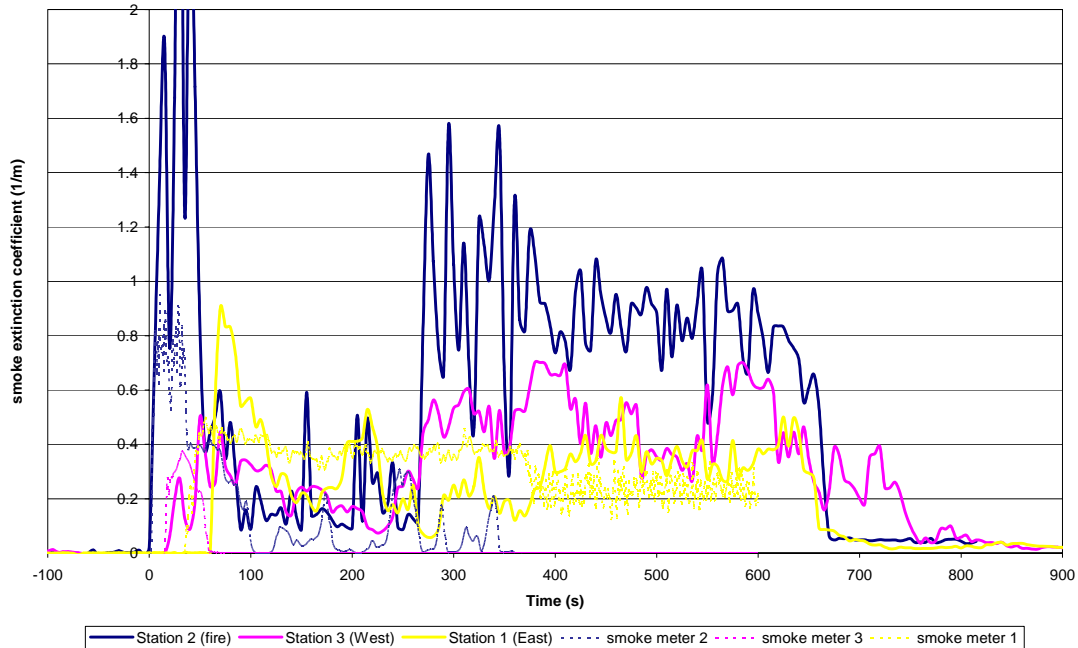


Figure 51. Smoke extinction coefficient all stations – test 2

The obscuration at station 2 is slightly under-predicted for the duration of the test.

Station 3 is well predicted for 30 seconds, but after that not at all well.

Station 1 is reasonably well predicted in both plume arrival time and obscuration.

9.7 Discussion of comparison

Some aspects of the FDS modelling satisfactorily predict the temperature, air velocity and obscuration of the hot smoke tests performed. Activation of smoke exhaust systems dramatically changed the ventilation conditions within the building and the model did not simulate this well. The air speed is not well simulated after the activation of the smoke exhaust fans. This shortcoming can be picked up in both the simulation of the anemometer measured air speed, the speed of the ceiling plume traveling along the concourse, prevention of backlayering and in the visualization of the amount of tilting of the plume. The difference between the simulation and the witnessed test may be due to one or more of the following:

- The lack of information on the make up air locations,

- the building leakage, and
- modelling the satellite area as an “open space”.

The above modelling results may also be incorrect if the smoke exhaust volumes stated in the report are not precisely being achieved by the systems. There was no way of verifying the actual quantities being achieved by the smoke exhaust systems.

9.8 Results of test 2 model with concourse exhaust at 50% and comparison with test data.

It was decided to investigate the possibility that the exhaust rates in the concourse were not as high as they were supposed to be. The reasons are two fold. In hindsight the exhaust from the gate lounges was decidedly more noticeable, in both noise and air movement, than that in the concourse.

The results of the FDS run assumed that each of the concourse fans was operating at 50% of the expected value. Input file melbairtest2c.data is plotted below showing the comparison with the experimental data. The results are described as Test 2: 50% to indicated the reduction in the concourse exhaust rate.

9.8.1 Air velocity – Test 2: 50% concourse extract

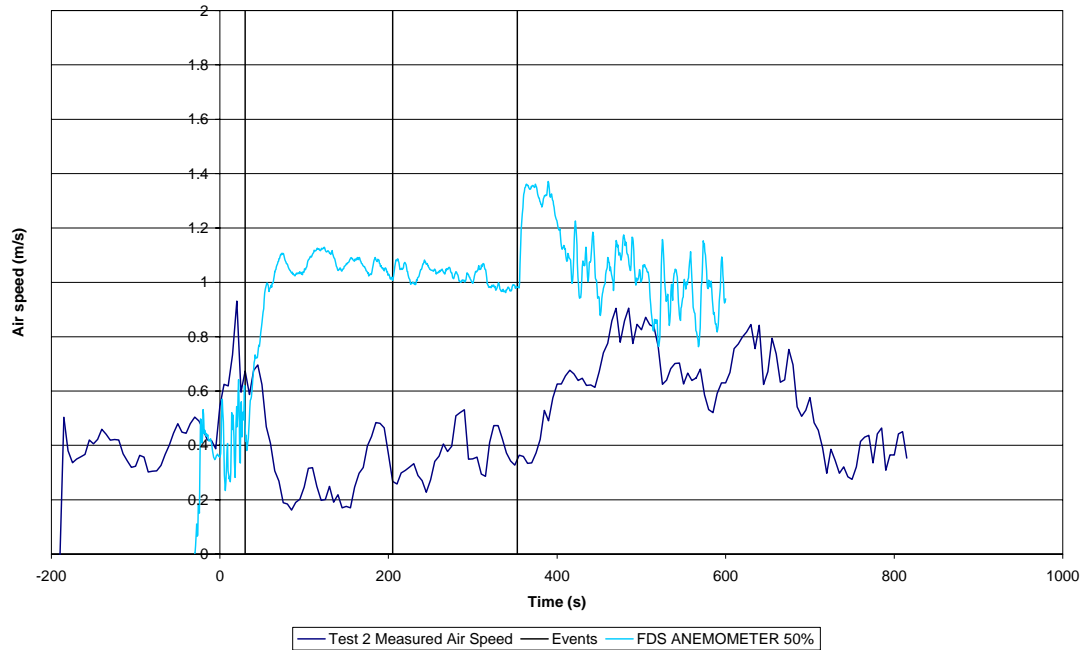


Figure 52. Air velocity station 2 – Comparison of Test 2: 50% simulation and measured data

Comparison of Figure 48 with Figure 52 shows that there may not be much difference given a lower concourse exhaust rate.

9.8.2 Temperature – Test 2: 50% concourse extract

Comparison of Figure 50 with Figure 53 shows that the reduction of exhaust rate in the concourse has dramatically improved the prediction of temperature at all the instrumentation stations. The temperature at station 1, east of the fire, is predicted well for the entire test duration. The temperature at station 2, near the fire, is predicted very well from the start of the test until 400 seconds, when the influence of the exhaust activating in gate lounge 1 takes affect. The prediction of station 3, west of the fire, is improved slightly, however it may still not be considered acceptable. Modelling a ramping-up of the exhaust rate over a 10 - 30 second period may well improve this aspect. Use of the RAMP_Q function could easily be applied to the smoke exhaust fans in the FDS model.

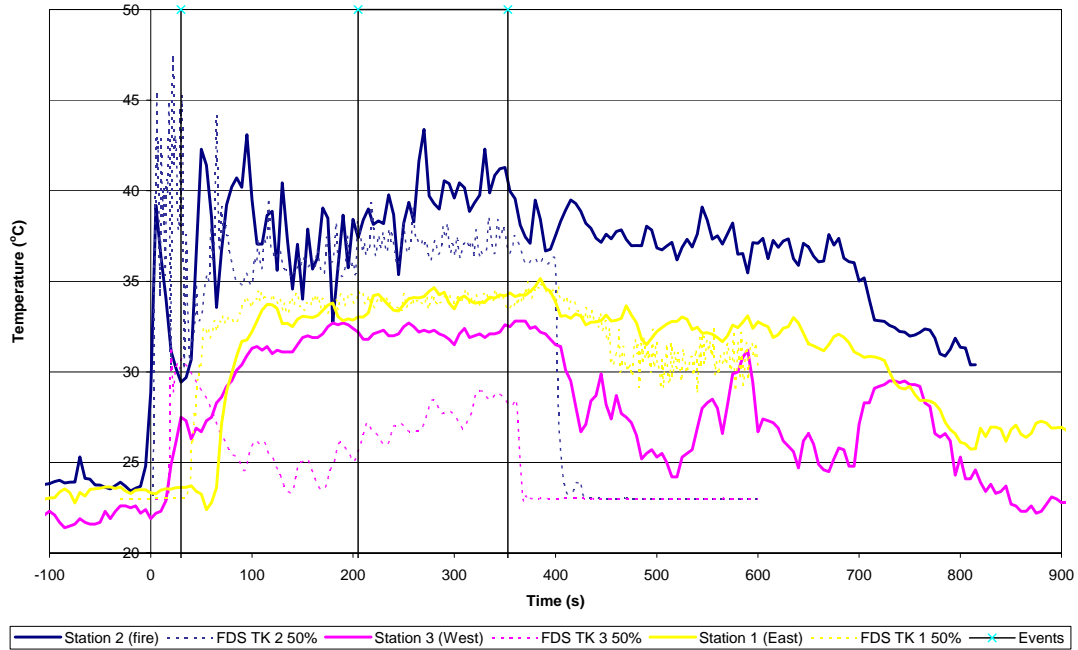


Figure 53. Temperature all stations – test 2: 50%

9.8.3 Smoke – test 2: 50% concourse extract

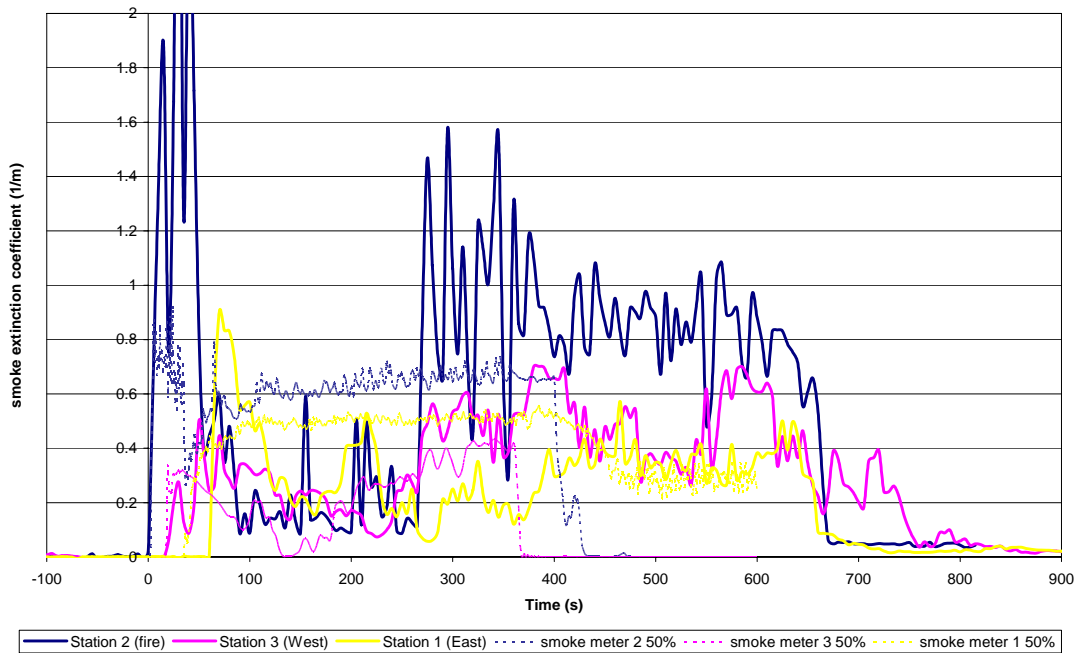


Figure 54. Smoke extinction coefficient all stations – test 2: 50%

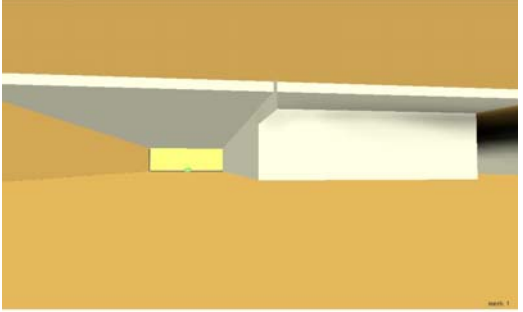
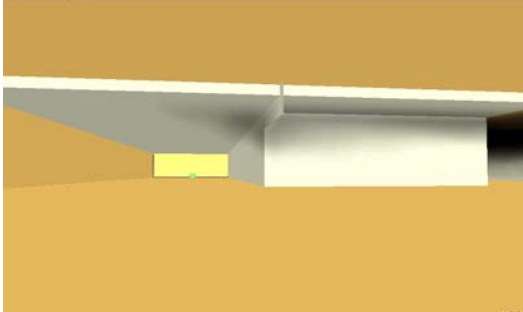
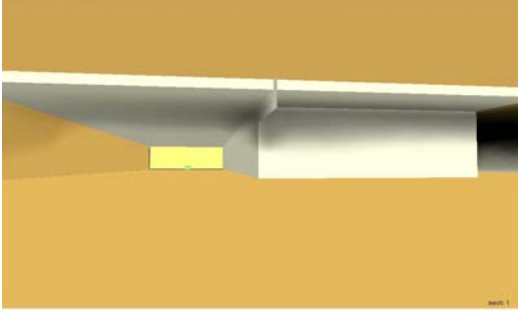
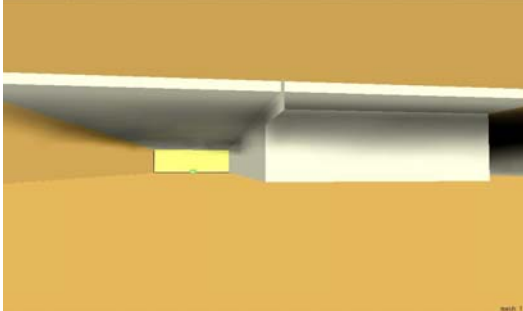
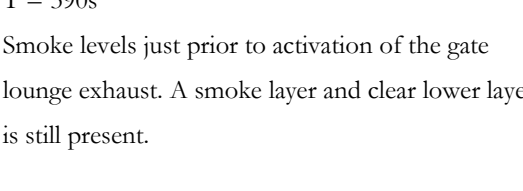
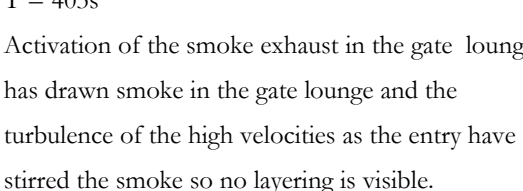
A comparison of Figure 51 with Figure 54 concludes that there is an improvement of the prediction of smoke at Station 1, but not a noticeable improvement at the other stations.

9.8.4 Test 2: 50% concourse extract impact of gate lounge exhaust

Test 2 and the test carried out in September 2003 both showed that when the gate lounge smoke exhaust systems were activated smoke was drawn into the gate lounge from the concourse. The high air velocities through the gate lounge entry corridor and spaces caused turbulence that resulted in smoke logging in the gate lounge. The FDS prediction picked up this event, which is best described by the Smokeview visualization of soot, which is included as Figure 55. The rendering at 390 seconds is 5 seconds after the activation of the gate lounge exhaust and it shows the first ball of smoke entering the lounge,

The smoke quantity of $9 \text{ m}^3/\text{s}$ drawn through the entry of a cross sectional area of 9m^2 would keep the design velocities through the corridor throat to about $1\text{m}/\text{s}$, which is below the BCA requirement of $2.5\text{m}/\text{s}$ from make-up air. The hot smoke test and FDS modelling indicate the untenable conditions may occur within the gate lounge in 400 seconds of a fire event in the concourse. The zoning of the gate lounge as a separate smoke zone has resulted in an improvement on the test in 2003, when the gate lounge was logged in 240 seconds. This discussion must of course be considered in the framework of time required to evacuate the occupants from the area, and the response of the safety systems to a “real” fire.

Figure 55 Pictures of the FDS rendering of smoke entering the Gate lounge 1.

<p>T = 113s Light smoke enters the gate lounge entry corridor.</p>	<p>T = 151s A small puff of smoke goes under the smoke baffle into the gate lounge.</p>
 <p>Smoke is visible as a thin yellow layer entering the corridor from the left. The gate lounge area is mostly clear.</p>	 <p>A small, distinct puff of smoke is shown passing under the horizontal smoke baffle into the lounge area.</p>
<p>T = 201s The smoke entering the gate lounge has reached the wall opposite the corridor.</p>	<p>T = 315s Smoke continues to drift into the gate lounge.</p>
 <p>The smoke layer has expanded and is now touching the wall opposite the entry corridor.</p>	 <p>The smoke layer has grown significantly and is drifting further into the lounge area.</p>
<p>T = 390s Smoke levels just prior to activation of the gate lounge exhaust. A smoke layer and clear lower layer is still present.</p>	<p>T = 403s Activation of the smoke exhaust in the gate lounge has drawn smoke in the gate lounge and the turbulence of the high velocities as the entry have stirred the smoke so no layering is visible.</p>
 <p>A clear, stratified smoke layer is visible at the top of the lounge, with a clear lower layer below it.</p>	 <p>The smoke is now fully mixed and stirred, with no visible layering, indicating the effect of the exhaust system.</p>



9.9 Grid Sensitivity analysis.

A grid sensitivity study was carried out on the run with the concourse exhaust rates at 50 %. The run title was Melbairtest2c, which had cells 50mm on a side in the fire area. The grid resolution was considered appropriate based on the analysis in Section 5 and the guidelines of ensuring 20 to be within the diameter of the fire (28). Each fire tray was 300mm x 200mm and there were $6 \times 4 = 24$ cells to the fire grid.

Melbairtest2e was set up with grids 1, 2 and 3 having 1/8 as many cells as Melbairtest2c. A reduction in the number of cells was a simple job, however, increasing the number of cells and keeping the same co-ordinates is not as easy. A simple doubling of the number of cells

in each direction results in over 5 million cells which, would take a week or more of computer time to complete.

Melbairtest2d was set up with the fire grid split into 3 grids and the concourse east split into 2 grids with the same number of nodes. It was realized that this would still lead to long computation times once the grid resolution was refined. Therefore Melbairtest2f was created with a total of 10 grid blocks and with the same number of cells as Melbairtest2c.

Melbairtest2g based on the 10 grids of Melbairtest2f but the fire grid was divided into 4 grids; three of these had the same resolution as Melbairtest2c; plus the 2m x 2m by 1.5m high region around the fire with double the resolution. 12m either side of the fire in the “west concourse” and “east concourse” was doubled in resolution.

The number of cells for each run is described in Table 10.

The results for the smallest and mid size domains are compared in Figure 56. The smaller grid predicts higher temperatures for Station 2 (near the fire) and station 3 (west of the fire). Station 1 is still reasonably well predicted.

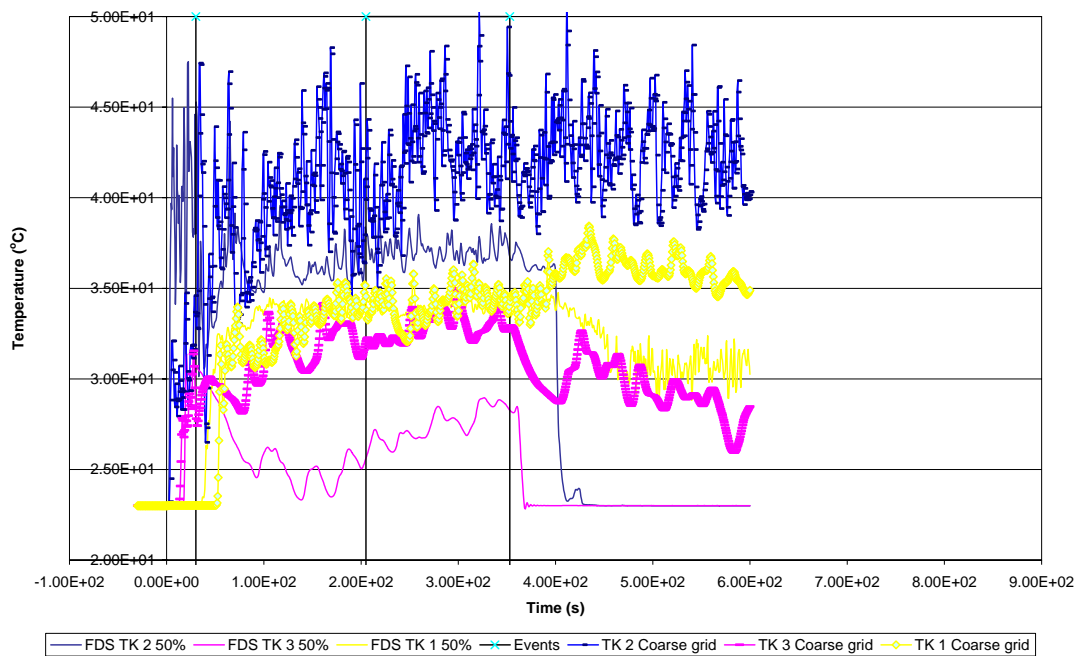


Figure 56. Grid sensitivity comparison of thermocouple readings 750,000 cells (Melbairtest2c) vs 114,000 cells (Melbairtest2e)

The prediction of higher temperatures is an indication of a lack of resolution of the turbulence leading to less mixing of ambient air into the plume in turn leading to over prediction of temperatures.

The comparison of the finest resolution grid and that of the base calculation shows that only minor variation occurred in the temperatures (Figure 57). The conclusion can be drawn that the grid resolution originally selected and used for the majority of the calculations was adequate, and that the model is insensitive to further increase in grid resolution. The grid resolution was 0.05m around the fire and 0.3 throughout the remainder of the domain.

Note that in comparison to other reported simulations the number of nodes is high. The *International Collaborative Project to Evaluate Fire Models for Nuclear Power Plant Applications* (22) analyzed a test designated as Benchmark Exercise #2. In all, 216,000 grid cells were used in that calculation (22).

Simulation of the WTC fire by NIST (22) were made using a 500mm by 500mm by 400mm.

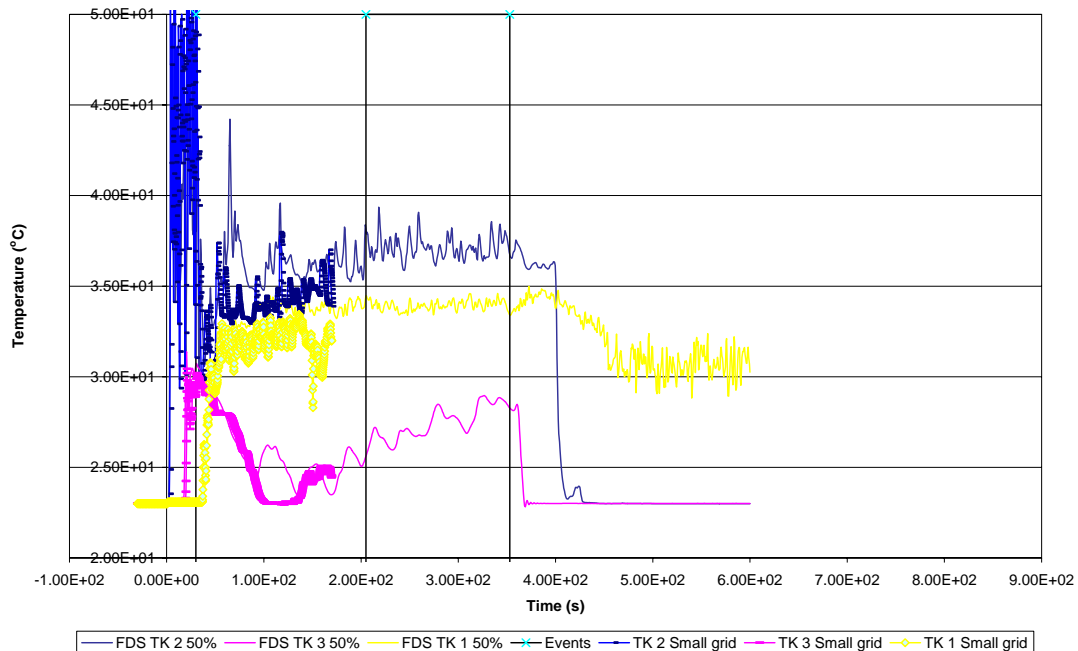


Figure 57. Grid sensitivity comparison of thermocouple readings 750,000 cells (Melbairtest2c) vs 1,440,900 cells (Melbairtest2g) for the first 200 seconds.

Table 10. FDS grid sensitivity runs

Grid	Melbairtest2c	Melbairtest2e	Melbairtest2d	Melbairtest2f	Melbairtest2g
1. Fire	IBAR=40 JBAR=180 KBAR=60 TOT 432k	IBAR=20 JBAR=90 KBAR=30 TOT 54k	1a IBAR=40 JBAR=40 KBAR=60 1b IBAR=40 JBAR=80 KBAR=60 1c IBAR=40 JBAR=60 KBAR=60 TOT 432k	1a IBAR=40 JBAR=40 KBAR=30 1b IBAR=40 JBAR=40 KBAR=30 1c IBAR=40 JBAR=50 KBAR=60 1d IBAR=40 JBAR=90 KBAR=60 TOT 432k	<i>1a IBAR=80</i> <i>JBAR=80</i> <i>KBAR=60</i> 1b IBAR=40 JBAR=40 KBAR=30 1c IBAR=40 JBAR=50 KBAR=60 1d IBAR=40 JBAR=50 KBAR=60 TOT 768k
2. Concourse west	IBAR=150 JBAR=30 KBAR=10 TOT 45k	IBAR=75 JBAR=15 KBAR=5 TOT 5.6k	= Melbairtest2c	2a IBAR=75 JBAR=30 KBAR=10 2b IBAR=75 JBAR=30 KBAR=10 TOT 45k	<i>2a IBAR=150</i> <i>JBAR=60</i> <i>KBAR=20</i> 2b IBAR=75 JBAR=30 KBAR=10 TOT 202k
3. Concourse east	IBAR=160 JBAR=150 KBAR=10 TOT 240k	IBAR=80 JBAR=75 KBAR=5 30k	3a IBAR=80 JBAR=150 KBAR=10 3b IBAR=80 JBAR=150 KBAR=10 TOT 240k	3a IBAR=40 JBAR=30 KBAR=10 3b IBAR=40 JBAR=150 KBAR=10 3c IBAR=80 JBAR=150 KBAR=10 TOT 192k*	<i>3a IBAR=80</i> <i>JBAR=60</i> <i>KBAR=20</i> 3b IBAR=40 JBAR=150 KBAR=10 3c IBAR=80 JBAR=150 KBAR=10 TOT 276k
4. Duty free	IBAR=108 JBAR=45 KBAR=5 TOT 24.3k	= Melbairtest2c	= Melbairtest2c	= Melbairtest2c	<i>4 IBAR=216</i> <i>JBAR=90</i> <i>KBAR=10</i> TOT 194k
Total number of cells	741,000 4 grids	113,925 4 grids	741,000 7 grids	693,000* 10 grids	1,440,900 10 grids
For first 200 seconds of the simulation.					
Time taken on desktop	16 hours 06 min Total CPU time 18.93hr	6:34 Total CPU time 24.67hr	16hours 34min Total CPU time 20.11hr	TBC??	NA
Time taken on HPSC	48 hours 14min Total CPU time 183.7 1hr	NA	13hours 34 minutes 89.12 hours	NA	TBC??

Notes: Grids in Melbairtest2g in *italics* are those with increased resolution.

* reduction in total node number is due to deletion of nodes within obstacles made possible by re-gridding.

9.10 Computation Sensitivity analysis.

The results for Melbairtest2d from the desktop and the HSPC multi processor are compared in **Figure 58** and **Figure 59**. The slight differences between the results is probably due to the fact that *FDS*

...uses the random number generator that is a standard feature in Fortran 90 to initialize the flow field with a small amount of *noise* to break up any unphysical symmetric flows that can occur when the initial and boundary conditions are symmetric. Each processor generates a unique sequence of random numbers that lead to the different results. However, these different results ought to be very slight, comparable to (sic) the different results one would expect from two fire experiments with the exact same parameters and procedures (50).

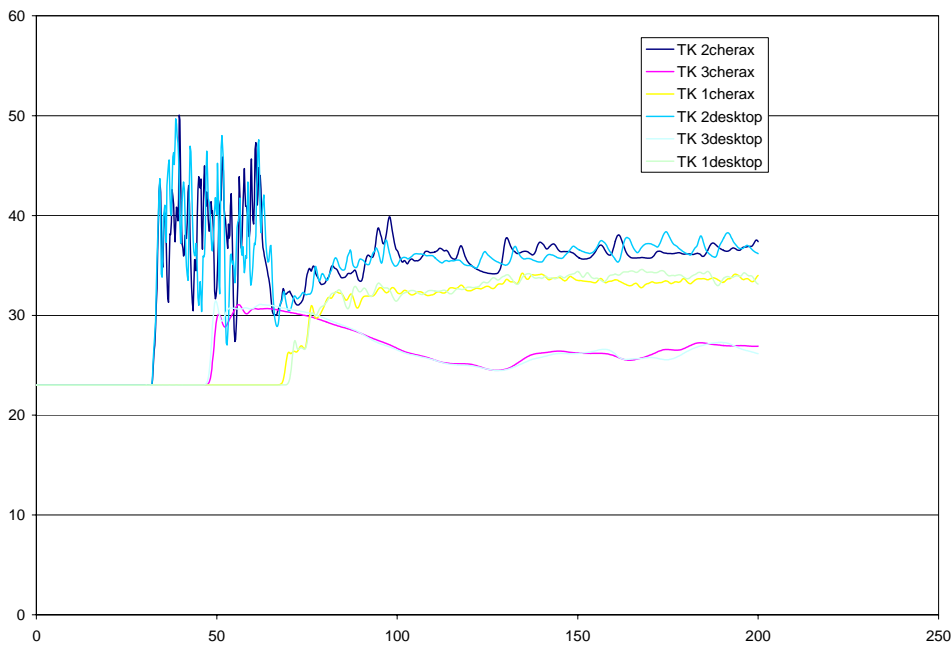


Figure 58. Grid sensitivity comparison desktop and the HSPC temperatures

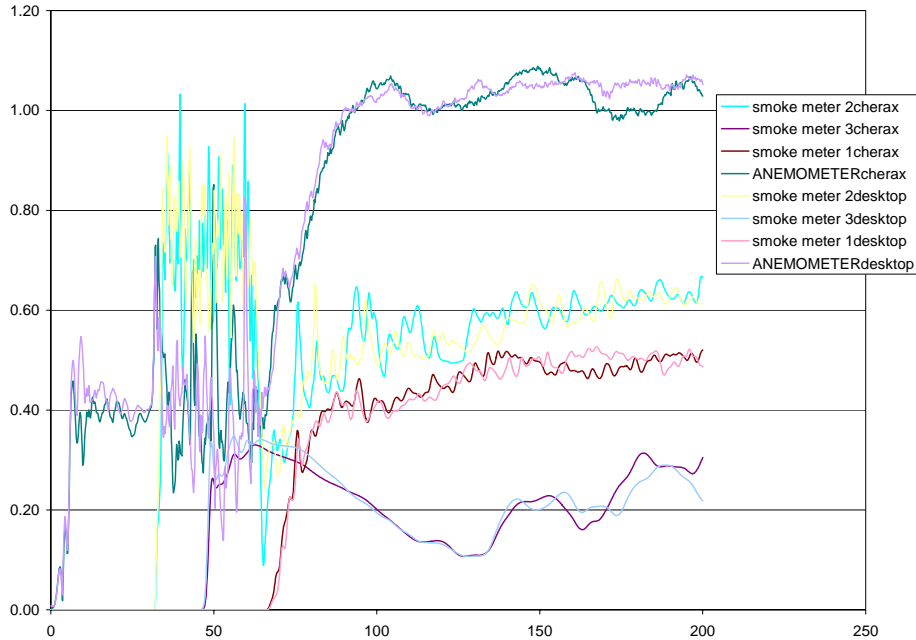


Figure 59. Grid sensitivity comparison desktop and the HSPC temperatures smoke and air speed

10 DISCUSSION

The above analysis of the fuel tray fire, cinema complex and airport HST have been performed with consideration to the typical limitations on resources that confront many fire protection engineers. The analysis then steps beyond, as most would not have access to multiprocessor capability.

Section 5 showed the difficulty in predicting the plume temperatures of the fire. Further work is needed in this area.

The cinema HST was reasonably well predicted in a qualitative fashion given the simple geometry, exhaust and make up air locations. It is expected that a typical fire protection engineer, with due diligence could satisfactorily use FDS for prediction purposes.

The test in the airport concourse contained issues that would challenge “typical modelers”. Some aspects of the FD modelling satisfactorily model the temperature, air velocity and obscuration of the hot smoke tests performed. In contrast, activation of smoke exhaust systems dramatically changed the ventilation conditions within the building and the model

did not simulate this well. The air speed is not well simulated after the activation of the smoke exhaust fans due to one or more of the following:

- the lack of information on the make up air locations;
- the building leakage; and
- modelling the satellite area as an “open space”.

A typical fire protection engineer would have difficulty predicting a hot smoke test in the given building geometry and complexity. Given these deficiencies however the results were none-the-less promising in that with further information on the building a simulation may be much closer to the measured values.

10.1 Improvements to the testing

Improvements that could be applied to the test and gathering of data are:

- Air velocity measurements taken further from the fire location to reduce the impact of local turbulence, unless multiple anemometers are available;
- A smoke meter located at the smoke source to get a baseline smoke density. CSIRO has built, and sells, smoke meters air cooled and temperature compensated, and that can withstand high temperatures;
- Development of an easy-to-set-up instrument station with temperature, air velocity and smoke with radio modem, that can be transported to site and placed with a minimum of on-site work.; and
- Mass and oxygen consumption calorimetry could be carried out for methylated spirit fires and all trays sizes. Plume temperatures should also be measured and comparisons made with Chow's measurement (60) and HRR estimates in the standard.

10.2 Improvements to the modelling

The following improvements could be applied to the FDS modelling:

- The temperature prediction of the fuel tray fire plume must be improved to get a reasonable comparison at 2 to 3m height above the fire.
- Inclusion of the satellite space as a further grid to better model the influence of the large but enclosed space;
- Include AHU locations and flow rates. Modelling of the gate lounge AHU supply would improve the prediction of the initial smoke entering the lounge and subsequent smoke detection;
- Ramp up exhaust fan flow rates over 30 s. using RAMP function instead of the near instantaneous smoke exhaust which would better simulate the typical flow rate increase for a fan start up;

- Modelling of smoke detection and corresponding activation of the smoke exhaust fans would further calibrate the FDS model ability to simulate detection systems;
- Model the building leakage using typical leakage rates as documented in NFPA 92A Table 4.5 (45) would better simulate make air and the influence of air velocity with the spaces;
- Compare the HST to a real fire scenario of a growing fire that may be expected in the airport would provide further information on the relevance of HST in simulation of real fires;
- Model the smoke generator as a particulate source independent of the methylated spirit fire to more closely simulate the HST set up;
- Investigate cooling of the tray due to water i.e. metho/tray doesn't get over 100°C. Also cooling of the plume by air moving over the water; and
- Investigate the time lag coefficient of the thermocouple model in FDS and adjust it for 2mm ungrounded MIMS type K thermocouple as FDS default is 1mm.

11 CONCLUSIONS

The author and staff of Commonwealth Scientific and Industrial Research Organization (CSIRO) performed hot smoke tests (HST) according to Australian Standard AS 4391 -1999 in two buildings. In some tests air temperatures, air speed and smoke optical density were recorded at several locations during some of the tests.

These were later modelled in Fire Dynamic Simulator (FDS) to show that a computer model may accurately predict results comparable to a full-sized simulation scenario within the limits of complex building systems. As expected the more complex the building and air movement the greater the discrepancy between the prediction and the test data. The modelling was improved by an investigation and resulting understanding of the relationship between fuel properties; plume temperature and dynamics, and grid sensitivity. This work may be considered beyond what a "typical" engineer would apply to the problem and further work is required to refine the input data to an acceptable level. Although the FDS hot smoke model predicted comparable results to the actual fire test, computer modelling should obviously never be used as a system installation certification tool.

The study showed that tightly controlled fire experiments will always provide much more accurate data for model verification than a hot smoke test in a complex “real life” building. However, data from hot smoke tests, if gathered cost effectively on tests that are occurring for the commissioning or certification of safety can still be a valuable resource for computer model verification. FDS modelled the major aspects of the smoke movement witnessed during the testing, however several aspects created limitations to the ability of the model to predict air temperatures, air speed and smoke optical density at the later stage of the tests.

The study also concluded that the use of Morgan’s method may lead to under prediction of temperature of the upper layer during a hot smoke test. Further work in this area may be focused on the potential improvements identified for future tests as well as additional improvements that could be applied to the FDS modelling.

12 ACKNOWLEDGEMENTS

I would like to thank the following people. The CSIRO staff: Glenn Bradbury, Nathan White, Ashley Bicknell and Dave O'Brien for the data gathering assistance; the Sydney HST team Atul Bhargava, Russell Collins, Jim Hooke and Hugh Allan for making the late nights wandering through the fog seem less like work. CSIRO for the time and money to attend WPI. Julie McInerney for her Procite finesse. My advisor Jonathon Barnett for the encouragement and patience to sort the ADLN challenges when he has a plethora of advisees. Judith Jones for the editorial adjustments. Yunlong Liu for the wrestling tips to tame cherax. Most importantly the support and love of my family Anna, Max and Ben. Above all, to all of the above, my affection for your patience during my glacial progress over the last years.

13 REFERENCES

Reference List

1. Allan H. Testing smoke control in atriums and other complex buildings. Fire Australia 1991;5-6.
2. Allan H, Delichatsios M. Hot smoke testing in tunnels: Melbourne's Citylink. Fire Australia 1999 Nov;28-30.
3. Allan, Hugh; Hooke, Jim, Hot Smoke Tests used to advance smoke control methodology ASIAFLAM '95, Proceedings of the 1st International Conference; Kowloon, Hong Kong. 1992. pp. 345-50.
4. Associated Engineers. Subway Environment Design Handbook, Volume II, Subway Environment Simulation (SES) Computer Program, Version 3.0, Part 1: User's Manual. Prepared for the Transportation Systems Center of the U.S.D.O.T.: Associated Engineers, a Joint Venture of Parsons Brinckerhoff Quade and Douglas, Inc, De Leuw Cather and Company, and Kaiser Engineers.; 1980.

5. Australian Building Codes Board. BCA 2004, Building Code of Australia, Class 2 to 9 Buildings. Canberra: CanPrint Communications Pty Ltd; 2004.
6. Australian Building Codes Board. International Fire Engineering Guidelines. Canberra: Australian Building Codes Board; 2005.
7. Baum, H. R.; Rehm, R. G.; Lozier, D. W.; Tang, H.; Sims, J. Buoyant Convection in an Inclined Enclosure *Fire Safety Science – Proceedings of the Third International Symposium*, International Association for Fire Safety Science, 1991. p. 313–323.
8. BS. Application of fire safety engineering principles to the design of buildings - Part 2:(Sub-system 2) Spread of smoke and toxic gasses within and beyond the enclosure of origin. British Standards; 2002. Report No.: BS 7974-2:2002.
9. Chow WK, Li YZ, Cui E, Huo R. Natural smoke filling atrium with liquid pool fire up to 1.6MW. *Building and Environment* 2001;36:121-7.
10. Colt International. [Web Page]; <http://www.coltinfo.co.uk/products-and-systems/smoke-control/car-parks.html>.
11. Colt International Limited. Car park ventilation - full scale "live" smoke tests. Hampshire: Colt International Limited; 2004. PD56:12/04.
12. Colt International Limited. Car park ventilation - full scale live smoke tests. Impulse ventilation or smoke control. Hampshire: Colt International Limited; 2006. PD61:04/06.
13. "Basic Considerations" Combustion Fundamentals of Fire. Academic Press; 1995.
14. Cox, Geoff; Kumar, Suresh. Section 3 Chapter 8 Modelling enclosure fires using CFD. DiNenno 3rd ed. Quincy: National Fire Protection Association; 2002.
15. FirecalcCSIRO Suite of fire models Version 3.2. 1995.
16. Davis, W.; Notarianni, K.; McGrattan, K. Comparison of Fire Model Predictions with Experiments Conducted in a Hangar with a 15 Meter Ceiling. Gaithersburg, Maryland: National Institute of Standards and Technology; 1996 Dec. Report No.: NISTIR 5927.
17. Dey, Monideep K.; Hamins, Anthony; Miles, Stewart. International Collaborative Project to evaluate fire models for nuclear power plant applications: summary of 5th meeting. Gaithersburg, MD: National Institute of Standards and Technology; 2002 May 2-2002 May 3. Report No.: NISTIR 6986. Main report.
18. Emmerich, S. J. Use of Computational Fluid Dynamics to Analyze Indoor Air Quality Issues. Gaithersburg, Maryland: National Institute of Standards and Technology; 1997 Apr. Report No.: NISTIR 5997.

19. Emmerich, S. J.; McGrattan, K. B. Application of a Large Eddy Simulation Model to Study Room Airflow. *ASHRAE Transactions*, 1998. Report No.: 104(1):1-9.
20. Floyd, J. D. ; Baum, H. R.; McGrattan, K. B. A mixture fraction combustion model for fire simulation using CFD. *Proceedings of the International Conference on Engineered Fire Protection Design* San Francisco, CA; 2001. pp. 279-90.
21. Forney, G. P.; McGrattan, K. B. User's Guide for Smokeview Version 4.0 – A Tool for Visualizing Fire Dynamics Simulation Data. National Institute of Standards and Technology; 2004. Report No.: NIST Special Publication 1017.
22. Gann, Richard D.; McGrattan, Kevin. B.; Hamins, Anthony, et al. Federal Building and Fire Safety Investigation of the World Trade Centre Disaster. Reconstruction of the fires in the World Trade Centre towers. Gaithersburg, MD: National Institute of Standards and Technology; 2005 Sep. Report No.: NIST NCSTAR 1-5. 186 pages.
23. Hamins, A.; Maranghides, A.; McGrattan, K. B., et al. Report on Experiments to Validate Fire Dynamic and Thermal-Structural Models for Use in the World Trade Center Investigation. Gaithersburg, Maryland: National Institute of Standards and Technology, 2004 Sep. Report No.: NIST Special Publication 1000-B.
24. Hansell, G. O.; Morgan, H. P. Design approaches for smoke control in atrium buildings. Garton: Fire Research Station, Building Research Establishment; 1994. Report No.: BR 258.
25. Hansell, G. O.; Morgan, H. P. Design approaches for smoke control in atrium buildings. Garton: Fire Research Station, Building Research Establishment; 1994. Report No.: BR 258.
26. Hansell, G. O.; Morgan, H. P. Design principles for smoke ventilation in enclosed shopping centres. Borehamwood: Fire Research Station, Building Research Establishment; 1994.
27. Hansell, G. O.; Morgan, H. P. Design principles for smoke ventilation in enclosed shopping centres. Borehamwood: Fire Research Station, Building Research Establishment; 1994.
28. Hietaniemi, J.; Hostikka, S.; Vaari, J. FDS Simulation of Fire Spread – Comparison of Model Results with Experimental Data. Espoo, Finland: VTT Building and Transport; 2004. Report No.: VTT Working Paper 4.
29. Hostikka, S. ; McGrattan, K. B.; Hamins, A. Numerical Modeling of Pool Fires using Large Eddy Simulation and Finite Volume Method for Radiation. *Fire Safety Science – Proceedings of the Seventh International Symposium*: International Association for Fire Safety Science, pages 383–394.

30. Hughes Associates Inc. [Web Page];
<http://www.haifire.com/download/slipsheets/SmokeControl.pdf#search=%22hot%20smoke%20test%22>.
31. Kashef, Ahmed. [Web Page]; http://irc.nrc-cnrc.gc.ca/fr/smbe/maurice_e.html.
32. Labein Tecnalía. [Web Page]; http://www.labein.es/isai/Index_en.htm.
33. Land Transport Authority. [Web Page];
http://app.lta.gov.sg/corp_press_content.asp?start=1470.
34. Marchant, Roger. Personal communication 2005 Oct.
35. McGrattan, K. B. Fire Dynamics Simulator (Version 4) – Technical Reference Guide. National Institute of Standards and Technology; 2004. Report No.: NIST Special Publication 1018.
36. McGrattan, K. B. Fire Dynamics Simulator (Version 4) – Technical Reference Guide. National Institute of Standards and Technology; 2004. Report No.: NIST Special Publication 1018.
37. McGrattan, K. B. Fire Dynamics Simulator (Version 4) – Technical Reference Guide. National Institute of Standards and Technology; 2004. Report No.: NIST Special Publication 1018.
38. McGrattan, K. B. Fire Dynamics Simulator (Version 4) – Technical Reference Guide. National Institute of Standards and Technology; 2004. Report No.: NIST Special Publication 1018.
39. McGrattan KB , Baum HR, Rehm RG. Large Eddy Simulations of Smoke Movement. Fire Safety Journal 1998;30:161–17.
40. McGrattan, K. B.; Forney, G. P. Fire Dynamics Simulator (Version 4) – User’s Guide. National Institute of Standards and Technology; 2004. Report No.: NIST Special Publication 1019.
41. McGrattan, K. B.; Forney, G. P. Fire Dynamics Simulator (Version 4) – User’s Guide. National Institute of Standards and Technology; 2004. Report No.: NIST Special Publication 1019.
42. Milke, A. J.; Klote, J. H. Smoke management in large spaces in buildings. Melbourne: Building Control Commission; 1998.
43. Morgan HP, De Smedt J-C. Hot smoke test: testing the design performance of smoke and heat ventilation systems and of impulse ventilation systems. International Journal on Engineering Performance-Based Fire Codes 2004;6(number 1):7-18.

44. Morgan, H. P.; Ghoush, G.; Garrad, G., et al. Morgan, H. P.; Ghoush, G.; Garrad, G., et al. Design methodologies for smoke and heat exhaust ventilation. London: CRC; 1999. Report No.: BR 368. (Building Research Establishment report.
45. National Fire Protection Association. NFPA 92A: Recommended Practice for Smoke Control Systems. Quincy, MA: National Fire Protection Association; 2000.
46. National Fire Protection Association. NFPA 92B: Guide for Smoke Management Systems in Malls, Atria, and Large Areas. Quincy, MA: National Fire Protection Association; 2000.
47. National Fire Protection Association. NFPA 92B: Guide for Smoke Management Systems in Malls, Atria, and Large Areas. Quincy, MA: National Fire Protection Association; 2000.
48. National Fire Protection Association. NFPA 204 Standard for Smoke and Heat Venting. Quincy, MA: National Fire Protection Association; 2002.
49. National Fire Protection Association. NFPA 204 Standard for Smoke and Heat Venting. Quincy, MA: National Fire Protection Association; 2002.
50. NIST. FDS Frequently Asked Questions. [Web Page]; <http://www.fire.nist.gov/fds/docs/fdsfaq.html>. [Accessed 9 Jun 2006].
51. Patankar, Suhas V. Numerical Heat Transfer and Fluid Flow. New York: McGraw-Hill Book Company; 1980. 197 .
52. Rehm RG, Baum HR. The Equations of Motion for Thermally Driven, Buoyant Flows. *Journal of Research of the NBS* 1978;83:297-308.
53. Smagorinsky J. General Circulation Experiments with the Primitive Equations. I. The Basic Experiment. *Monthly Weather Review* 1963 Mar;93((3)):99-164.
54. Standards Australia. Australian Standard 4391- Smoke management systems - hot smoke test. Standards Australia; 1999. Report No.: AS 4391:1998.
55. Standards Australia. Australian Standard 1670 Part 1- Fire detection, warning, control and intercom systems - System design, installation and commissioning - Fire . Standards Australia; 2004. Report No.: AS 1670.1:2004.
56. Standards Australia. Australian Standard 1670 Part 1- Fire detection, warning, control and intercom systems - System design, installation and commissioning - Fire . Standards Australia; 2004. Report No.: AS 1670.1:2004.
57. Tewarson, A. Section 3 Chapter 4 Generation of Heat and Chemical Compounds in

- Fires. 3rd Edition ed. National Fire Protection Association; 2002. pp. pp.3-111.
58. Tewarson, A. Section 3 Chapter 4 Generation of Heat and Chemical Compounds in Fires. 3rd Edition ed. National Fire Protection Association; 2002. pp. pp.3-111.
59. Vision Systems. [Web Page];
http://www.fpemag.com/archives/article.asp?issue_id=27&i=154.
60. Wang J, Hua J, Kumar K, Kumer S. Evaluation of CFD modeling methods for fire-induced airflow in a room. *Journal of Fire Sciences* 2006;24:393-411.
61. Xin, Y. Baroclinic Effects on Fire Flow Field. *Proceedings of the Fourth Joint Meeting of the U.S. Sections of the Combustion Institute*. Pittsburgh, Pennsylvania: Combustion Institute; 2005.

CMMT(C)-2006-437
END OF REPORT